Chem Soc Rev

This article was published as part of the

2008 Gold: Chemistry, Materials and Catalysis Issue

Please take a look at the full table of contents to access the other papers in this issue

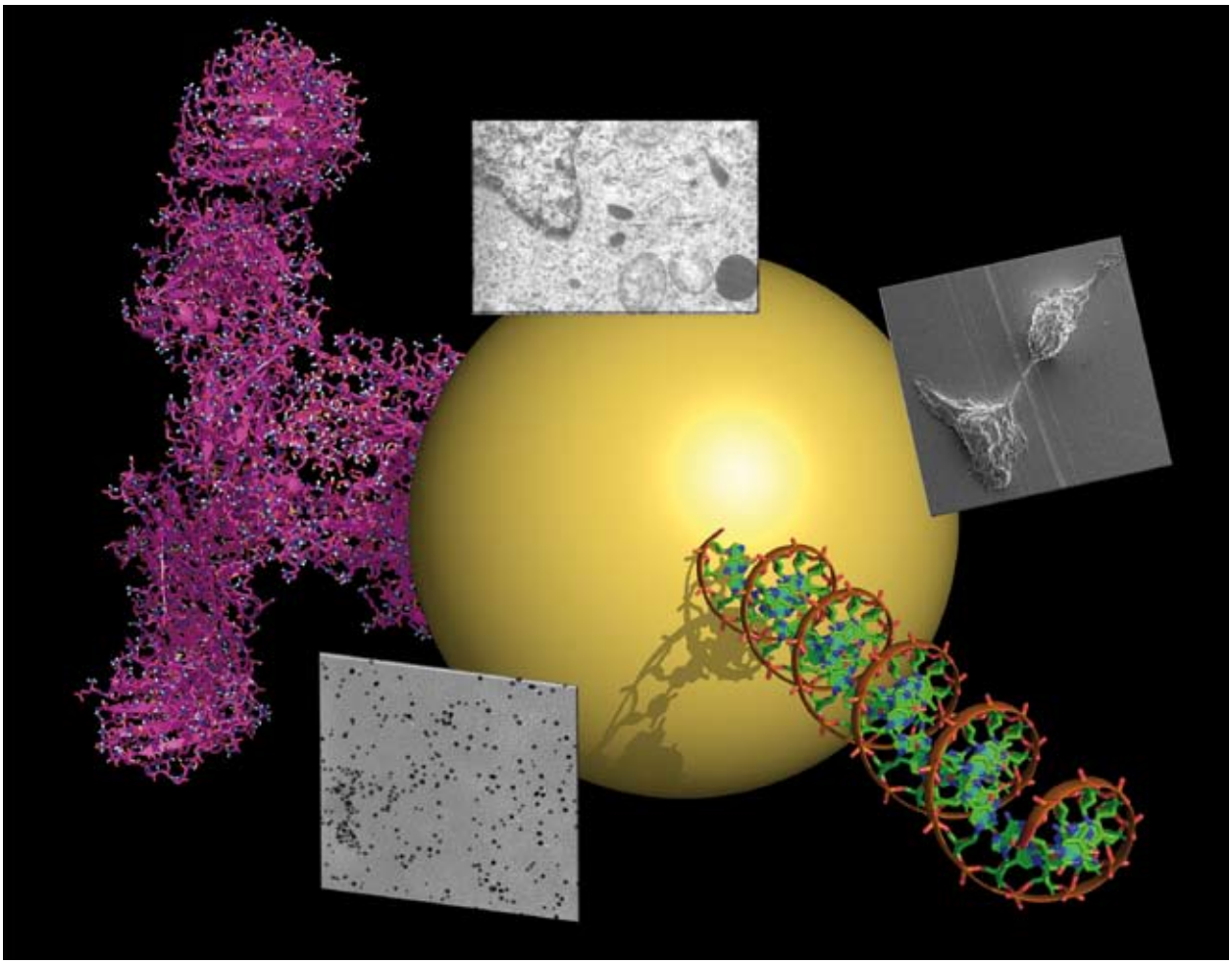

Theoretical chemistry of gold. III†‡

Pekka Pyykkö*

Received 28th February 2008
First published as an Advance Article on the web 3rd July 2008
DOI: 10.1039/b708613j

Gold is an element whose unique properties are strongly influenced by relativistic effects. A large body of appropriate calculations now exists and its main conclusions are summarized in this *critical review*. The present paper completes the recent reviews by Pyykkö (2004, 2005) (529 references).

I Introduction

The theoretical chemistry of gold is right now undergoing an explosive development. The present review continues the two previous ones by the author[1,2] and basically covers the work from mid-2005 to 2007. An independent review on theoretical chemistry of gold has been compiled by Schwerdtfeger and Lein.[3]

The numerous acronyms used are explained in Table 1. A given contribution may appear in the text, in the tables, or both.

II Physical principles and computational methods

A: Relativity and chemical trends

In several cases further insight is obtained by considering the trends for the entire Group 11.

Department of Chemistry, University of Helsinki, P.O.B. 55 (A.I. Virtasen aukio 1), FIN–00014 Helsinki, Finland. E-mail: Pekka.Pyykko@helsinki.fi; Fax: 358-9-191 50169

† Part of a thematic issue covering the topic of gold: chemistry, materials and catalysis.

‡ Theoretical chemistry of gold. Parts I and II, refs. 1 and 2. Figure of graphical abstract from ref. 141.

Pekka Pyykkö

Pekka Pyykkö was born in 1941 in Hinnerjoki, Finland, and received his formal education in the nearby city of Turku with a PhD in 1967. After working at the Universities of Aarhus, Göteborg, Helsinki, Jyväskylä, Paris XI and Oulu in 1968–74, he was Associate Professor of Quantum Chemistry at Åbo Akademi in Turku in 1974–84. Since then he holds at the University of Helsinki the Swedish Chair of Chemistry, established in 1908 as a parallel one to Johan Gadolin's former position, founded in 1761. He led the European REHE programme (Relativistic Effects in the chemistry and physics of the Heavy Elements) in 1993–98 and the Finnish CoE in Computational Molecular Science in 2006-08. His main interest is the theoretical chemistry of heavy elements, such as gold.

B: Methods of quantum chemical calculations

Already in 2001 Martin and Sundermann[4] proposed auxiliary $2f1g$ functions for the Stuttgart pseudopotentials of all nd-elements, n = 3–5, including gold. The exponents for Au were 0.498, 1.461 for f and 1.218 for g. Note that for aurophilicity the optimal f exponents were 0.2 and 1.19.[5] A g exponent of 1.1077 was used for $AuXe^+$ before.[6] New basis sets of double-, triple- and quadruple-zeta quality for the elements H–Rn were presented by Weigend and Ahlrichs.[7] The gold compounds in the test set were Au_2, Au_3^-, AuCl and $AuCl_3$. Peterson and Puzzarini[8] report new, systematically convergent basis sets for the Group 11–12 metals. They are consistent with the latest Stuttgart pseudopotential.[9]

Hou *et al.*[10] evaluated basis sets for various 11-VE pseudopotentials for DFT use. The PP were LANL1, Ermler-Christiansen and Troullier-Martins. Rousseau *et al.*[11] searched for a *local* one-valence-electron (1-VE) gold pseudopotential for modelling the Au–Au interactions in slab models. In Au–S bonds, to quote an example, the 5d electrons would also strongly hybridize.

Naveh *et al.*[12] introduced a real-space PP with SO coupling for Au and tested it on the diatomic AuH and Au_2. They report an SO-induced *de*crease of the Au_2 (not AuH) D_e by 0.33 eV while earlier work by van Lenthe *et al.* yields an *in*crease by 0.06 eV.[13]

For an optimized accurate auxiliary basis set for RI-MP2 and RI-CC2 calculations, see Hellweg *et al.*[14]

An 'optimized virtual orbital space (OVOS)' method was tested on diatomic coinage-metal hydrides and fluorides by Pitoňák *et al.*,[15] at levels up to CCSD(T).

A charge-selfconsistent density-functional based tight-binding method was introduced by Koskinen *et al.*[16] with applications on gold clusters Au_n^-, n = 4–14. A quintuple-zeta Slater basis is used. The method resembles somewhat the Extended Hückel one, but the matrix elements $H_{\mu\nu}$ are solved from the Kohn–Sham equations, instead of being parametrized. Tests against other DFT methods were carried out. The advantage is a low cost.

The developed interatomic potentials are summarized in Table 2.

Details on earlier methods. Methods for calculating the vibrational spectra of large molecules, such as $[(Ph_3PAu)_6C]^{2+}$ were developed by Neugebauer.[17]

Table 1 Acronyms and symbols used in the present work

Acronym	Method
ADF	Amsterdam density functional code
BDF	Beijing density functional code
BPMA	Bis(2-pyridylmethyl)amine
BSSE	Basis-set superposition error
B3LYP	A density functional
CASPT2	Complete active space 2nd-order perturbation theory
CASSCF	Complete active space self-consistent field
CBS	Complete-basis-set (extrapolated limit)
CCSD	Coupled-cluster method with single and double excitations
CCSD(T)	Ditto with perturbative triples
DC	Dirac–Coulomb (Hamiltonian)
DFT	Density functional theory
DKH	Douglas–Kroll–Hess (approximate relativistic Hamiltonian)
EA	Electron affinity
IP	Ionisation potential
MD	Molecular dynamics
MP2	Second-order Møller–Plesset theory
MRCI	Multireference configuration interaction
NHC	N-heterocyclic carbenes
ONIOM	A variety of QM/MM
PP	Pseudopotential = effective core potential
QM/MM	Interfaced quantum mechanical and molecular mechanical methods
SAPT	Symmetry adapted perturbation theory
SERS	Surface enhanced Raman scattering
SO	Spin-orbit
SR	Scalar relativistic (SO averaged)
STM	Scanning tunneling microscopy
SWNT	Single-wall nanotube
TDDFT	Time-dependent DFT
Tht	Tetrahydrothiophene
XANES	X-ray absorption near-edge spectroscopy
ZORA	Zeroth-order regular approximation

Table 2 Atom–atom potentials for molecular dynamics calculations on gold-containing systems

Authors	Year	Comments
Cruz *et al.*[389]	2005	Potentials for Au on TiN(001) from DFT
Lin *et al.*[189]	2005	A tight-binding Au–Au potential
Chen *et al.*[174]	2007	Gupta parameters for Ag–Au alloys
Fartaria *et al.*[25]	2007	A force field for ethanol on Au(111)
Pawluk *et al.*[23]	2007	Reparametrize Sutton–Chen potential
Schaposchnikow *et al.*[390]	2007	Lennard-Jones 12–6 fits for Au–CH_x and Au–S interactions

Atomic properties. Itano[18] reported MCDF calculations for Au^+. Values for the atomic quadrupole moment, nuclear quadrupole moment and magnetic hyperfine coupling constants were obtained.

The performance of usual quantum chemical approaches (MP2, CCSD(T), various DFT) on the EA and IP of the 4d and 5d metal atoms was tested by Wu and Kawazoe.[19]

Concerning the electronegativity of gold in auride compounds, Belpassi *et al.*[20] considered the entire series MAu; M = Li–Cs. They conclude that in them the gold behaves as a halogen, intermediate between Br and I.

Fivet *et al.*[21] measured the radiative lifetimes of several odd-parity states of both Au I and Au II (for chemists Au^0 and Au^+, respectively). The results were related to relativistically corrected Hartree–Fock calculations including a core-polarization potential.

Zeng *et al.*[22] calculated oscillator strengths for highly ionized, Co- to Ge-like gold ions.

For the best available calibration values, see Table 3.

Molecular dynamics (MD). A comparison of the available MD potentials for Ag and Au was made by Pawluk *et al.*[23] using a model test reaction M_2 + M for different kinetic energies and collision angles. Coalescence was sensitive to the chosen potential. It was necessary to reparametrise the Sutton–Chen potential to get agreement with the DFT calculations.

The cluster studies of Xiao *et al.*[24] similarly suggested that the Sutton–Chen interatomic potential should be modified. A force field to describe the adsorption of ethanol on Au(111) was developed by Fartaria *et al.*[25] For summary of the potentials, recall Table 2.

Including pressure. Kohanoff *et al.*[26] presented a 'Langevin thermostat' method for simulating the effect of both an applied pressure and a finite temperature. They applied it on calculating structures of gold clusters.

Table 3 Latest relativistic benchmark results on atomic gold: R = relativistic, NR = non-relativistic

System	Property	Exp.	R	NR	R-NR	Method	Ref.
Au (atom)	*IP*1 [eV]	9.22554(2)	9.197	7.057	2.140	CCSD	391[a]
			9.219			PP-CCSD(T)	8
	EA [eV]	2.30863[b]	2.295	1.283	1.012	CCSD	391[a]
			2.307			MBPT2	392

[a] Including newer results from personal communication. [b] Ref. 393.

III Results from theoretical calculations

A: The oxidation states of gold

Mononuclear Au(II) is a rare oxidation state.[27] Barakat *et al.*[28] found that the main driving force for the disproportionation $2Au^{II} \rightarrow Au^{I} + Au^{III}$ is the favourable solvation free energy of the trivalent complex, for the ligands L = PH_3, CO, MeCN, MeNC, NH_3, OH_2, py. For free gas-phase ions, the disproportionation would be endothermic by 311 kcal mol^{-1} using experimental data. This is a natural consequence of the approximately quadratic increase of the IP_n as function of n.[29] Note, however, that the difference between $2 \times 2^2 = 8$ and $1^2 + 3^2 = 10$ is not large. Low-polarity solvents may be helpful in stabilizing mononuclear Au(II).

Riedel and Kaupp[30] showed at levels, up to CCSD(T), that the experimental claims by Timakov *et al.*[31] for a gold heptafluoride, AuF_7, were unlikely to be true. Later Himmel and Riedel[32] theoretically attributed the species, seen by Timakov *et al.* to $AuF_5 \cdot F_2$. The experimental evidence was based on elemental analysis, and a single IR line at 734 cm^{-1}, which now found a natural explanation as the F–F stretch in the complex. Thus the highest documented oxidation state of gold remains Au(V).

B: Coordination to gold

Trends in Group 11. Hancock *et al.*[33] considered the complexation of the M^+ cations, M = Cu, Ag, Au, Rg (röntgenium, E111) to one or two of the ligands L = NH_3, OH_2, SH_2 and PH_3. The heaviest member Rg invariably had the largest complexation energy. It was concluded to be the 'softest' metal ion.

The first *terminal* gold–oxo bonds were experimentally reported by Cao *et al.*[34] Opposite to the observed, multiple 176 pm O–Au bond there is a much longer coordination bond to OH_2. The equatorial plane has four oxygen atoms from a polytungstate. Theoretical model calculations were attempted. The recent triple-bond covalent radii[35] would predict a calculated Au–O bond length of 176 pm. The Au(III) oxidation state was supported by five independent experimental methods (chemical titrations, coulometric measurements, a d^8 optical spectrum, near-edge X-ray absorption, and the X-ray structure).

Au^+–L systems. The N-heterocyclic carbenes (NHC) have a potential to play the role of phosphines in gold chemistry. As an example, Laitar *et al.*[36] synthesized the first isolable gold fluoride as an (NHC)–Au–F complex. DFT calculations on a model complex suggest involvement of the Au 5d shell in the bonding.

Pyykkö and Runeberg[37] verified the strong bonding of L = NHC in the systems Au–L^+ and ClAu–L. The carbodiphosphoranes $R_3P{=}C{=}PR_3$ were found to be potentially even stronger ligands, L, than the phosphines. For further discussions on the bonding in these ligands, see ref. 38–41.

Li and Armentrout[42] presented new measurements of the 0 K bond dissociation energies of Au–CH_2^+ and Au–CH_3^+. The values were 3.70(7) and 2.17(24) eV, respectively. They agreed well with earlier and new calculations. Au gave much stronger bonds than Cu or Ag.

Olson *et al.*[43] calculated the binding energies of M^+, M = Ag, Au to propene at MP2 and CCSD(T) levels, extrapolating the result to a complete-basis-set (CBS) limit. The latter model gave 2.92 eV.

The MCN, MNC and triangular MNC forms of M = Cu–Au monocyanides were compared by Lee *et al.*[44] For Cu–Au the triangular form was a saddle point.

Yi *et al.*[45] studied the complexation of Group 10–12 ions to benzene, quinone and hydroquinone. The 6s ions (Au^+ and Pt^{2+}) were found to prefer η^2 coordination to η^6 coordination because this gave better donation from the ligand to the relativistically stabilized metal s orbitals.

The BO^- anion is isoelectronic with cyanide, CN^-, and has been proposed as a possible ligand, or a crystal anion.[46,47] Now, in a study of laser vaporized ^{10}B/Au samples, the group of Lai-Sheng Wang[48] identified, using mass selection and PES, the species Au_nBO^-; n = 1–3. The species Au_2BO^-($C_{\infty v}$, AuBO and Au_3BO have closed-shell structures. The bonding system covers the entire molecule.

The ions $Au^+(CO)_n$, n = 1−12 were experimentally observed by Velasquez *et al.*,[49] with n = 2,4 having large intensity. The n = 3 case is calculated to be trigonal planar and the n = 4 one tetrahedral.

Concerning the complexation of Au^+ with water, the bonding in the systems $[Au(H_2O)_n]^+$; n = 1–10 were analysed by Reveles *et al.*[50] As found before, the first two ligands form strong bonds. The subsequent ones form four-membered rings.

Au^-–L systems. In complexes to imidazole, the preferences for C-binding *vs.* N-binding depend on the metal fragment involved.[51] The ligands L = –AuCl, $–Au(NH_3)^+$ and $–Au(OH_2)^+$ favoured C-complexation by −8.4, −13.4 and −28.0 kJ mol^{-1}, respectively.

AuL_n systems, $n \geq 2$. Lee *et al.*[52] asked, why is the second hydration of Au^+ stronger than the first one, in a gas-phase situation. The special stability was attributed to a HOMO structure involving the Au 6s–5d hybrids and the water lone pairs.

The disproportionation of Au(II) to Au(I) and Au(III) was discussed by Barakat *et al.*[28] The ligands L = Cl, PH_3, CO, MeCN, MeNC, NH_3, OH_2 and pyridine were compared for 2 $AuL_3^{2+} \leftrightarrow AuL_2^{+} + AuL_4^{3+}$.

The complexation of Au(III) to azide ions in $Au(N_3)_4^-$ was analyzed by Afyon *et al.*[53] The experimental counterions were alkali metals K to Cs.

A four-coordinated dithiolate complex of Au(III) was studied by Kokatam *et al.*[54] Four different charge states, $[Au(L)_2]^q$, $q = -2$ to $+1$, could be produced. A one-electron oxidation had little effect on the Au–S distances but a large effect on the S–C distances of the dithiolate ligands. The magnetic and electric ^{197}Au hyperfine structure, however, indicated some spin presence at the metal. Structures and spin populations were calculated for the various charge states.

Agostic interactions, *i.e.* attractions from the H atoms of neighbouring C–H and N–H bonds to gold, were both experimentally observed and theoretically calculated by Räisänen *et al.*[55] for certain pyridine thiolates. They also quote earlier studies on such interactions.

Comments on particular ligands: halides. Krawczyk *et al.*[56] studied the structural change of coinage-metal halide clusters $(MX)_n$ with increasing n. Up to $n = 4$, rings are obtained for all metals, M = Cu–Au. A clear transition to a 3D structure occurs at $n = 6$ for CuBr. The gold halides adopt ring structures at $n = 6$. These rings are related to the chains in the macroscopic gold halides.

Diphosphines. The coordination of the diphosphines dppp = 1,3-bis(diphenylphosphino)propane and depp = 1,3-bis-(diethylphosphino)propane to Au_n^+(n = 2–5) was studied by Golightly *et al.*[57] The latter was found to be a poor model for the former. While dppp is a net electron ($\sigma + \pi$) electron acceptor, depp is a net electron donor. The purpose was to model gas-phase electrospray mass-spectrometry data where $[Au_{11}(dppp)_5]^{3+}$ was observed but its depp analogue not. (As discussed in Part I (ref. 1, p. 4435), counting one Au as a central, 11e atom, and the others as 1e atoms, the total electron count becomes $11 + 10 - 3 = 18$.

van der Waals complexes with neutral gold atoms. Granatier *et al.*[58] calculated the interaction energies for M···SH_2 systems, M = Cu–Au. All were found to be non-planar. The complexation energies were compared with the analogous OH_2 and NH_3 complexes by Antušek *et al.*[59] Both partial charge-transfer from the donor lone-pair to the half-filled metal s orbital, induction effects and dispersion mechanisms count. Relativistic effects strongly increased the M···SH_2 complexation energies.

C: Aurophilicity

A 'recapitulation' on the nature of aurophilicity is given at the end of this article. In addition to the references there on interactions between polarisable ions, we mention the qualitative discussions on possible quadrupolar polarisability effects by Bilz.[60] A review on typical aurophilic structures was published by Muñiz and Sansores.[61]

From the experimental side we record the first experimental, EXAFS studies of aurophilic interactions in solution.[62]

A statistical analysis of the experimentally observed numbers of aurophilically bound gold atoms and their local geometries in various systems was given by Anderson *et al.*[63] The data base contained 336 compounds with Au–Au distances in the range 300–400 pm. The dihedral L–Au–Au–L angles tended to be either 0, 90 or 180°.

A dimer and trimer study of Au(CO)Cl structures at MP2 level was reported by Elbjeirami *et al.*[64]

Methodological questions: The basis-set limit. Pyykkö and Zaleski-Ejgierd[65] studied the basis-set limit of the aurophilic attraction at MP2 level using both the Dunning-type correlation-consistent sets and the Stuttgart-type sets. Both gave ultimately the same results for the perpendicular $[ClAuPH_3]_2$ free dimer model and for $[E(AuPH_3)_3]^+$, E = P. The latter systems were earlier found to be T_d for E = N and C_{4v} for E = P, As [66] but that E = P MP2 result was contested by Fang and Wang.[67] For the free dimer, the 'Andrae + 2f(0.2,1.19)' level, used since 1997,[5] was found to give about 74% of the basis-set-limit aurophilic attraction energy, thus verifying the earlier body of work.

DFT. No proof has been given that any supramolecular DFT treatment would reproduce the aurophilic attraction for a good physical reason. At operative level it has been found that certain functionals give results in the neighbourhood of wavefunction-based correlated ones. Such cases comprise the series $X(AuPH_3)_4^+$, X = N–Sb with $X\alpha$.[67] Of the functionals studied, the venerable Slater $X\alpha$ performed best.

A-frames and pyramids. For A-frames, the latest study remains the one on $[S(MPH_3)_2]$; M = Cu–Au at levels up to CCSD(T) by Riedel *et al.*[68]

Cation–cation and anion–anion interactions. Carvajal *et al.*[69] considered the interactions between $[AuL_2]^+$monomers, L = $C(NHMe)_2$. The interaction in a free dimer is dominated by Coulomb repulsion but inclusion of the anions does restore aurophilic attractions. The calculations were at MP2 level, including one compact f function.

To bracket this result, recall that for a very small dication, such as Au_2^{2+}, the ground-state potential indeed is purely repulsive, like in the case of Carvajal.[70,71] To the contrary, in a globally neutral chain tetramer, such as $[AuCl_2]$-$[Au(PH_3)_2][Au(PH_3)_2][AuCl_2]$,[72] a (− + + −) or (+ − − +) type contact was found to be possible, both theoretically and experimentally.

Other oxidation states. A new example on Au(I)–Au(III) and an example on Au(III)–Au(III) aurophilic interactions were produced by Cao *et al.*[73] The monomer structures were calculated and their frontier orbitals discussed for $[AuCl(BPMA)]^{q+}$, q = 1,2.

Closed-shell interactions between gold and other metals. Fernández *et al.*[74] reported comparative studies at HF, B3LYP and MP2 levels for an $[AuPh_2]^-$unit, interacting with $[Ag_4(CO_2H)_5]^-$ in a square-pyramidal configuration for the metals. An attraction between the two anions was reproduced and the metallophilic stabilization was estimated to be around 13 kJ mol^{-1} per Au(I)–Ag(I) interaction.

The Pt–Au bonding in the hypothetical complex $[Pt(PH_3)_3Au]^-$ was analyzed by Mendizabal *et al.*[75] The nature of the bonding was analyzed by starting from the large-R limit. It then transpired that the charge-induced-dipole term and the induction term, behaving like R^{-4}, dominate the interaction at large distances. The isoelectronic system with Tl^+ instead of Au^- is experimentally known. The isoelectronic system with Hg(0) shows a metallophilic R^{-6} interaction.

The first compound with an Au(I)···Bi(III) interaction (of 373 pm) was synthesized by Fernández *et al.*[76] A comparison of HF and MP2 calculations suggested that the interaction was 79% ionic and 21% dispersion.

The d^{10}–s^2 interactions in Au(I)–Tl(I) complexes were modelled at MP2 level by Fernández *et al.*[77]

Many aurophilic systems exhibit optical absorption and phosphorescence, see Table 4.

IV Further aspects

A: Gold as a halogen; auride chemistry

For a summary of the calculations, see Table 5.

B: Gold as hydrogen-bond acceptor

Experimental examples of the auride anion as a hydrogen-bond acceptor in N–H···Au^- systems were presented by Nuss and Jansen.[78] Theoretical predictions for such N–H···Au[79–82] and F–H···Au [83] interactions were published by Kryachko and Remacle.

C: The chemical analogy between gold and hydrogen

As mentioned in earlier reviews, an R_3PAu– group, or even a plain gold atom, can show similar chemical behaviour as a hydrogen atom. Khairallah *et al.*[84] considered both experimentally and computationally the resulting H_3^+ analogs. The lowest-energy structure was a hydrogen-bridged R_3PAu–$AuPR_3$ cation.

Zubarev *et al.*[85] considered the structures of $B_xAu_x^{2-}$ clusters and found them similar to those of the $B_xH_x^{2-}$ *closo* boranes.

Kiran *et al.*[86] compared the clusters $Si_3Au_3^q$; $q = -1, 0, 1$ with their hydrogen analogs, finding similar structures for both. An example is the D_{3h} structure of the 2π aromatic cation.

D: Multiple bonds to gold

Recall here the study on $Au = CH_2^+$ by Li and Armentrout.[42] Very short Au(II)–Au(II) bonds of about 245 pm in polyatomic gold guanidates were synthesized by Mohamed *et al.*[87] Theoretical model calculations on $[Au_2(hpp)_2Cl_2]$ (hpp = hexahydropyrimido(pyridine)) and related systems reproduced the

Table 4 Some calculations of optical properties for molecules or molecular models

Authors	Year	Method	System and comments
Barakat *et al.*[394]	2003	DFT	Jahn–Teller distortion in phosphorescent excited state of three-coordinate Au(I) phosphine complexes
Roman *et al.*[186]	2003	DFT	Circular dichroism spectra of bare and thiol-passivated Au_n
Bojan *et al.*[395]	2005	MP2	Models for three-coordinated $[Au_2Ph_2Sb)_2O_3]^{2+}$ dimer. Jahn–Teller distortion at only one centre
Cao and Zhang[396]	2005	CASSCF	H_3PAu–$(C{\equiv}C)_n$–Ph; $n = 1$–6
Fernández *et al.*[397]	2005	Review	Luminescence in Au(I)–Tl(I) systems
Del Vitto *et al.*[222]	2005	TDDFT	Optical properties of Au and Au_2, adsorbed on amorphous SiO_2
Guo *et al.*[398]	2005	MP2, TDDFT	$[Au_2(S_2CS)_2]^{2-}$-type systems. Solvent effects. Au–Au shortening upon excitation
Saha and Mookerjee[399]	2005		Random CuAu alloys
Sinha *et al.*[400]	2005	TDDFT	$Au(PPh_3)_2Cl$. T-shaped exciplex
Aikens and Schatz[252]	2006	TDDFT	Au_{20}, pyridine/Au_{20}. Opt. excit. and SERS
Bardají *et al.*[401]	2006	TDDFT	A mixed Au(I)–Au(III) species has no luminescence
Cottancin *et al.*[230]	2006	TDDFT	The plasmon resonance size effect for Cu, Ag and Au clusters
Fa *et al.*[127]	2006	DFT	Hypothetical icosahedral and low-symmetry Au_{32}
Fernandez *et al.*[402]	2006	TDDFT	Luminescence of tetranuclear Au_2M_2 units
Liao *et al.*[403]	2006	CIS, TDDFT	Luminescence of (diethylfluorenyl)$AuPH_3$
Mendizabal *et al.*[404]	2006	TDDFT	Spectra of $[M(CN)_2]_n^{-n}$ (M = Au(I), Ag(I); $n = 1$–3)
Pan *et al.*[405]	2006	CIS	Spectra of *trans*-$[Au_2(PH_2CH_2SR)_2]^{2+}$, R = H, Me, Cy
Zhang *et al.*[406]	2006	CIS	$Au_3(HN{=}COH)_3$. Luminescence
Arvapally *et al.*[407]	2007	MP2 vert. tr.	$M[Au(SCN)_2]$ and related species; M = Li–Cs. Excited triplet in dimer covalently bound
Bosko *et al.*[226]	2007	TDDFT	Optical spectra of M, M_2; M = Cu–Au at regular sites and oxygen vacancies on MgO(001)
Elbjeirami *et al.*[64]	2007	TDDFT	$[Au(CO)Cl]_n$, $n = 1$–3. CO stretch blue-shift reproduced
Fernandez *et al.*[408]	2007	DFT	T-shaped [Tl(η^6-benzene)][$Au(C_6Cl_5)_2$]. Ground state short ionic bond, CT state has long bond. Intense, blue phosphorescence
Fernandez *et al.*[409]	2007	DFT	$[Au_2Ag_2(C_6F_5)_2(CF_3CO_2)_2(tht)_2]$ and related systems. Lowest triplet transitions
Liu *et al.*[410]	2007	3D ED model	Rodlike and bipyramidal Au nanoparticles
Mendizabal *et al.*[411]	2007	TD-DFT	$[Au_3(MeN{=}COMe)_3]_n$; $n = 1$–4. DFT *vs.* MP2. Stack of triangles. MMCT, MLCT found
Muñiz *et al.*[412]	2007	TDDFT	$[AuS_2PPh(OCH_2CH{=}CH_2)]_2$ luminescence
Perrier *et al.*[413]	2007	TDDFT	Dithienylethene + Au_n; $n = 3, 9$. Photochromicity
Stener *et al.*[414]	2007	TDDFT	Optical spectra of Au_6^{4+}, Au_{44}^{4+}, Au_{146}^{2+}
Wong *et al.*[415]	2007	TDDFT	Luminescence in a new class of cyclometalated alkynylgold(III) complexes
Zhu *et al.*[416]	2007	TDDFT(+SO)	Group-11 M(III) complexes in N-confused (M–C bonded) porphyrins
Pan *et al.*[417]	2008	TDDFT, MP2	$[MM'(CN)_n(PH_2CH_2PH_2)_2]^q$; M, M′ = Pt, Au; $n = 0$–4

Table 5 Available *ab initio* calculations on aurides

Authors	System	Comments
	Molecules	
Belpassi *et al.*[20]	MAu; M = Li–Cs	'Au as halogen' between Br and I
Cui *et al.*[418]	Na_nAu_n, $Na_nAu_n^-$; $n \leq 3$. PES interpreted	Bonding highly ionic. MP2, CCSD

experimental geometry. Frontier orbitals were analysed. Recall, as another short experimental Au(II)–Au(II) distance, the one of 249 pm in solid $AuSO_4$, containing formally Au_2^{4+} clusters.[88]

E: Bonds between noble gases and gold

Ghanty[89] considered the insertion of the noble gases Kr or Xe into AuF or AuOH. Local minima with barriers were found but the processes were strongly endothermic. The species AuXeF, AuKrF and AuXeOH were characterized as having a covalent Au–Rg bond. A comparison with the other coinage metals and Ng = Ar–Xe was added later.[90] For the radicals AuBX; X = F–Br Ghanty[91] found a stability, comparable to that of the known HBX radicals.

The interaction potentials between the coinage metal cations of Cu–Au and the noble gases He–Rn in the diatomic MNg^+ species continue to attract attention.[92–94] These potentials were brought to the CCSD(T) basis-set limit and related to transport properties of the metal cation in the gas by Yousef *et al.*[94] At least for the heaviest members of the series, $AuKr^+$ and $AuXe^+$, a clear covalent bonding character was detected. Compared to the earlier, predicted $D_e(AuXe^+)$ (PP-SR-CCSD(T)) of 1.314 eV,[6] the newest values are 1.248[94] (PP-SR-CCSD(T)), 1.305[93] (PP-SR-CCSD(T) with CBS extrapolation) and 1.33 eV[92] (DC-CCSD(T)). Belpassi *et al.*[92] also compared the bonding in the $NgAu^+$ cation and NgAuF molecule, and made a methodological comparisons between four-component MP2, CCSD(T) and DFT calculations.

The electronic spectra of the neutral Au–Ar complex were obtained and analysed by Plowright *et al.*[95]

F: Gold as interatomic glue

Hakala and Pyykkö[96] suggested a new possible structure for solid AuCN. The known structure consists of infinite –CN–Au–CN–Au– chains, packed to a hexagonal lattice, with all Au(I) ions in the same plane. The predicted, new low-density structure consisted of cyanuric C_3N_3 six-rings, coupled to each other by N–C–Au bonds in the same plane. A quinoline-based series of nanostrips (one-dimensional polymers) was predicted to exist by Pyykkö *et al.*[97] Depending on the number of valence electrons, varied by C/N substitutions, the systems could be semiconducting or metallic. The other coinage metals are slightly less likely to accept this structure.[98]

These nanostrips were further bent to finite nanorings by Pyykkö and Zaleski-Ejgierd.[99] Their elastic properties were analysed by treating the entire molecule as an elastic body. Then the bending energies and deformation frequencies scale as R^{-1} and R^{-2}, respectively, where R is the radius of the nanoring. The deformation energies of these polyauronaphthyridines were comparable with those of polyacenes.

Larger, triangular complexes held together by linear N–Au–C bonds were also theoretically studied. Sansores *et al.*[100] considered [2-pyridyl–Au]$_3$, similar pyrazolates and related systems. Experimental geometries were reproduced.

Repp *et al.*[101] observed by an STM method chemical bonds, made by a single gold atom between a pentacene molecule and an NaCl layer, supported by a Cu(100) surface. The individual bonding orbitals were studied by DFT methods.

Sterrer *et al.*[102] modelled the case of an OC–Au group, bonded to MgO(001)/Mo(001). Strong chemical interaction throughout was discovered, and this influences the CO stretch.

G: Individual spectroscopic species

For a summary, see also Table 6. Starting with diatomic species, the following advances are reported:

Group 14. Accurate studies of AuC and AuC^+ appeared.[103]

Group 18. See for MNg^+ and MNg diatomics the chapter IV. E.

Inorganic systems: general. It was predicted earlier by Gagliardi and Pyykkö[104] that very short triple bonds of about 210 pm could exist between late 5d metals and uranium. The first such compound, $IrUO^+$, was subsequently observed by Santos *et al.*[105] In such compounds, iridium is a chemical analog of nitrogen, and platinum one of oxygen. Now, a similar isoelectronic series of such *metalloactinyls* was predicted for thorium by Hrobárik *et al.*[106] As seen from Table 5, several of the predicted species contained gold.

Li and Miao[107] found the planar clusters M_5H_5X; M = Ag, Au; X = Si, Ge, P^+, S^{2+} quite stable.

The Au(III) monohalides were earlier predicted to suffer a Jahn–Teller distortion from D_{3h} symmetry. This was verified for $AuCl_3$ using matrix spectroscopy.[108]

Organometallic systems. Grönbeck *et al.*[109] calculated the structures of the cyclic thiolate clusters $(MeSAu)_x$, x = 2–12. For $x > 4$, crown-like conformations were obtained.

H: Clusters and wires

Reviews. For a review on both pure Au_n clusters, Au alloy clusters and CO-chemisorbed Au clusters in the gas phase, see Zhai *et al.*[110] Garzón[111] reviewed the bare and passivated Au_n with emphasis on disorder and chirality aspects.

Highly-charged clusters. Chen *et al.*[112] used special electron-counting rules for approximately spherical clusters, mostly with high charges (from 6− to 4+) to arrive at the predicted minima Au_6^{2-}(O_h), Au_8 (double tetrahedron, T_d), Au_{10}^{2+} (D_{4d}) and Au_{14}^{4-} (D_{2d})). Note that the fragment $[CAu_6]^{2+}$ could be seen as a C^{4+} inside Au_6^{2-}. This species was already reported at HF level in ref. 113 and it was synthesized, with $-Au(PPh_3)_3$ groups instead of –Au, in Schmidbaur's group.

Table 6 *Ab initio* production results for molecules containing gold. See also the text

System and comments	Ref.	Method
Diatomics, Groups 1–18		
AuH. Excited states at DFT level using non-collinear xc kernel	419	TD-DFT
MH; M = Ag, Au in a cylindrical confining potential. Effect on SO	420	DK-MC
MAu; M = Li–Cs. 'Au as halogen' between Br and I	20	Dirac-DFT
NaAu, $NaAu^-$. PES interpreted	418	MP2, CCSD
CsM; M = Ag, Au. Excited-state dipole moments	421	Dirac
MH, MF; M = Cu–Au; dipole moments, polarizabilities	15	CCSD(T)
$AuPt^q$; $q = -1, 0, +1$	422	DFT
Au_2 as test of new, systematically convergent basis sets	8	PP-CCSD(T)
Au_2 and Rg_2 as tests for a two-spinor minimax finite-element method	423	DFT-FEM
MSi^q; M = 3d, 4d or 5d metal; $q = -1, 0, +1$	424	DFT
MM′; M = Cu–Au; M′ = Ge–E114	425	DFT
AuO. Electronic spectrum and spectroscopic parameters	426	DK CASPT2
AuX^q (X = O, S, Se, Te, $q = +1, 0, -1$)	427	DFT
Triatomic gold clusters		
Metalloactinyls containing thorium: $FThAu^{2+}$, $OThAu^+$, NThAu, $AuThAu^{2+}$, $AuThPt^+$, AuThIr	106	DFT
Larger gold clusters		
M_4 (D_{2h}); M = Cu–Au	428	DFT
Au_n; n = 2–7. Effect of SO on structure and magnetic moments discussed. Results agree with Table 7	260	DFT
Au_n; n = 4–7. Most minima wrong	429	DFT
Au_6. D_{3h}. Comparisons with MP2 and DFT	115	PP-CCSD(T)
Au_8. Large-basis CCSD(T) gives planar, D_{4h} structure	114,115	CCSD(T)
Au_n; n = 2–10. Planar up to n = 11	430	DFT
Au_n; n = 2–12. Mentions zigzag chain alternative	431	DFT
Au_{13}. C_{2v} 'buckled biplanar'	432	DFT
Au_n^{q+}; n = 9, 13; q = 0, 1, 3	334	DFT
Au_n; n = 2–14. 2D-to-3D at n = 12. Polarizabilities	433	DFT
$Au_{16}^{2-} T_d$ dianion predicted to be stable	167	DFT
M_n; M = Cu–Au; n = 2–20	434	ADF
Au_n^-, n = 15–19. Hollow cages for 16–18	128	DFT
Au_n^-, n = 15–19. Flat cages for 15–16, hollow cages for 17–18, pyramidal n = 19	119	DFT
Au_n^-; n = 11–24. DFT and el. diffr. 2D-to-3D for n = 12–14, cages for n = 16, 17, T_d for n = 20, symmetric tubulars for n = 24	133	DFT
Au_{20}^q; q −2 to +2	120	DFT
Au_n^-; n = 15–24. Structures and reactivity with O_2	135	DFT, exp.
Au_n; n = 18, 20, 32, 34, 38. Also n = 18 a stable one. C_{2v}	130	DFT
Au_n^-, n = 21–25. Pyramids for 21–23, hollow tube for 24, endohedral for 25	134	DFT
Au_n; n = 26–28. The Au_{26} is tubelike, the others add atoms to it	127	DFT
Au_{32}^- calculated and experimentally produced. Low-symmetry structure favoured by free energy above 300 K	136	DFT
Au_{32} optical and IR lines calculated. I_h and low-symmetry forms give different signals	435	DFT
$Au_{32}^{-1,0,+1}$. Low-symmetry structures for the ions reproduced, also at T = 0, Neutral remains I_h	436	DFT
Au_{38}. Lowest structure amorphous	437	DFT, MD
Au_n; n = 32, 38, 44, 50, 56. The C_2 Au_{50} is hollow	125	PP DFT
Au_n; n = 32, 38, 44, 50 and 56. All can be cage or space-filled. Dipole moments and polarisabilities	149	DFT
Au_{34}^-. A C_s covered pyramid structure	137	DFT
Au_{50}. New, lowest-energy cage structure of D_{6d} symmetry	126	DFT
Au_n; n = 2–55. Linear and zigzag chains, flakes, 3D clusters	24	DFT
M_n; M = Cu, Au; n = 2–60	438	EAM MD
Au_n, n = 55, 147 under pressure, up to 10 GPa	26	CP DFT
$Au_{6,13,19,38,44,55,147}$. s-Orbital ferromagnetism	261	DFT
Au_n, n = 13–171. *fcc* fragments. Cuboctahedra frequently preferred	143	PAW DFT
Au_n, $n \leq 162$. For n = 162, an icosahedral structure studied	131	DFT
Heteroatomic clusters		
$AuPt_3$. Reaction with H_2	439	MP2, MC-SCF
$Au@Sn_{12}^-$. Icosahedral stannaspherene. PES	440	DFT
Au_nBO^-; n = 1–3	48	DFT
$AuAl_4^-$ found to be planar, C_{2v}	441	DFT
Au_nPt_2, n = 1–4.	442	DFT
Au_nPt_m, up to $Au_{12}Pt$, which is planar. +CO	329, 443	DFT

Table 6 (*continued*)

The Au/H chemical analogy in $Si_3Au_3^q$; $q = -1, 0, 1$	86	DFT
$[Au_3Ge_{18}]^{5-}$. Coupled Ge_3–Au_3–Ge_3 triangles	176	Exp. + DFT
$[Au_3Ge_{45}]^{9-}$. Au(I) coordinated to four Ge has almost isoenergetic planar and tetrahedral $[Au(Ge_4)_2]^{n-}$ coordinations	444	Exp. + DFT
M_nTl_n; M = Cu–Au; $n = 1, 2$	445	HF, MP2
$Na_nAu_n^-$; $n = 1$–3. $n = 2$ quasilinear + some D_{2h}, $n = 3$ 3D C_s bent-flake. Neutral Na_2Au_2 planar D_{2h}, Na_3Au_3 planar D_{3h}, Na_4Au_4 T_d	418	MP2, CCSD; PES
Cu_3Au_3 clusters. Planar cyclic D_{3h} ground state. Cu in, Au out. Magnetic, NMR, optical, vibrational properties	446	DFT
M_4A^-; M = Cu–Au; A = Li–K. Ring currents and PES studied	447	PP-CCSD
Au_iCu_{6-i}; $i = 0$–6. Lowest energy flat, D_{3h}-type. Largest binding energy at $i = 3$. D_{3h}, Au at corners	448	DFT
X_4Y_4 (X = Cu, Ag, Au, Ti); Y = C, Si). Often cubic	449	DFT
$B_7Au_2^q$; $q = -1, 0$. Planar C_{2v}. Photoelectron spectra	450	DFT
$B_xAu_x^{2-}$; $x = 5$–12. Structures similar to $B_xH_x^{2-}$	85	DFT
Au_6Pt. Lowest energy D_{6h}. O_2, CO adsorption	422	DFT
Au_yAg_x; $x + y = 7$	451	MD
M_nAl^q; M = Ag, Au; $n = 4$–7; $q = -1, 0$. Large gap for $n = 7$, large EA for Al_6Au	452	DFT
Au_mAg_n; $2 \leq m + n \leq 8$	453, 454	DFT
$Au_{n-1}Cu$, Au_n; $n = 2$–9. Au_4Cu C_{4v}, Au_5Cu C_{4v}	455	DFT
Au_nS; $n = 2$–10	430	DFT
Au_nS^+; $n = 1$–8: what will the sulfur do?	456	DFT
Pt_6Au. 38 conformations located. 3D $S = 2$ ground state	457	DFT
E–Au_n; $n = 1$–4, 10; E = Hg, E112. Models for adsorption energy of E on gold. E112 adsorbs more weakly than Hg	304	DFT
$Ag_mAu_n^+$; $m + n = 4$–6, reactions with CO	458	DFT
M_4Li_2; M = Cu–Au (D_{4h}). NICS and σ(Li) at the centre	459	DFT
M_4Li_4, M_6Li_2; M = Cu–Au (D_{4h}). NICS at the centre	460	DFT
Small-basis WAu_{12} as illustration of an I_h 18e system. The p-like component is mainly based on the ligands; the s- and d-like components bond to W	129	DFT
$Si@Au_{16}$, a 20e endohedral system. Binds O_2^-. Based on the hollow Au_{16}^{2-}	167	DFT
Later shown to be exohedral	168, 169	Exp., DFT
$M@Au_n$; $n = 8$–17, M = Na, K, Mg–Sr, Sc–Y, Zr, V–Ta, W, Mn, Re, Ru, Rh, Pd 18-electron systems investigated	165	DFT
C_5Au_{12}, aurated neopentane	184	DFT
$Zr@Au_{14}$ large gap, $Sc@Au_{14}^-$ large IP. The calculated $Sc@Au_{14}$ EA 4.13 eV	164	DFT
$Cu@Au_n^-$; $n = 16, 17$	166	DFT, exp
$[M_{13}@Au_{20}]^-$; M = Co, Mn. High total spins	170	DFT
$(CuAu)_n$, $n = 5$–22. GGA minima differ from Gupta ones. $n = 20$ icosahedral	461	DFT
Au–Cu, Au–Ni, Au–Co clusters. Up to 38 atoms. Compared to Ag	130	DFT
Cu_nAu_{38-n}, Cu_3Au_{22}. Au atoms prefer surface	462	MD
Ag_nAu_{38-n}. Ag atoms prefer surface. Gupta potential	463	MD
M_{55} Mackay icosahedral clusters, M coinage-metal mixture	464	MP

Clusters with ligands and/or endohedral atoms

M_n–Ph^-; M = Ag, Au; $n = 1$–3. Photoelectron spectra	465	DFT
$(Au_nO_m)^-$; $n = 2, 3$; $m = 1$–5. Reactions with CO	310	DFT
Au_3 rings with ligands	466	DFT
$(HS)Au_3$, SAu_4. C_{3v}.	274	DFT
Au_nBO^-; $n = 1$–3. PES explained	48	DFT
M_3L; M = Ag, Au; L = glycine, cysteine	467	DFT
Au_n–L; L = CO, NO; $n \leq 8$. Oscillations of NO stretch observed	335	DFT
(Au_nM_m)–CO; $m + n = 2, 3$; M = Cu, Ag, Pd, Pt. Nondissociative adsorption for 22 species	327	DFT
$[Ag_2Au_3(CCH)_6]^-$. Both metallophilicity and electrostatics count	468	DFT
Pyridine on small Au_mAg_n ($m + n = 1$–4) clusters	469	DFT
Au_n–SH_2; $n = 1$–4. Vibrations	470	DFT
Au_n^q–H_2, –SH_2; $n = 1$–8; $q = 0, +1$	471	DFT
Au_5M; M = Na, Mg, Al, Si, P, S. Planar Au_5Na, Au_5S ($S = \frac{1}{2}$) have high IP	472	DFT
MAu_6^q; M = Ti, V, Cr; $q = -1, 0$. D_{6h}. Magnetic	171	DFT
$[(Ph_3PAu)_6C]^{2+}$. Vibrational centre-ligand couplings	17	DFT
Au_6 anion with 0–3 carbonyls on the corners	473	DFT
$Au_{11}(SCH_3)_n$ go from 2D to 3D for $n \geq 1$	161	DFT
VAu_{12}^- as adsorbant for CO or O_2 molecules	162	DFT
C_5Au_{12}. Gold-plated diamondoid. Neutral, anion	184	DFT
Au_n–acetone; $n = 2,\ldots,13$. Also acetaldehyde, diethyl ketone	474	DFT
$[Au_m(NH_3)_n]^{0,\pm1}$. $m = 1, 3, 4, 20$; $n = 1$–3. Both Au–N bonds and N–H···Au hydrogen bonds occur	81	DFT
Pyridine/Au_{20}. Adsorption, optical excitation, SERS	252	TDDFT
Au_{24}^q + O_2; $q = 0, -1$. Tubular adsorbs stronger than amorphous	475	DFT
Au_{32}, I_h or C_1 + H_2, CO or O_2.	476	DFT
Au_{38} clusters with phosphine or thiolate ligands	180	DFT

Clusters on surfaces		
Au atom on pentacene molecule. A σ bond to central C most stable	477	DFT
Au_n (n = 1–7) on rutile TiO_2(110). The n = 1, 3 negative, 5, 7 positive and 2, 4, 6 almost neutral	478	DFT
Au_{13} on graphene sheets and flakes. CO, H chemisorption	479	DFT
M_n on graphene sheets, M = Ag, Au; n = 1, 2, 6, 13	225	DFT, dispersion model
Surfaces, surface models and heterogeneous catalysis		
M_4 on MgO(001); M = Cu–Au	428	DFT
Polyatomic Au–L systems		
MBX; M = Cu–Au; X = F–Br. Most stable radical for gold. Cp. known HBX	91	DFT
$(MX)_n$; M = Cu–Au; X = F–I; n = 5, 6. Structure changes from rings to 3D	56	DFT
$Au(H_2O)^+$ and isoelectronic systems. R/NR	480	PP or Dirac DFT
(Au^+)–L; L = H, C, CH, CH_2, CH_3. Bonding and D_0 measured and calculated	42	DFT, QCISD(T)
MER, M_3–EMe; E = S, Se; M = Cu–Au; R = C_1 to C_6. Chain-length effect small	481	DFT, MP2
$M(C_3H_6)^+$; M = Ag, Au. Binding energy at CBS limit	43	MP2, CCSD(T).
AuXeF, AuKrF, AuXeOH have covalent Au–Rg bonds	89	DFT
$Au(PPh_3)_2Cl$. 'Beyond T-shape'. Singlet and triplet states	400	DFT
Centred $Au(L)_n$ systems, $n > 1$		
AuX_2^-; X = Cl–I. SO effects on photodetachment spectra	482	CAS, CCSD(T)
$XAuY^-$; X, Y = Cl–I. SO effects on photodetachment spectra. Geometry	483	CAS, CCSD(T)
AuF_5, AuF_7. Former exists, latter not. The experimentally claimed AuF_7 attributed to AuF_5F_2	30, 32	DFT, CCSD(T)
$Au(OH)_2$. C_{2h}. IR spectra	484	DFT
$M(OH)_2$; M = Cu–Au. C_{2h}. IR spectra and experiment	485	DFT
$[Au(H_2O)_n]^+$; n = 1–10. First two strong	50	DFT
OAuCO, (OO)AuCO, (OC)Au(O_2CO). IR spectra	486	DFT
M_nPo; M = Cu–Au; n = 1, 2. Geometries	487	HF/MP2
$[Au(C_2H_4)_3]^+$. D_{3h} minimum, AuC_6 in same plane. This structure agrees with experiment in $[SbF_6]^-$ salt	488	DFT
(Imidazole)AuX, X = Cl, NH_3^+, OH_2^+. Favour C- over N-coordination on the imidazole.	51	DFT, MP2, MP4
$X(AuPH_3)_4^+$; X = N–Sb. X = P predicted to be T_d	67	HF, DFT, MP2, CC2
$Au(N_3)_4^-$. Bonding analyzed by ELF	53	DFT
Aurophilic dimer models		
Au_2O^-. Photodissociation to AuO^- + Au or Au^- + AuO studied experimentally. Long-lived excited state found	489	Exp
$[M_2Te]_n$; M = Cu–Au; n = 2, 3	490	MP2
$[AuL_2]_2^{2+}$ model, L = C(NHMe), repulsive as naked but attractive with counterions	69	MP2
Larger aurophilic systems		
$[Au(CO)Cl]_n$, n = 1–3. CO stretch blue-shift, Au–Au reproduced	64	TDDFT, MP2, CCSD(T)
$[AuS_2PPh(OCH_2CH{=}CH_2)]_2$. DFT *vs.* MP2	412	DFT, MP2
$[Au_3(MeN{=}COMe)_3]_n$; n = 1–4. DFT *vs.* MP2. Stack of triangles	411	DFT, MP2
Other metallophilic systems		
First Au(I)–Bi(III) interaction. $[Au(C_6F_5)_2][Bi(Me_2)(NR_3)_2]$-type models	76	HF, MP2, DFT.
Further complexes		
The first Rh(II)–Au(II) bond in $Rh^{II}Au^{II}(HN[PH_2]_2)_2(CNH)_2Cl_2^{2+}$	491	DFT
Group-11 M(III) complexes in N-confused (M–C bonded) porphyrins	416	DFT
Other, larger inorganic and organometallic systems		
$(MeSAu)_x$, x = 2–12	109	DFT
Benzenedithiolate on gold	344	DFT
Fumaramide on M(111); M = Ag, Au	492	DFT

Table 6 (*continued*)

Chemical reactions and solvation effects		
M_2, PdM; M = Cu–Au. Reactions with H_2	493	DFT
$(Au_nO_m)^-$; n = 2, 3; m = 1–5. Reactions with CO	310	DFT
$Ag_mAu_n^+$; $m + n$ = 4–6, reactions with CO	458	DFT
Aminocarbene $(CO)_5Cr{=}C(NR_2)CH_3 + H_3PAu^+$ has C→Cr bonding. Alternatives with thiocarbenes prefer S→Cr bonding	494	DFT
Model for propylene epoxidation using hydrogen peroxide. Au_3 model for the gold particle. Ti-based support	495	QM/MM

Structures and energies for gold clusters. For a summary over the structural data, see Table 7. Basically we now include data that are verified either by experiments or by CCSD(T)-level calculations. While the DFT structures often agree with experimental ionisation potentials or scattering cross-sections, the MP2 or small-basis CCSD(T) calculations can favour wrong structures. As an example, Olson and Gordon[114] went up to CCSD(T) level on Au_8. While MP2 strongly favoured non-planar structures, CCSD(T) with a large enough basis restored the planarity. The newest technology was used *viz*. the Peterson-Puzzarini basis[8] and the latest Stuttgart pseudopotential by Figgen *et al*.[9] For sufficiently large basis sets and CCSD(T), the planar D_{4h} structure emerges as the lowest-energy structure of Au_8. Core-valence correlation is not able to reverse this conclusion. Han[115] also found at CCSD(T) level Au_8 to be planar D_{4h}.

The search for the lowest-energy structures, or interesting alternatives to them, for Au_n species continues to attract interest. The role of SO effects in stabilizing the D_{3h} isomer of Au_3 was again demonstrated by Rusakov *et al*.[116], now at DFT level (cp. Table 7). For neutral species, Fa *et al*.[117] place the transition from planar (2D) species to three-dimensional (3D) ones in the interval $13 \leq n \leq 15$. The structures for $16 \leq n \leq 25$ were characterized as pyramid-based. In the particular cases of n = 24 and 26, tubular structures were found, all at DFT level. In a comparison with trapped-ion electron diffraction experiments and DFT calculations, for anions with n = 11–13, Johansson *et al*.[118] place the transition from 2D to 3D structures at n = 12.

Bulusu *et al*.[119] predict for n = 15 and 16 flat cages, for 17 and 18 more spherical, hollow cages, and for n = 19 the first structure of tetrahedral type. The possibility of $M@Au_{17}$ was evoked, where M is a monovalent metal.

Concerning Au_{20}, Kryachko and Remacle[120] remind the reader that its closed-shell character was already evident in a low measured EA by Taylor *et al*.[121] Kryachko and Remacle calculate possible structures for the five charge states from 2− to 2+. The second EA is still 0.43–0.53 eV.

Among the most intriguing recent predictions were those of a hollow icosahedral cage structure for Au_{32} at 0 K.[122,123] Experimental evidence for such a structure, with all 32 atoms on the surface, was found by Oila and Koskinen.[124] Their compound, however, had as many bridging thiolates as it had gold atoms on the surface. Thus it is quite remote from the free Au_{32}.

Wang *et al*.[125] theoretically verify this prediction for the hollow Au_{32} and find another hollow system which is an energy minimum, *i.e*. an Au_{50} of C_2 symmetry. It also is stabilized by spherical aromaticity and shows large NICS shifts and a large HOMO–LUMO gap. The surface layer of the cluster resembled the reorganized surface layer of helical multishell gold nanowires. Also recall the reorganization of the surface of bulk gold (ref. 1, ch. 4.7). Tian *et al*.[126] discovered theoretically a new, lowest-energy structure for Au_{50}: a hollow shell of D_{6d} symmetry. It is thought to be stabilized by the spherical aromaticity of the 50e electron count. Note that the 0 K total energy, not a finite-temperature free energy, was calculated.

A further hollow system is Au_{26}. Fa and Dong[127] predict it to have a lowest-energy D_{6d} structure which is a segment of a (6,0) single-wall nanotube (SWNT). The n = 27, 28 cases add atoms to that. The first hollow gold cages were experimentally discovered in the Wang group.[128] They were Au_n^- anions with n = 16–18. Note, that they then exactly or nearly fulfill the 18-electron rule.[129] Thus their stability may come from that nodal structure of the surface orbitals.

Ferrando *et al*.[130] found that, in addition to the earlier cases with n = 20, 32, the Au_n cluster with n = 18 and C_{2v} structure would have an enhanced stability.

The general question of planar (2D) and 3D structures, and relativistic effects promoting the 2D ones, was considered by Fernández *et al*.[131] With relativistic effects included and a GGA functional, 2D prevailed until n = 11 for neutral clusters. Cagelike magic Au_n structures were found, not only for the earlier n values of 32 and 50, but also of the icosahedral 162.

Concerning anions, a long-lived excited state was discovered in the planar Au_6^-.[132] It was assigned to an unpaired π^1 electron in the field of the neutral, triangular Au_6.

Xing *et al*.[133] combined DFT calculations and electron diffraction measurements to verify that Au_n^-, n = 11–24, go from planar to 3D for n = 12–14, cages for n = 16–17, tetrahedron for n = 20, and a tubular structure for n = 24. The tubular Au_{24}^- was confirmed by combined PES measurements and DFT calculations by Bulusu *et al*.[134] They also find that the tetrahedral structure type extends from n = 20 up to n = 23. Finally, Au_{25}^- is the first anion with an endohedral gold atom.

The structures in the size range Au_n^-; n = 15–24 were studied by Yoon *et al*.[135] by combining DFT calculations and PES experiments. For n = 15 and 16, flakes were predicted but 3D structures observed. For n = 17 and 18, probably a combination of cages and other structures was seen. The cases n = 19–21 were tetrahedron-based. The n = 22 and 23 were characterized as 'pita pockets'. Finally, n = 24 was a capped cylinder.

The Au_{32}^- anion was produced by Ji *et al*.[136] Its photoelectron spectrum suggests a low-symmetry solid structure. The

Table 7 Structures of free Au_n^q clusters. For further calculations, especially on neutral clusters, see the Parts I–II or Table 6

N	q	Method	Structure	Ref.
3	−1	CCSD(T)	Linear	496
3	−1	DFT, exp.	Linear	497
3	0	CCSD(T)	Bent, C_{2v}. No SO	496
3	0	CI, exp.	D_{3h}. SO included	498
3	1	CCSD(T)	D_{3h}	496
3	1	DFT, exp.	D_{3h}	499
4	−1	DFT, exp.	Y-shaped, C_{2v} + possibly rhombic D_{2h}	497, 500
4	0	DFT	D_{2h}	500
4	1	DFT, exp.	Rhombic D_{2h}	499
5	−1, 0	DFT, exp.	Planar 'W' or 'half-cake'	497, 500, 501
5	1	DFT, exp.	Planar 'X' D_{2h}	499
6	−2	DFT	Octahedral, O_h	112
6	−1	DFT, exp.	Planar D_{3h}, $S = \frac{3}{2}$	497, 500
6	0	PP-CCSD(T)	Planar D_{3h}	115
6	1	DFT, exp.	Planar, quasi-D_{3h}	499
7	−1	DFT, exp.	Planar C_{2v}. Square with 3 bridges	118,497
7	−1	DFT, exp.	Coexisting planar C_s and C_{2v}	500
7	0	DFT	Planar C_s	500, 502–504
7	1	DFT, exp.	Planar D_{6h}	499
8	−1	DFT, exp.	2D D_{4h} star	497
8	−1	DFT, exp.	2D coexisting D_{4h} and C_{2v}	500
8	0	PP-CCSD(T)	2D D_{4h} star	114, 115
8	1	DFT, exp.	3D C_s	499
8	1	PP-CCSD(T)	3D C_{2v}	114
9	−1	DFT, exp.	Planar C_{2v}	497, 500
9	1	DFT, exp	3D C_{2v} capped pyramid	499
10	−1	DFT, exp.	Two planar structures, D_{3h} and D_{2h} possible	497, 500
10	1	DFT, exp.	3D distorted T_d pyramid	499
10	2	DFT	D_{4d}	112
11	−1	DFT, exp.	Planar C_s and C_{2v}	118, 497, 500
11, 12	1	DFT, exp.	3D structures	499
12–14	−1	DFT, exp.	Transition region from 2D to 3D	118, 133, 497, 500
13	−1	DFT, exp.	C_{3v} 3D	118
13–15	0	DFT	Transition region from 2D to 3D	117
13	1	DFT, exp.	3D C_{2v} fragment of solid	499
14	−4	DFT	D_{2d}	112
15, 16	0	DFT	Flat 3D cages	119
15, 16	−1	DFT, exp.	3D observed	128,135
16, 17	−1	DFT, exp.	Hollow cages	133
16–18	−1	DFT, exp.	Hollow cages	128
16–23, 25	0	DFT	Pyramid-based 3D	117
17, 18	0	DFT	Hollow 3D cages	119
19	0	DFT	Pyramid-based	119, 153
19–21	−1	DFT, exp.	Tetrahedron-based	135
20	−1, 0	DFT, exp.	Tetrahedral T_d	505
21–23	−1	DFT, exp.	Pyramid-based structures	134
22, 23	−1	DFT, exp.	'Pita pockets'	135
24, 26	0	DFT	Tubular. R/NR Au_{24}	117
24	−1	DFT, exp.	Tubular	133–135
25	−1	DFT, exp.	First anion with an endohedral Au	134
26	0	DFT	SWNT D_{6d}	127
27, 28	0	DFT	Derivatives of $n = 26$	127
28	0	DFT	Amorphous	182
32	0	DFT (0 K)	I_h single-wall nanosphere	122, 123, 125, 136
	−1	DFT, exp.	Low-symm., 3-atom core, 29-atom shell	136
34	−1	DFT, exp.	Covered-pyramid C_s	137
34	−1	DFT, exp.	A fluxional core-shell cluster, $Au_4@Au_{30}^-$	506
38	0	DFT, MD	Amorphous	437
50	0	DFT	Hollow C_2	125
		DFT	Hollow D_{6d}	126
55	−1	DFT, exp.	Low-symm., unlike Ag_{55}	140
55	0	MD, DFT	Amorphous	182, 507
72	0	DFT	Chiral, symmetry I single-wall nanosphere	141

reasons were traced to the entropy contribution to the free energy. They yield a lower energy around room temperature.

The Au_{34}^- was studied by DFT calculations and experimentally by PES and by gas-phase electron diffraction by Lechtken *et al.*[137] The mass-selected ions were held during the diffraction measurement in a radiofrequency ion trap of Paul type. As predicted earlier from molecular dynamics calculations, a covered-pyramid C_s structure was found. Such

low-symmetry structures lack an S_n axis and are hence perforce chiral. For a comment, see ref. 138.

The dissociation energies of Au_n^+ clusters for n = 7–27 were measured by Hansen *et al.*[139]

Häkkinen and Moseler[140] verified that the symmetry-breaking from icosahedral Ag_{55}^- to various low-symmetry isomers for Au_{55}^- can be attributed to relativistic effects.

The spherically aromatic Au_n clusters can be sought at $n = 2(N+1)^2$. the case n = 32 corresponding to N = 3. Karttunen *et al.*[141] found the case n = 72 (N = 5) to be energetically more than 20 kJ mol^{-1} per atom below the known Au_{20} for both H and G. The symmetry was the chiral, icosahedral I, possibly unprecedented for a molecule. For illustration, see the Graphical Abstract.

As to the morphologies of very big clusters, Grochola *et al.*[142] find from MD simulations that lower temperatures and early coalescence favour pancake decahedron, D_h shapes while ideal, atom-by-atom growth conditions produce icosahedral, I_h particles. Barnard and Curtiss[143] focussed on *fcc* nanocrystals. Below 1 nm, the cuboctahedron is frequently preferred.

Curley *et al.*[144] considered the alternative, cuboctahedra, inodecahedral, icosahedral and puckered icosahedral structures for a four-layer Au_{309} cluster. The last one was lowest but the differences were small, below 0.01 eV atom^{-1}. The neighbours with 309 ± 15 atoms also gave highly faceted structures. The Gupta potential and the authors' own 'genetic' search algorithm were used.

Algorithms for global structure optimization are an issue. Dong and Springborg[145,146] introduced a genetic algorithm, supposedly able to find minima that are otherwise difficult to discover. The electronic method was a tight-binding DFT one. A broad study of Au_n; n = 2–58 was carried out, and a C_1 structure with no symmetry found for most species. This is in clear contradiction to both experiment and all other calculations for Au_{20}. Similarly, for neutral Au_{32} at 0 K all other workers obtain a lowest-energy I_h icosahedral shell structure.[122,123,125,136] A third case of deviations are the tubular structures around n = 24, 26.[117] Au_{33} was particularly stable. Future will show whether the differences are due to too approximate quantum chemistry of Dong and Springborg, or due to the inability of other theoreticians and Nature to find the truly lowest-energy minima.

For an early, general discussion on disordered *vs.* ordered cluster structures, including gold, see Soler *et al.*[147,148] A specific driving force is the tendency of the low-coordinated, surface atoms to contract their bonds.

Properties of clusters. Wang *et al.*[149] calculated the dipole moments and dipole polarizabilities of gold clusters Au_n with n = 32, 38, 44, 50 and 56. All of these had both cage and space-filling isomers. The dipole moments were larger for the latter. The polarisabilities were larger for the cages, and roughly correlated with the cluster volume.

Popescu *et al.*[150] studied experimentally the mean inner Coulomb potential in gold nanoparticles through a phase-shift in transmission electron microscopy. The increased surface tension in smaller particles was found to contribute.

Melting of clusters. Molecular dynamics simulations yielded a broad transition from solid-like to liquid-like clusters for Au_n, n = 7 and 13 but an abrupt transition at 1200 K for the case of n = 20.[151] This value may be too high due to technical limitations, see ref. 153.

For anions in the size range n = 11–14, Koskinen *et al.*[152] found both normal three-dimensional (3D) droplets and two-dimensional (2D) liquid systems at about 750 K. No such *flat liquids*, in a 3D space, are previously known to the authors. They could be seen as a further manifestation of the 6s–5d(zz) hybridization, so common for gold.

The comparison between Au_n, n = 19,20 by Krishnamurty *et al.*[153] revealed an interesting dynamical difference: Both are 'tetrahedral', Au_{19} missing one corner atom. While the Au_{20} has a sharp melting point around 770 K, Au_{19} has a continuous melting transition between 650 and 1000 K.

Inversely, the crystallization of a large, Au_{10179} cluster was treated at MD level by Chui *et al.*[154] The crystallization was found to start at the surface, not in the interior.

Similarly, concerning the freezing of an Au_{456} nanoparticle, Mendez-Villuendas and Bowles[155] also found that it starts at the vapour-surface interface at all temperatures, in agreement with earlier work.

The melting of gold clusters in excited electronic states during a photochemical process was discussed by Stanzel *et al.*[156]

Aromaticity. The aromaticity-related aspects of certain gold clusters, notably studied by the theoretical device of 'Nucleus-Independent Chemical Shifts (NICS)' were included in the reviews of Chen and King.[157,158]

Doped or covered clusters. Experimentally, Kornberg's group[159] determined the crystal structure for an [Au_{102}(MBA)$_{44}$] cluster (MBA = *p*-mercaptobenzoate). It was found to consist of a truncated decahedral Au_{79} inner cluster, covered by further, coordinated gold atoms. For a commentary, see Whetten and Price.[160] The 58-electron count (102-44) is reached through two (sp) shells plus single (dfg) shells. The exact roles of covalent bonding and aurophilic attractions between the 5d cores require further study.

While the neutral Au_{11} was calculated to be planar, Spivey *et al.*[161] found that already a single -SCH_3 substituent made them 3D. For further data on thiolate-covered gold surfaces and clusters, see Table 6.

In the WAu_{12} valence isoelectronic family, five members are now known. The potential of the $V@Au_{12}^-$ anion as catalyst for CO oxidation was explored by Graciani *et al.*[162] Sun *et al.*[163] started from the WAu_{12} core and studied, what happens when more gold is added. For instance WAu_{20} and WAu_{32} become strongly asymmetric, with the WAu_{12} structure side-on bonded to a remaining gold cluster. The latter part was more hydrophilic than the former. A dimer, W_2Au_{21}, and a closed W_9Au_{81} nanoring were also considered.

Gao *et al.*[164] had the idea of replacing the central, Group 6 atom by a Group 4 atom and adding at the same time two gold atoms. These species, such as $Zr@Au_{14}$ (D_{2d}) have a large calculated HOMO–LUMO gap of 2.23 eV. The valence isoelectronic anion $Sc@Au_{14}^-$ corresponds to an electron affinity of about 4 eV. Note that they are still 18-electron systems.[129]

The same group[165] mapped further systems of type $M@Au_n$; n = 8–17; M = Pd, ···Na–K. With the exception

Table 8 Studies of alkali thiolates on an Au(111) surface

Authors	Year	Method	Comments
Perebeinos and Newton[345]	2005	FP-LAPW	Periodic Ph–S– lattice on Au(111). '2PPS' spectra
Miao and Seminario[508]	2007	VASP	Oligophenylene ethynylene thiolates on Au(111). Nontop below top. Large spin imbalance found for 'top'
Schaposchnikow *et al.*[390]	2007	MD	Selectivity of adsorption of different alkyl thiols on Au(111) and nanoparticles
Wang and Selloni[509]	2007	DFT	Influence of end groups X and surface structure on current–voltage characteristics of $-SC_6H_{12}-X$ monolayers on Au(111)
Wang *et al.*[510]	2007	DFT	Formation of MeS–monolayers on Au(111) from MeSSMe. $Au(SMe)_2$ adatom structures found

of Pd in $PdAu_8$, the heteroatoms stayed inside a gold sheath. Thus these other systems can still be regarded as 18-electron systems, despite of the often low symmetry. See for earlier examples the Table 8 of Part I.[1]

The clusters $Cu@Au_n^-$; n = 16, 17 were experimentally produced by Wang *et al.*[166] They were endohedral and DFT calculations, coupled with PES, suggested little distortion of the parent Au_n cage, which had an autonomous stability.

Concerning $Si@Au_{16}$, Walter and Häkkinen.[167] first predicted it to be a 20e endohedral system with two occupied a_1 or s-like shells. This structure was based on the hollow Au_{16}^{2-}. It also was predicted to bind oxygen molecules to the superoxide species O_2^-. Later experimental and theoretical work, however, showed that the Si atom prefers to bind outside, not inside the gold cage.[168,169] An Si atom is not happy inside this nano gold system, although solid Au–Si phases are known.

A large magnetic moment was calculated to exist in $[M_{13}@Au_{20}]^-$; M = Co, Mn by Wang *et al.*[170] The icosahedral Au_{20} cage is large enough to house the M_{13} dodecahedron. For M = Co, Mn the total spins S_z were 20 and 44 μ_B, respectively. For the naked M_{13} core, values of 30 and 2, respectively, were obtained. Similarly, the magnetic moments of the central atom survived in the planar D_{6h} clusters MAu_6^-, M = Ti, V, Cr,[171] characterized by PES and by DFT calculations.

Ferrando *et al.*[130] studied mixed Au–Cu, Au–Ni and Au–Co nanoclusters with up to 38 atoms. Of them, Au–Cu forms several bulk phases and this is reflected in the formation of clusters. Au and Ag were juxtaposed. The search procedures for the optimum structures were reviewed by Ferrando *et al.*[172]

Cheng *et al.*[173] calculated the optimum structures of 55-atom decahedral Cu–Au clusters. The segregated structure had Au on surface and at centre, and Cu in between. Smaller model clusters were also considered. The 55-atom Ag–Au 'nanoalloys' were studied at MD level by Chen *et al.*[174] Minimum-energy structures were predicted for the entire range n(Au) = 0–55. The calculated melting or glass-transition temperatures and the phase boundary between icosahedral Au-poor and amorphous Au-rich clusters were obtained. At the level of Monte Carlo simulations, Cheng *et al.*[175] found both Cu_1Au_{54} and $Cu_{12}Au_{43}$ to be icosahedral. The latter had a triple-shell, $Au@Cu_{12}@Au_{42}$ structure. A study of the melting revealed that even the single copper atom at the centre could raise the calculated melting point from 380 K for Au_{55} to 530 K.

A novel bonding motive was experimentally discovered by Spiekermann *et al.*[176]: an $[Au_3Ge_{18}]^{5-}$ in crystals. It could actually be seen as two $[Ge_9]^{4-}$ anions, coupled by three gold atoms in a nominal Au^+ oxidation state, as stated. Taking the covalent radii of Au and Ge as 134 and 122 pm, respectively, the predicted Au–Ge is 256 pm, not very far from the experimental average of 245 pm. The Au–Au distances range from 290 to 310 pm and may be a little inside the aurophilic minimum distance. This system is the first binary Au–Ge cluster. The calculated HOMO–LUMO gap was 2.60 eV.

Kryachko *et al.*[83] studied the hydrogen bonding between planar gold clusters and up to four HF molecules. Kryachko and Remacle[82] studied the interaction of DNA bases and small neutral gold clusters. Special attention was attached to 'nonconventional' N–H···Au hydrogen bonds, involving a doughnut hybrid on gold. Kumar *et al.*[177] also considered the interaction of the AT or GC base pairs with Au_n clusters, n = 4, 8. Neutral clusters and anions led to different structures.

Batista *et al.*[178] considered covering the C_{60} fullerene by n = 32 to 92 gold atoms. A moderate binding energy of 0.05 eV per gold atom was found for n = 92. Thiolates were added to some of the systems.

Adsorption of molecular N_2 on planar Au_n; n = 1–6, was found to occur in the cases n = 2–4. Anionic clusters did not adsorb. The resulting N_2–gold vibrations were around 200–300 cm^{-1}.[179]

Au_{38} clusters with phosphine or thiolate ligands were calculated to develop molecular gold-thiolate rings on their surface.[180] Various, open-structured, phosphine-stabilized gold–arsenic clusters were synthesized and theoretically modelled by Sevillano *et al.*[181] For earlier work on $Au_{28}(SMe)_{16}$ and $Au_{38}(SMe)_{24}$, including their chirality aspects, recall Garzón *et al.*[182] The corresponding optical activity had earlier been seen in glutathione-passsivated gold nanoclusters in the 20–40 gold atom range.

An MD study of Au–Ag nanoparticle formation by Negreiros *et al.*[183] produced silver segregation to the surface. Up to 3456 atoms were used. Apart from different M–M′ interaction strengths, another driving force was the stability of (111) faces.

Gold-covered clusters. Naumkin[184] considered the case of C_5Au_{12}, a neopentane where all hydrogen atoms would be substituted by gold atoms. Although the Au atoms are much larger than the H atoms (and the C atoms), and the system is expected to be very 'floppy', the idea is interesting.

Feeling the chirality. As already mentioned, the gold clusters whose symmetry groups lack an S_n axis are chiral. López-Lozano *et al.*[185] calculated the energy differences felt by

cysteine, adsorbed on the edges of a chiral Au_{55} cluster. The final results were of the order of 0.1 eV, compared with a total chemisorption energy of 2–5 eV. Circular dichroism spectra of both bare and thiol-passivated gold nanoclusters were calculated by Roman *et al.*[186]

Pure wires. Zhou and Gao[187] studied by molecular dynamics the solidification of liquid gold nanowires of about 1.84 nm diameter. The cooling rate was found to have an effect on the final structure. With decreasing cooling rates, they obtained first amorphous, then helical multishelled structures and finally crystalline, fcc ones.

Park and Zimmerman[188] simulated the inelasticity and failure in gold nanowires at room temperature. Long helical wires of 2.588 nm diameter were frequently obtained.

MD simulations for multishell helical nanowires were reported by Lin *et al.*[189] Their Young modulus increased with decreasing radius. The elongation and compression modes had different moduli.

The changes of the inner crystal structure and the phenomenon of shape memory in nanowires were discussed at MD level by Park *et al.*[190]

Bond-length alternation in hypothetical finite linear Au_n nanowires (n = 4–9) was studied by Seal and Chakrabarti.[191]

Suspended wires of gold continue to attract interest. Ayuela *et al.*[192] considered the structural effect of extra electric charge, drawn from the electrodes. Au_n with n = 2–4. Only a small effect on the equilibrium distance was found.

For wires of 2–5 gold atoms, Skorodumova *et al.*[193] find that longer chains are weaker. The odd–even alternation was discussed in terms of the band structure of a periodic model.

Yanson *et al.*[194] observed conductance oscillations in the histograms of a large number of gold nanowire samples at both 4.2 K and room temperature.

Doped wires. Both pure wires of Au and Pt and their bimetallic linear, zigzag, double zigzag and tetragonal wires were investigated by Asaduzzaman and Springborg.[195] The structures were optimized and all chains were shown to be metallic.

A particular question is the nature and stability of the apparently monoatomic gold chains, usually stretched between electrodes. Novaes *et al.*[196] added oxygen clamps. This impurity would strengthen the entire Au–Au–O–Au chain, thus making it possible to add further Au atoms. The impurities H, C, O, N, B, S, CH, CH_2 and H_2 were also considered.[197] They always led to local strengthening over a pure Au–Au bond. The best candidate to explain the observations was atomic H. Hobi *et al.*[198] return to the question of H-atom impurity effects on the stability of monatomic gold chains. With improved technical assumptions an Au–H–Au distance of 3.5(1) Å was calculated, in agreement with experiment.

Anglada *et al.*[199] considered the heteroatoms H, C, O, S, added to the gold wire during growth of the monoatomic gold wire under stretch. Single hydrogen atoms always evaporated, carbon and oxygen had a low probability of staying and sulphur almost always remained as a bridging atom in the monoatomic chain. The starting point was an amorphous column of frozen liquid gold. The calculated stretching for at rupture was close to the experimental one of 1.5 nN, and the Au–Au distance 280(20) pm.

Infinite nanotubes of gold. In a comparison of the three coinage metals, both Ag and Au produced surprisingly stable multishell nanotubes for certain filled shells; the experiments could be extended to room temperature.[200]

The structures of single-walled (5,3) gold nanotubes were calculated by Yang and Dong.[201] A longer version of the theoretical study of gold SWNTs by Senger *et al.*[202] appeared. A discussion of the electronic transport was included.

Zhou and Dong[203] calculated the phonon dispersion relations for seven different single-wall gold nanotubes (SWGT). The calculated frequency of the Raman breathing mode (RBM) (in cm^{-1}) increased with decreasing diameter, d (in Å), as $\omega_{RBM} = 338.8/d + 16.2$.

The hypothetical icosahedral Au_{32} cluster was polymerized to an infinite nanotube by Tielens and Andrés.[204] The calculated energy was comparable with that of the experimentally known (5,3) nanotube. The predicted tube was conducting, rather than insulating.

Gold atoms, clusters or chains on other surfaces. Barcaro *et al.*[205] studied small coinage-metal clusters M_n (n = 1–3) on MgO(100) surfaces. The formation of metal 'islands' was also observed.

Walter *et al.*[206] wanted to explain two experimental observations. Firstly, gold evaporated on a MgO surface formed small islands of 8–20 atoms. Secondly, a scanning tunneling microscope showed pictures, corresponding to the electronic states of the entire cluster, not pictures of individual atoms, *i.e.* quantum-dot behaviour. The picture had the symmetry of these quantum states rather than the symmetry of the cluster.

Ferullo *et al.*[207] studied small coinage-metal clusters M_n (n = 1–3) on reduced SiO_2 surfaces at a neutral $\equiv$Si–O$^\bullet$ site. Lim *et al.*[208] placed Au or Au_2 on a surface model for amorphous silica, modelling in turn MCM-41 or eddingtonite.

Molina and Alonso[209] considered the gold clusters Au_n, n = 4–10 and their interactions with TiO_2 or MgO surfaces, with or without defects. The molecular reactivity with the free or supported gold cluster was studied using a hydrogen atom as test particle. 'Upright' cluster orientations were preferred in most cases.

Locatelli *et al.*[210] pointed out that on a perfect TiO_2(110) surface, Au atoms are very weakly bound and consequently form 3D clusters, even at submonolayer coverage. Stronger bonding occurs at oxygen vacancies. When these form linear rows, so do the adsorbed gold atoms. The experimental Au–Au distance was 295 pm. A theoretical model suggested a mainly covalent interaction between the Au and the substrate.

Pillay and Hwang[211] studied M_n clusters (M = Cu–Au; n = 2–4) on rutile TiO_2(110). For M = Au only the vicinity of an oxygen vacancy was considered. Moreover the surface was reduced by removing the bridging oxygen atoms. For the lowest-energy dimer the Au–Au distance was calculated to be 5 pm shorter than for gas-phase Au_2. For the trimer, a chain structure was preferred, and for the tetramer, a 'Y'.

Okazaki *et al.*[212] calculated the inner potentials for electrons in TiO_2-supported gold nanoparticles, in order to simulate

scanning tunneling microscopic studies. The mean potential rises above the bulk one for particle sizes below 5 nm. Both stoichiometric, Ti-rich and O-rich TiO_2(110) surfaces were included.

Au_n clusters (n = 2, 4) on TiC(001) were found to bond to the carbon atoms by Rodriguez *et al.*[213] M atoms (M = Cu–Au) on ZrO_2(111) were found to prefer a Zr–O bridging site.[214]

In a beginning series on Au_n on rutile TiO_2, Chrétien and Metiu[215] studied the case n = 1–7 on a stoichiometric (110) surface. Structural differences from the gas-phase clusters occur; for instance Au_7 is 3D instead of 2D. The main chemical interaction occurs between the cluster HOMO and the surface oxygens. Between adsorbed Au_1 and Au_n with n odd, a through-support interaction arises.

If species, like –OH, alkali metals Na–Cs or gold clusters Au_n (n = 3, 5, 7) were preaadsorbed on the TiO_2(110) surface, they were found to donate electrons to the conduction band and to influence that way the subsequent adsorption of Au_1 or O_2, both of them Lewis acids, on the surface.[216]

Neyman *et al.*[217] studied M_4 (M = Cu–Au) clusters interacting with oxygen vacancies on an MgO(001) surface. The vacancies were neutral or charged. For the planar tetramer, one M atom is bound to the vacancy and another to a nearby O atom. The core-level IP's were calculated and mentioned as fingerprints for this adsorption situation. The calculation was improved by embedding the treated area to the solid.

The optical absorption of magnesia-supported gold clusters Au_n:MgO; n = 1, 2, 4, 8 was calculated by Walter and Häkkinen.[218]

Ricci *et al.*[219] considered the bonding trends and dimensionality crossover of gold clusters Au_n; n = 8, 16, 20 on MgO(100). A supporting metal-layer below it promoted a transition to 2D gold structures, notably for Au_{20}. For a later discussion, see Landman *et al.*[220] In a later study of Au_n on MgO(100) on Mo, Frondelius *et al.*[221] found that all the gold clusters were close to mononegative, and that the structures of these adsorbed flat anions were close to their gas-phase counterparts.

Del Vitto *et al.*[222] provided both DFT calculations and measurements for the optical properties of Au atoms or Au_2 molecules, adsorbed on amorphous silica. The trapping centres could be both silicon dangling bonds [$\equiv$Si$^\bullet$], nonbridging oxygen [$\equiv$Si–O$^\bullet$] or silanolate groups [$\equiv$Si–O$^-$]. The first of these makes particularly strong bonds to Au.

Cruz Hernández *et al.*[223] compared the bonding of single coinage metal atoms on α-Al_2O_3(0001). While Cu and Ag bonded to a three-fold oxygen site, Au preferred the top of a single oxygen atom. As a technical remark, in such metal-support interactions, the correction for the basis-set superposition error (BSSE) was found to be important. The most important bonding contribution for gold was the polarisation of the Au atom.

Akola and Häkkinen[224] studied gold adatoms or Au_6 clusters on defects of graphite (0001) surfaces. The defects considerably increase the adsorption energy.

M_n clusters on graphene sheets, M = Ag, Au; n = 1, 2, 6, 13, were studied by Jalkanen *et al.*[225] by combining DFT calculations with a classical dispersion model, based on atomic polarizabilities. The latter contribution was found to be significant. The adsorbed Au_6 preferred to be 3D although the free Au_6 is 2D (D_{3h}). This raises the question, would gold wet graphite?

The optical properties of M, M_2 (M = Cu–Au) on regular sites or on oxygen vacancies on MgO(001) were calculated by Bosko *et al.*[226]

Grids of clusters. Batista *et al.*[227] consider the electron states in a 2D lattice of Au_{38} nanoclusters, capped by methylthiols and possibly functionalized by dithiolated aromatic groups. Even under 2D compression the systems remain insulating.

A bi-icosahedral, vertex-sharing chain cluster $[Au_{25}(PH_3)_{10}(SCH_3)_5Cl_2]^{2+}$ was studied by Nobusada and Iwasa.[228] The HOMO–LUMO gap for this charge-state is over 2 eV. This was rationalized by a Mingos electron count $8n_p$, where n_p is the number of polyhedrons. That gives 16e for this dimer. As discussed in ref. 1, p. 4435, one actually has to include the 5d shell of the central atom in the electron count, bringing one back to the 18-electron rule (see ref. 129) for it. A corresponding tri-icosahedral Au_{37} covered cluster was also considered. Such polyicosahedral clusters had already been synthesized by Teo (see ref. 1, p. 4436).

Gold layers on other metals. Shikin *et al.*[229] studied Ag and Au monolayers on W(110) and Mo(110). The spin–orbit effects of the W substrate caused a splitting of the surface monolayer.

Colours of nanoparticles. The optical properties of coinage-metal nanoclusters in the size range 1.4–7 nm were measured and simulated as function of particle size by Cottancin *et al.*[230] As the size decreases, the surface-plasmon resonance shows a small blue-shift for silver, as contrasted to a stronger blue-shift and damping for gold. For copper the peak vanishes entirely. The theoretical simulations used either Mie theory or a 'semi-quantal' TDDFT model (DFT = LDA) where the dynamical screening from the d electrons was accounted for through its contribution to the dielectric constant. Hao *et al.*[231] modelled the plasmon resonances of a tetrahedral gold nanostar through hybridization of the core and the tip plasmons.

See also Table 4.

I: Solids, liquids and surfaces

For a summary of solid-state calculations, see Table 9.

Pure gold can be heated to temperatures of tens of thousands of K by laser pulses. Mazevet *et al.*[232] studied the optical properties, electrical conductivity and structure of the system. The initial fcc structure was maintained for several picoseconds, even under such extreme conditions. Ping *et al.*[233] measured the dielectric function in the 450–800 nm area for gold, heated by a laser pulse to 10^6–10^7 J kg^{-1}. Shifts and enhancements of the transitions from the 5d band were observed. Although the electrons are heated rapidly, the nuclei are not yet displaced in the femtosecond scale.

As to high-pressure studies, Dubrovinsky *et al.*[234] predicted a transition to an *hcp* structure around 240 GPa. No such transitions are predicted for Cu or Ag and this was related to the larger d $\rightarrow$ sp gap. Above 250 GPa gold has more complicated stacking structures of close-packed layers.

Table 9 Calculations on solids. For aurides, see Table 5

Authors	Year	Method	System and comments
Filippetti and Fiorentini[511]	2005	PAW	Structures of M_2O; M = Cu–Au
Hou *et al.*[10]	2005	PP DFT	Monatomic Au chain. Band structure, bond length
Hsu *et al.*[512]	2005	FLAPW	AuM_2; M = Al–In. XANES spectra interpreted
Li and Corbett[513]	2005	LMTO	Bonding in Na_3MIn_2; M = Ag, Au
Reichert *et al.*[514]	2005	GGA	Au_3Ni. Order *vs.* phase separation
Yu and Zhang[237]	2005	APW+lo	AuN_2. New nitride predicted
Zhang and Alavi[515]	2005		Superabundant vacancies in hypothetical *fcc* AuH
Gegner *et al.*[516]	2006	LDA, LDA+U	RAuMg and RAgMg (R = Eu, Gd, Yb). XPS interpreted
Lange *et al.*[517]	2006	TB-LMTO-ASA	AuSn, $AuNiSn_2$. Mössbauer and bonding
McGuire *et al.*[518]	2006	EHT	New compound AuTlSb predicted to be metallic, like $AuSb_2$
Miyazaki and Kino[519]	2006		(BEDT-TTF)$AuCl_2$. Pressure effects up to 24 GPa
Semalty[520]	2006		Dilute, $Au_{0.96}Cd_{0.04}$ alloy. Specific heat, density of states
Ugur and Sovalp[521]	2006		AuE_2; E = Ga, In. Structure, electronic, dynamical properties
Winkelmann *et al.*[255]	2006		$CeCu_{6-x}Au_x$. Cu NMR, NQR properties interpreted
Dai and Corbett[522]	2007	EHTB	AAu_2In_2; A = Sr, Ba. Metallic. A inside Au_6In_6 hexagonal prism
Dal Corso[523]	2007	DFPT	Au metal. SO included, small. Lattice dynamics from PT
Hodak *et al.*[524]	2007	Grid DFT	Au, as test for a real-space grid-based method
Dubrovinsky *et al.*[234]	2007	Exp., calc.	Au exhibits an *fcc* to *hcp* transition around 240 GPa
Lee and Hwang[525]	2007	DFT	Amorphous Au–Si alloys
Lin and Corbett[526]	2007	Exp., LMTO	$Ca_4Au_{10}In_3$. Au–Au, Au–In bonding
Song *et al.*[527]	2007	MD	Point defects in Au_3Cu ordered alloy
Shi *et al.*[528]	2007	DFT-GGA/VASP	Au_2O_3, Au_2O. Bonding, heat of formation discussed
Kurzydłowski and Grochala[529]	2008	DFT	AuF stable above 22.6 GPa wrt AuF_3 + Au

In a general discussion on high-pressure phases, Grochala *et al.*[235] mention without further proof the interesting possibility of a gold(I) auride phase, $(Au^+)(Au^-)$.

An analytic model for the optical properties of gold was presented by Etchegoin *et al.*[236] It combines a high-frequency limit dielectric constant, a Lorentzian for the plasma oscillation and two terms for interband transitions.

Alloys and compounds. The so far experimentally unknown gold nitride AuN_2 was calculated to have the fluorite structure. The nitrogen atoms occupy all tetrahedral holes in the *fcc* structure of the metal. The relative energy of this compound was not given.[237]

Predictions for several ordered Au–Pd alloys were made by both Barabash *et al.*[238] and by Sluiter *et al.*[239]

The structures of the eutectic alloys of Au with Si and Ge were simulated by Takeda *et al.*[240] They occur at 636 K, 19 at.% Si and 629 K, 28 at.% Ge, respectively. Substitutional structures were found.

Surface reconstruction. Adatoms. Feng *et al.*[241] studied the reconstruction of an Au(100) surface as function of the surface charge. For neutral surfaces a hexagonal reconstruction was found. For an increasing positive charge, the square lattice becomes the lower state. This is calculated to happen at achievable electrochemical potentials.

Surface states. Silkin *et al.*[242] calculated the dynamical response of M(111) surfaces (M = Cu–Au). The partially occupied surface-state band yielded acoustic surface plasmons with linear dispersion at small wave vectors. These plasmon states were calculated to exist from 0 to 0.4 eV.

Walls and Heller[243] studied the Au(111) surface states in presence of an imposed local potential from additional adatoms, a 'quantum corral'. Then the surface-induced SO effects cause new states in the DOS and new spatial interference patterns.

Gold-atom impurities in or on other solids. Feng *et al.*[244] considered M/Al_2O_3 interfaces, M = Ag, Au. At high Al activity or low O_2 pressure gold prefers Al_2 termination. Ag prefers O-termination. The Al activity, a_{Al}, is connected to the chemical potential *via* $\Delta\mu_{Al} = kT \ln a_{Al} + \Delta_{Al}{}^0(T)$. The latter term makes the temperature correction from 0 to T K.

Karttunen and Pakkanen[245] presented a cluster-model study of Au^+ adsorption on Au(111).

Kyriakou *et al.*[246] obtained both experimental and theoretical data for gold atom chains on Cu(110). The packing density of the chains was limited by the strain in the copper, not by interchain interactions.

The adsorption of Pd, Rh, Ir and Pt on Au(100) and Au(111) was studied by Gotsis *et al.*[247] The hollow sites are favoured over on-top ones.

J: Optical properties and photochemistry

For high-temperature laser experiments on bulk gold, see the previous chapter IV. H.

The colour of gold and related questions. Romaniello and de Boeij[248] developed a two-component time-dependent current-density functional theory. SO effects were now included and gave new, experimentally observed features for Au.

Systems with metallophilic attractions. For calculations on absorption and emission spectra of metallophilic systems, see Table 4. The available data on luminescence of gold–heterometal complexes were reviewed by Fernández *et al.*[249]

Clusters. For a review on the experimental optical properties of nanoclusters, see Hodes.[250] The theories for the surface plasmon resonances of both single and coupled gold nanoparticles were comprehensively reviewed by Ghosh and Pal.[251]

Aikens and Schatz[252] chose the tetrahedral Au_{20} as a surface model for surface-enhanced Raman scattering (SERS), using pyridine as a test adsorbant. For the pure cluster, the TDDFT spectrum starts with an intraband (sp–sp) peak at 2.89 eV

while the higher bands at 3.94 and 4.70 eV have mixed intra- and interband (sp-d) character. The SERS enhancement factors for vertex and surface adsorption were in the range of 10^3–10^4 and 10^2–10^3, respectively, and much smaller than those of up to 10^5 for pyridine/Ag_{20}. The Au/Ag differences were attributed to relativistic effects.

Macroscopic plasmon models. See Colours of nanoparticles under Chapter IV.H.

K: Hyperfine properties

For the magnetic dipole A and electric quadrupole B constants of the 6s and 6p states of the Au atom, Song *et al.*[253] presented MCDF calculations. Similar work for Cu and Ag were included. The agreement with experiment for A was better than 1%. For another calculation of lower accuracy, recall Itano.[18] The good agreement of the Song A with experiment depended on error cancellations and a much more involved calculation is actually required.[254]

For NMR and NQR properties of the heavy-fermion compounds $CeCu_{6-x}Au_x$, see Winkelmann *et al.*[255]

The spin-densities for a complex of dithiolate radicals and Au(III) were calculated by Kokatam *et al.*[54] Both magnetic and electric hyperfine signatures were experimentally seen but the unpaired electron had 5% or less Au character.

The redetermination of the ^{197}Au nuclear quadrupole moment Q continues to attract interest. The classical table value from muonic hyperfine structure is 547(16) millibarn (mb). Yakobi *et al.*[256] used the Au atom $5d^96s^2$ measurements to extract a value of 521(7) mb. It is below the muonic one, as is the molecular value of 510(15) mb from AuX and NgAuX molecules (Ng = noble gas, X = F–I) by Belpassi *et al.*[257] In both cases, 4-component coupled-cluster methods were used to extract the electric-field gradient, q. Thierfelder *et al.*[258] obtain 526 mb using 4-component DFT.

Magnetic shielding effects. David and Restrepo[259] calculated at HF and 4-component DF level the RPA magnetic shieldings, σ(M, F) for the MF molecules, M = Cu–Au. For the heaviest member, over half of the σ(Au) arose from spin–orbit effects. In the series AuX, X = F–I the case X = F stood out, having a twice larger σ than the other cases X = Cl–I

L: Magnetism in clusters

Unlike the hyperfine properties, the distributions of magnetic currents in isolated clusters are not direct observables. Nevertheless, studies have appeared for Au_{2-7}[260] and $Au_{6,13,19,38,44,55,147}$.[261] Luo *et al.*[261] emphasised the s-orbital origin of the ferromagnetism. Note that they found for icosahedral Au_{13} a magnetic moment of $5\mu_B$, corresponding to five unpaired electrons in the h_g LUMO of the isoelectronic WAu_{12}.[262]

Michael *et al.*[263] developed a temperature-dependent mean-field model for ferromagnetism in gold nanoparticles. For thiol-capped particles, a maximum was predicted around a diameter of about 3 nm.

Recall also the $[M_{13}@Au_{20}]^-$; M = Co, Mn by Wang *et al.*[170] For M = Co, Mn the total spins S_z were 20 and 44 μ_B, respectively. For the naked M_{13} core, values of 30 and 2, respectively, were obtained. Similarly, the magnetic moments of the central atom survived in the planar D_{6h} clusters MAu_6^-, M = Ti, V, Cr,[171] characterized by PES and by DFT calculations.

M: Electrochemistry and solvation

A model for 1-decanethiol self-assembly on Au(111) surfaces from an ethanol solution was developed by Fartaria *et al.*[264]

N: Electron transport from gold electrodes

Take first the electron transport in stretched gold wires. The conductivity is of the order of the quantum unit $G_0 = 2e^2/h$. Grigoriev *et al.*[265] considered monoatomic chains of 3–7 gold atoms, suspended between (111) surfaces. The geometric structures were different, flat and spiral zigzag, for odd and even numbers of atoms, respectively. The conductivity could be effectively quenched by making the transmission channel pass the Fermi level, as function of stretching.

Fujii *et al.*[266] measured the conductance just before contact breaking. Current-induced breaks were found. Differences between the coinage metals occurred: Au had a break at 1 G_0 while Ag and Cu also had breaks at 2.5, 5 and 7.5 G_0. Dreher *et al.*[267] combined, for atomic-sized Au contacts, MD calculations of their structure with tight-binding model for the conductance. The disappearance of conducting channels with decreasing size was observed.

Electron transport through molecules. A pair of gold clusters or tips are frequently used for measuring the electric conductivity of molecules, attached to them. The results can deviate from those, calculated by DFT, by orders of magnitude.

Basch and Ratner[268] analysed at the orbital level the electron transfer between electrodes, including gold, and molecular bridges, such as benzene dithiolate.

Ning *et al.*[269] studied the electron transport through dithiolate molecules between two gold electrodes. The same problem from the point of view of inelastic electron tunneling spectra was considered by Solomon *et al.*[270]

Remacle and Levine[271] studied the electrical transport in saturated and conjugated molecular wires, tethered between two gold electrodes by sulfur atoms using both PP DFT and Extended Hückel wave functions. The I–V curves were obtained using a Landauer type formalism.

Viljas *et al.*[272] included the effect of molecular vibrations on the problem.

Zheng *et al.*[273] considered electron transport through the hypothetical Au_{32} fullerene, suspended between two gold electrodes.

The interaction strength between different small gold clusters, up to Au_4, and the groups phenyl–X (X = O–Te, NC), S or SH was studied by Seminario *et al.*[274] A particularly strong bond of 116.8 kcal was obtained between an S atom and μ_3-Au_4.

The specific case of the bonding modes and conduction of an aromatic amine between two gold electrodes was investigated by Quek *et al.*[275] both theoretically and experimentally.

Diode action. Yan *et al.*[276] considered the electron transport through molecules like a Si cluster, cyclohexane or benzene, between one gold electrode and one silicon electrode. For

diode action the gold side needed a positive bias of 0.8 V. The general, barrier tunneling conditions for molecular rectification by an electrode–molecule–gap–electrode assembly were formulated by Armstrong *et al.*[277]

O: Chemical reactions of gold species

A number of examples are shown at the end of Table 6.

P: Studies of dynamic processes

As mentioned in subsection I, the laser experiments and related simulations on warm, dense gold were discussed by Mazevet *et al.*[232]

Samela *et al.*[278] simulated Xe ions striking Au(111) surfaces with energies of 0.1 to 200 keV at MD level. A particular question were the 'thermal spikes'. Sputtering yields and crater formation were studied.

V Catalysis

A: Reviews

A monograph on catalysis by gold was published by Bond, Louis and Thompson.[279]

A thorough review on the homogeneous catalysis by gold complexes, with a special emphasis on the relativistic shifts, was provided by Gorin and Toste.[280] One aspect emphasized was the Lewis acidity of Au, directly related to the 6s stabilization. Another was the 5d back donation in carbenoid species, related in turn to the 5d destabilization.

More experimentally oriented reviews were given by Hashmi and Hutchings[281–283] and by Edwards and Thomas.[284] Burks[285] covered the question for the readers of *C&E News*. Kung *et al.*[286] reviewed the case of low-temperature CO oxidation. Conflicting results on the role of the support were identified. Poisoning by residual Cl^- was discussed. The evidence for several Au oxidation states and the role of moisture were presented. A possible reaction mechanism was proposed, where adsorbed CO is inserted to an Au–OH bond, the hydroxycarbonyl is oxidized to bicarbonate, which is decomposed to Au–OH and CO_2. The role of the small Au particle size, traditionally ascribed to numerous low-coordination sites, was left open.

Other reviews on the suggested mechanisms for CO oxidation comprise those by Louis[287] or Landman *et al.*[220] The latter specifically considered the 'non-scalable' domain of up to 20 gold atoms.

The industrial reactions of interest for sustainable chemistry were reviewed by Ishida and Haruta.[288] Other reviews with a more applied view include those by Corti *et al.*,[289] Thompson.[290]

B: Homogeneous catalysis

Roithová *et al.*[291] studied both mass-spectrometrically and computationally the coupling reaction of alkynes and alcohols. The theoretical test system was $Au^+/C_2H_2/CH_3OH$, a case with no reaction observed.

A single-site homogeneous or heterogenized gold(III) Schiff-base catalyst for the hydrogenation of olefins was studied by Comas-Vives *et al.*[292] They combined calculations and kinetic experiments. Both the solvent and the solid support chosen influenced the results. Note the valence isoelectronic relation between Au(III) and the previously used Pd(II). The critical step was the cleavage of the H_2.

Rabaâ *et al.*[293] modelled the reaction of alkynes with furan, catalysed by $AuCl_3$ and AuCl and found that a [4 + 2] Diels–Alder reaction of Au(III) was thermodynamically favoured. On the other hand a route, involving a carbene complex, was kinetically favoured. Solvent effects, in a continuum model using the acetonitrile dielectric constant, decreased the activation energies. Note that monomeric $AuCl_3$ in condensed matter is not known, the present Au(III) species were effectively tetracoordinated planar, with one of the reacting carbons in the fourth corner. The $AuCl_3$ is introduced to the system by dissociation of the dissolved species Au_2Cl_6.

C: Surface adsorption and heterogeneous catalysis, including cluster work

Methodology. The theoretical methodology for studying the ultrafast dynamics in and on atomic clusters, including ones containing gold, is being developed by Bonačic-Koutecký and coworkers, for a review see ref. 294 Both precalculated potential-energy surfaces and "on-the-fly" nuclear dynamics are used. An example on the processes studied is the NeNePo (negative-to-neutral-to-positive) ionisation of Ag_2Au or Au_4 in a time scale of a few ps.

The surface adsorption of various single species is discussed below. A general remark by Loffreda[295] is that, the adsorption energies to Au(110) being small, a sufficient accuracy to obtain phase diagrams is difficult to obtain. A large number of adsorbates was considered (acrylonitrile, nitoethene, propenoic acid, methacrylate, propene imine, propenal, propene amide, but-3-ene-2-one and nitroso ethene). Concerning the coadsorption of several species, Zhang *et al.*[296] find both theoretically and experimentally that a predose of NO_2 or another electronegative substituent will promote the subsequent adsorption of CO on Au(111). A concomitant blue-shift of the CO stretch was seen and explained.

In addition to gold nanoparticles, ultrathin gold layers on titania surfaces were shown to be catalytically active. A high C–O stretch of adsorbed CO was used as indicator. It should be underlined that the gold then wets the metal oxide surface.[297]

Hydrogen on gold. The adsorption and possible dissociation of H_2 on gold was studied by several workers.[298–300] Dissociation was found on an Au_{13} cluster,[298] Au_{14} cluster, which strongly deformed, and Au_{29}.[299] No dissociation occurred on Au(111) and Au(100) bulk surfaces.[299,300] An extended line defect on the surface led to dissociation and the general conclusion is that low-coordinated gold atoms are necessary for it.[300] Further experimental support, that hydrogen is only chemisorbed at cluster edges and corners on Au_n/Al_2O_3, was presented by Bus *et al.*[301]

In a study of M_6 metal particles in a hydroxylated faujasite zeolite framework, Ivanova Shor *et al.*[302] found gold to be the only metal that preferred M_6/(zeo)3H over the hydrogenated cluster form M_6(3H)/zeo. The latter case is termed 'reverse hydrogen spillover'.

Mercury on gold. Sarpe-Tudoran *et al.*[303] were interested in providing a value for the adsorption energy of a single eka-mercury (E112) atom on an (100) gold surface, using a large cluster model of up to 36 atoms for the latter. E112 always adsorbed more weakly than Hg. The difference depended on the site. The same conclusion was reached by Rykova *et al.*[304]

Oxygen on gold. Ding *et al.*[305] found that hybrid functionals, such as B3LYP, gave good agreement with experiment for the adsorption energies of both anionic, cationic and neutral gold clusters with up to six gold atoms. The GGA, such as PW91, overestimated the adsorption energy.

Molina and Hammer[306] studied the adsorption of O_2 on Au_n clusters (n = 1–11), either as free clusters or adsorbed ones on MgO(100). The adsorption of O_2 on an Au_{11} + gold surface nanotip model was studied by Tielens *et al.*[307]

For experimental and DFT studies of adsorption of O_2 on free Au_n clusters, n = 15–24, see Yoon *et al.*[135] The O_2 prefers end-on bonding to a low-coordinated gold atom.

Various gold–oxygen cluster structures were studied experimentally and theoretically by Kimble *et al.*: $Au_nO_m^-$ ($n \geq 4$),[308] AuO_n^- (n = 1–3),[309] $Au_2O_n^-$ and $Au_3O_n^-$ (n = 1–5),[310] $Au_6O_2^-$.[311] The interactions of CO with these cluster structures were also studied. $Au_2O_2^-$ and $Au_6O_2^-$oxidise CO but $Ag_2O_2^-$ and Ag_6^- do not (see ref. 311). The very different sticking probabilities of O_2 onto M_6^- (M = Ag, Au) clusters in the gas phase were attributed to their different dynamical properties concerning the internal vibrational redistribution. The gold cluster is stiffer, leaving the excitation energy at the O–O part and thereby promoting an oxidation reaction.

Barrio *et al.*[312] considered O_2, H_2, or both together on bare Au_n clusters (n = 14, 25, 29). For n = 14 and 29, superoxo and peroxo moieties were formed, respectively. For n = 25, no interaction with O_2 was found. The surface models Au(100) and Au(111) were found to be inactive. With predissociated hydrogen present, hydroperoxo groups were formed. A concerted, exothermic (−30 kcal mol^{-1}) reaction mechanism to form H_2O_2 was identified.

Fajín *et al.*[313] studied the adsorption of both O and O_2 on periodic Au(321). The atoms were found to prefer cavity sites. The molecules preferred terrace or bridge sites. The O_2 dissociation was exothermic.

Okumura *et al.*[314] studied both O_2 and H_2O adsorption on Au_{10} clusters. The presence of water was found to promote the activation of O_2. For the Au_{10} cluster, a 3D C_{3v} structure was taken. Hydrogen bonding was found to occur between the water and the O_2, when coadsorbed on the cluster.

Experimental evidence for *subsurface oxygen species* was found by Lim *et al.*[315] for gold nanoparticles, resting on graphite and subjected to bombardment by a mixture of O atoms and electronically excited O_2. This happened on graphite for diameters below 6 nm diameter. On silica surfaces the opposite behaviour was found, with larger particles forming Au-oxide.

Concerning atomic oxygen on a periodic, Au(111) surface, Shi and Stampfl[316] find a weak adsorption, energetically close to molecular O_2. The lowest-energy structure had oxygens, bound to three inner Au atoms, and capped by a fourth Au.

Tielens *et al.*[317] constructed a two-dimensional periodic array of pyramidal, 29-atom subunits to model modified Au, Au/Pt or Pt surfaces. Then end-on O_2 adsorption was achieved. A combined experimental study of oxygen desorption from gold field-emitter tips and theoretical study of O_2 on Au_{10} nanotips by Visart de Bocarmé *et al.*[318] showed weaker end-on interaction with Au_{10} but stronger interaction with an Au-adatom-on-Au(100) model. The addition of electric fields in the DFT calculation could increase the activation energy for oxygen dissociation.

The adsorption of organic molecules on gold electrodes was treated by Teobaldi and Zerbetto[319] at the level of an Embedded Atom glue model. The three applications comprise the deposition of citric acid on Au(111), ditto for a porphyrin derivative and the voltage-dependent desorption of thiolate chains in self-assembled monolayers.

Cyanide on gold. Anionic cyanide is found to adsorb on a metallic gold surface. Beltramo *et al.*[320] carried out a combined SERS and DFT slab model study for three different surfaces. 'Stark tuning slopes' of the molecular vibrations, as function of the electrode voltage, were obtained.

Carbonyl on gold. A useful signature for the effective charge of a gold cluster could be the dependence of the adsorbed CO stretching frequency. Such an experimental correlation was shown for gas-phase Au_8 by Fielicke *et al.*,[321] see Fig. 1.

Phala and van Steen[322] qualitatively related the adsorption energy of CO to a 1–10 nm gold nanoparticle to the energetic distance between the Fermi level and the 5d-band centre, calculated at EHT-level. McKenna and Shluger[323] studied the shape deformation of a gold cluster, following CO adsorption. It was found to promote further low-symmetry sites. The deformation of Au_{79} was related to the CO Pressure.

Giordano *et al.*[324] studied the vibrational and ESR properties of a CO ligand on an Au atom on MgO. The results were compared with free AuCO. Upon adsorption to MgO, a charge transfer from a surface oxide to the ligand takes place

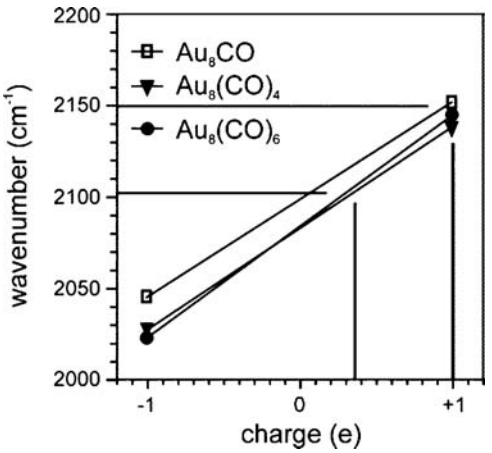

Fig. 1 The experimental correlation between the particle charge, q of −1, 0 or +1 for an Au_8^q cluster, and the observed CO stretch frequency for carbonyls, adsorbed on it. From Fielicke *et al.*[321] Copyright American Chemical Society.

and this increases the CO stretching frequency by about 290 cm^{-1}. The adsorption of only the Au atom on MgO, in turn on a metal like Ag, was considered in a related work.[325]

Fernández and Balbás[326] considered CO adsorption on gold/alumina substrates, the gold being a single atom or Au_8. The substrate was modelled by an amorphous $(Al_2O_3)_{20}$ cluster or by an Al-terminated (0001) surface. The preferred sites for the combinations were reported.

Joshi *et al.*[327] performed a DFT study of non-dissociative CO adsorption on 22 diatomic or triatomic binary Au-alloy (Au_nM_m) clusters with M = Cu, Ag, Pd and Pt. The data set was big enough to study correlations between the CO bond length, vibrational frequency and the binding energy of CO to the cluster.

On mixed, small Pt_mAu_n; n, m = 0–4 clusters, Wang[328] found that the adsorption of CO upside down, M−OC, is less bound than the normal M–CO adsorption but still binding, compared to the separated M + CO. The M − CO adsorption was strongest around 25% Pt composition.[329]

In a series of combined experimental and theoretical studies of CO adsorption on Au surfaces, Loffreda *et al.*[330–332] gave evidence for restructuration of the gold surface itself.

Tielens *et al.*[333] studied the interaction between an Au atom, or monovalent ion, and the ligands CO, NO and OO. An external electric field could be imposed. Both DFT and CCSD(T)/MP2 methods were used. The bonding was analysed.

O_2 *vs.* CO on gold clusters. Prestianni *et al.*[334] studied these two species on neutral or cationic gold clusters with up to 13 atoms. While O_2 interacts better with neutral clusters, being an electron acceptor, CO binds more strongly to cationic clusters, acting as an electron donor.

NO *vs.* CO on gold clusters. While CO adsorption on Au_n^+ did not show oscillations in the adsorbate stretch frequency, NO adsorption did.[335] This experimental observation was reproduced by DFT calculations and rationalized in terms of strong and weak back donation from the Au_n cluster to the π orbital of NO and CO, respectively.

Silanes on gold. The chemisorption of monomethylsilane on a cluster model for Au(111) was studied by Ekström *et al.*[336] in order to interpret the Si K- and L-shell X-ray spectra. The gold bonded on a three-fold site.

Sulfur species, especially thiolates on gold. For an overview on the (mainly experimental) situation concerning sulfur or alkanethiol layers on Au(111), see Vericat *et al.*[337,338]

Gonzalez-Lakunza *et al.*[339] compared the bonding of L = S, Sh and SCH_3 on Au(111) and found similar Au–S bonding for all three.

Maksymovych *et al.*[340] suggested that the discrepancies between theoretical and experimental results concerning the structures of thiolates, adsorbed on Au(111) could be removed by actually reconstructing the surface. They introduced adatoms. One adatom would then bridge two thiolates, RS–Au–SR. Experimentally this 'stripe-phase' was very stable under the tunneling current. A similar suggestion was made independently by Mazzarello *et al.*[341] Yu *et al.*[342] verified by X-ray experiments the RS–Au(adatom) hypothesis for thiolates on Au(111), quoting for a theoretical prediction in 2005 Cometto *et al.*[343] Note that they have one thiolate per adatom. A calculated structure is shown in Fig. 2.

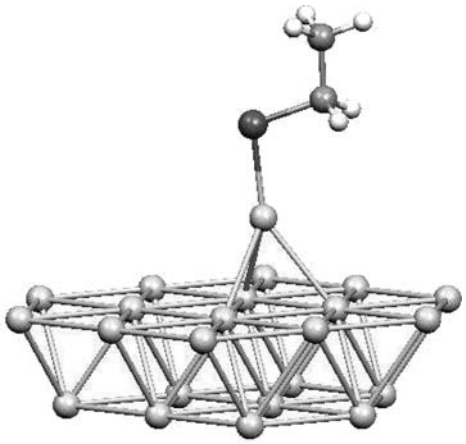

Fig. 2 The calculated structure for a thiolate, bound to an Au adatom, bound to Au(111). Reprinted with permission from ref. 343. Copyright American Chemical Society.

The bonding of benzenedithiolate on gold was studied by Leng *et al.*[344] at DFT level, comparing LDA, PBE0 and X3LYP functionals. The self-assembled monolayers (SAM) were studied at MD level.

A periodic treatment of phenylthiolate groups on Au(111) revealed significant lateral dispersion.[345] '2PPE' spectra were interpreted.

Heimel *et al.*[346] calculated the energetics of 4-mercaptobiphenyls on a gold surface.

The simplest way to model a gold surface is a single gold atom. This was used by Doneux *et al.*[347] to analyse the IR spectrum of adsorbed 2-mercaptobenzimidazole. The results support a thiolate anion structure and were compared with experiments.

Iwasa and Nobusada[348,349] considered a specific $Au_{25}(SCH_3)_{18}$ cluster model with net charges ranging from −3 to +3. Spin densities appeared at the central Au_7 part and this result was qualitatively related to experimental observations.

In addition to thiolates, a gold sulfide layer can exist on gold. Such an iccommensurate AuS layer on Au(111) was modelled by Quek *et al.*[350] The structure shows up familiar tetracoordinate Au(III) and two-coordinate Au(I) moieties, the latter paired to Au–Au-bonded dimers.

For further data, recall Table 8.

Water on gold. Neves *et al.*[351,352] developed a DFT-based force field for water on an Au(210) surface and performed MC simulations. Most water molecules lie on the surface side-on and form specific hydrogen bonds with the next solvation layer.

Alcohols on gold. Chen *et al.*[353] studied the adsorption and subsequent dissociation to CH_3O or HCHO of methanol on Au(111). The methoxyl radical was found to be a likely intermediate.

A DFT model for ethanol, adsorbed on Au(111), was developed by Fartaria *et al.*[25]

Phenol on gold. The adsorption of phenol on gold in a dilute aqueous solution was studied by Neves *et al.*[354] The simulation suggested a first, oxygen adsorption step, with the aromatic ring perpendicular to the surface. This is followed by turning it parallel to the surface.

Ammonia on gold. Kryachko and Remacle[81] studied the bonding of 1–3 ammonia molecules on $Au_n^{-1,0,+1}$ clusters, $n = 3, 4, 20$. Both traditional N→Au coordination and through-hydrogen N–H···Au bonding was found to occur.

Hydrocarbon radicals on gold. McDonagh *et al.*[355] reacted experimentally ethynylbenzene on an Au(111) surface in presence of oxygen. Theoretical calculations supported the stability of the obtained phenylacetic acid and phenyloxirane radicals, bound on-top to the gold surface.

Aromatics on gold. Benzene adsorption on a Au(100)-3 × 3 surface was studied by Chen *et al.*[356] Two opposite carbon atoms on the ring were found to rehybridize from sp^2 to sp^3 and make the bond from the benzene to the metal. "The hollow site" was preferred to "bridge" and "top" positions. Bilić *et al.*[357] studied benzene adsorption on Au(111) using a slab model and DFT. Because wave-function based calculations on a Cu_{13} cluster model suggest mainly dispersive interactions, the results are not very reliable.

The adsorption of pyridine on vertex and surface sites of tetrahedral Au_{20} was considered by Aikens and Schatz.[252]

The adsorption of metal porphines (M = Mn, Pd) on Au(111) was modelled by Leung *et al.*[358] The adsorbate preferred to lie flat. Top, bridge and hollow positions were comparable. Although DFT methods were used, the interaction was mainly characterized as dispersive. Electric fields could be added to the model and changed the Mn magnetic moment.

Lee *et al.*[359] studied the adsorption of pentacene on an Au(100) surface at DFT level, comparing a discrete basis set and a numerical basis set. After a counterpoise correction for the BSSE was added, the former agreed with the latter. Concerning the functionals, LDA was strongly overbinding while GGA is closer to experiment but underbinds. No detailed analysis was given on the adsorption mechanisms.

A superstructure inside a C_{60} monolayer on Au(111) was experimentally observed.[360]

Metal ions on gold. Karttunen and Pakkanen[245] studied the interactions with a stiff cluster model for an Au(111) surface of naked or hydrated Na^+ or alternatively naked or hydrated Au^+ ions. The hydrated Na^+ ion preferred to remain hydrated in the interaction with the surface while the Au^+ adsorbed directly to the metal. Note that in technological applications Au(I) usually appears as $[AuL_2]^-$, L being typically CN. No data on any hydrated Au^+ species appears to exist for bulk solutions. For gas-phase droplets such data are known, see chapter 3.2. of Part I.[1]

Heterogeneous catalysis. The reaction of SO_2 with Au/CeO_2(111) was studied by Rodriguez *et al.*[361] Oxygen vacancies were found important.

CO oxidation is perhaps the most widely studied reaction, catalysed by small (1–5 nm in diameter) particles of gold. Some key features are that the reaction can take place at low temperatures, down to 200 K and that a molecular oxygen, not predissociated oxygen, would be involved.[362]

Bongiorno and Landman[363] studied CO oxidation on free and MgO(100) supported gold clusters and found it to be enhanced by water. One key feature was the formation of an H_2O–O_2 complex with partial proton sharing and concomitant O–O bond activation.

Molina and Hammer[364] summarize their work on CO oxidation, catalysed by Au particles on MgO or TiO_2 surfaces. For small Au clusters, a certain active structure with low-coordinated Au atoms was found. Au_{34} was a typical cluster used.

The CO oxidation on Au/TiO_x/Mo(112) was studied by Liu.[365] His aim was to explain the observations by Chen and Goodman. The combined high stability and high reactivity of the mentioned 'two-layer Au phase' were rationalized. The same system was considered by Cruz Hernández *et al.*[366] To begin with, the gold layer wetted the titanium oxide and its thickness was between a mono- and a bilayer. The transition state for the reaction

$$CO(ads) + O_2(ads) \rightarrow CO_2(g) + O(ads)$$

was localised.

Remediakis *et al.*[367] considered CO oxidation on both free and surface-bound gold clusters, taken as Au_{10}. Again, the low-coordinated Au sites were found to do the job. Shiga and Haruta[368] simulated the CO oxidation pathways over Au_n ($n = 10, 13, 20$) using a 'paired interacting orbitals' (PIO) analysis of Relativistic Extended Hückel (REX) orbitals. Four different pathways were found.

Arenz *et al.*[362] summarized the available data for CO combustion on supported, small (<1 nm), size-selected gold clusters. The factors considered were the role of the oxide support, its defects, charging and structural fluxionality of the clusters, the cluster size and the promotional effect of water. No generalized explanation emerged. Little catalysis occurred up to Au_7. Different reaction mechanisms were found below and above 250 K. The fluxionality of the cluster was essential for catalysis; a frozen cluster did not work.

Kimble *et al.*[310] presented both gas-phase experimental results and DFT studies on reactions of CO with the anionic clusters $(Au_nO_m)^-$; $n = 2,3$; $m = 1$–5. Both atomic and diatomic oxygen moieties could play a role and otherwise forbidden reactions could occur with two CO groups.

The oxidation of CO on Au nanoclusters on MgO on Mo(100) was considered by Zhang *et al.*[369] In this case the gold wets the surface and the Au_{20} clusters were taken as planar. To the contrary, the gas-phase tetrahedral Au_{20} cluster would maintain its structure on the bulk MgO(100) surface. For the oxidation reaction, low barriers were found. No defects of the surface were required; an excess electronic

charge on the cluster was obtained by penetration of metal states through the thin oxide layer.

The adsorption of one or several CO or of O_2 on the vanadium-centred icosahedral cluster VAu_{12}^- was theoretically studied by Graciani *et al.*[162]

Concerning the effects of the ligands on the surface structure of an originally icosahedral Au_{13}, Guliamov *et al.*[370] found in a study of $Au_{13}[PPh_3]_4[SMe]_4$ that large tangential distortions occurred. The results were compared with experimental EXAFS/TEM measurements. The radial bonds were much stiffer.

Liu *et al.*[371] studied the O_2 supply pathway in CO oxidation on $Au/TiO_2(110)$. The OH radicals from dissociated water were found to play a role, see also ref. 220.

The oxidation of propene on Ag or Au surfaces, modelled by clusters, was compared to that of ethene by Kobayashi and Shimodaira.[372]

Wang *et al.*[373] investigated the formation of hydrogen peroxide from hydrogen and oxygen over Au_n^- clusters, $n = 1$–4. The reaction was suggested to proceed from initial H_2 dissociation to formation of OOH intermediates, to HOOH.

Marion *et al.*[374] studied both experimentally and computationally the [(NHC)Au^I]-catalyzed formation of conjugated enones and enals from propargylic acetates. The catalytically active species was found to be [(NHC)AuOH], produced *in situ* from [(NHC)$AuSbF_6$] and H_2O. The OH was then transferred to the –C≡C– bond, forming a gold-allenolate.

In a study of CO oxidation on Au_{10} clusters on a $TiO_2(110)$ surface Janssens *et al.*[375] emphasize the role of low-coordinated gold atoms. The role of different sites was expressed by power laws $1/d^n$, where d is the particle diameter. For corner atoms $n = 3$, for edges $n = 2$ and for surfaces $n = 1$.

The water–gas shift (WGS) reaction $CO + H_2O \rightarrow CO_2 + H_2$ is an important source of clean hydrogen. Rodriguez *et al.*[376] studied both experimentally and theoretically a catalyst where an Au(111) surface has a high concentration (20–30%) of CeO_x or TiO_x nanoparticles. It is concluded that the CO molecules adsorb on nearby Au sites and that the rest of the reaction takes place on the particle. The has predissociated on the oxide particle.

Role of cations in gold catalysis? The work on chemical adsorption on gas-phase Au_n^+ was discussed above. We now discuss cationic clusters adsorbed on surfaces. In many cases above, the gold cluster was supposed to be anionic. Wang and Hammer[377] compared the activities of Au_7 nanoparticles in different oxidation states on rutile $TiO_2(110)$. The real catalysis conditions correspond to oxidised (alkaline) TiO_2 supports. A full catalytic cycle of CO oxidation by O_2 could then be constructed and had only low activation barriers. The results were supported by comparing the calculated and measured CO-stretch frequencies. The Au_7 group had low or no symmetry during the process. The atomic or molecular oxygen was bound initially at the cluster-surface perimeter, and the CO further away.

For growing single-wall carbon nanotubes, gold clusters were *not* found to be useful catalysts, in contrast to 3d-metal clusters.[378]

VI Conclusion

We apologise for any papers that were inadvertently missed. Some general conclusions are suggested by the material.

1. The two 'gold standards' for calibrating the other theoretical results are experiments, or high-level wave-function-based calculations. An example on the level that may then actually be necessary, are the calculations of the lowest-energy structures of gold clusters,[114] which could be pushed to CCSD(T) level with large Peterson-Puzzarini[8] basis sets and the latest Stuttgart pseudopotential.[9] An explicit inclusion of the (5s5p) semicore correlation also was an issue.

It is generally thought that DFT calculations can reach the basis-set limit with smaller basis sets than wave-function-based methods. No reference on this point seems to exist, however.

Some caution must be exercised, when addressing a random problem with a random method.

2. Many innovative new gold species were experimentally verified during the review period. Some of them are the hollow Au_n^- around $n = 16$–17, or their derivatives, filled with Cu.

3. Surface problems can be complex. Although thiolates on a gold surface are *the* prototype for self-organized structures, it was only now realized that there is a gold adatom between the surface and the -SR group, or groups.

4. Even more complex is the catalysis by gold particles, whether in the gas phase or by particles on a surface, possibly one with a multiple sandwich structure.

5. While gold single-wall nanotubes are both seen in electron microscopy and theoretically verified, the thinner nanowires, down to stretched monoatomic ones, possibly with heteroatom links, continue to draw interest but are not so well documented.

6. One reason to study luminescent complexes is to use them for signalling, as chemical indicators. New complexes are being produced and the TDDFT method appears to be a reliable workhorse for studying their absorption and emission spectra.

7. Much activity goes on with the prediction and interpretation of the electron transfer through moieties suspended between gold electrodes.

8. Concerning the hybridization and bond character of gold, one recurrent theme is the facile d-sp hybridization. It was evoked to explain the flat liquids.[152]

9. Concerning multiple bonding to gold, the effectively double bond in gold carbenes is not doubted. At least partial triple-bond character occurs in the isoelectronic series AuC^+, AuB, ... and they were used for developing a set of triple-bond covalent radii,[35] for almost all elements.

10. The situation concerning the aurophilic attraction appears stationary. New experimental examples are steadily synthesized and theoretical examples are being treated. On the methodological side, the basis-set limit at MP2 level was now studied.[65] Not a single wave-function-based calculation disputes the earlier conclusion that the effect is mainly a dispersion effect. The virtual-charge-transfer (or 'ionic') terms are typically the next most important ones. Others, like induction terms between molecules having large dipole or quadrupole moments, occasionally exist.

There still is no reason to trust any supramolecular DFT calculations for the aurophilic attraction, or any other dispersion forces. The SAPT method could in principle work but has not been applied yet.

In case of the more general metallophilic attraction there are new examples, such as the first Bi(III)–Au(I) attraction. There it was estimated that Coulomb attraction between opposite atomic charges dominates over dispersion, which is the next term.

Recapitulation: The nature of aurophilicity

The *simplest* picture is that aurophilicity is just another van der Waals ('vdW' = dispersion) interaction, but an unusually strong one in an initially unexpected place.

How do we know? One basic property of such interactions is that, at large intermolecular distances, R, the interaction decays like R^{-6}. More quantitatively, it follows the London approximation

$$V(R) = -\frac{3}{4}\alpha_A\alpha_B\frac{I_A I_B}{I_A + I_B}R^{-6}, \qquad (1)$$

where the α's are electric polarisabilities and the I's the ionisation potentials of the interacting systems A and B. When other contributions were eliminated, eqn (1) was found to fit well (refs. 70 and 379 and later work). A further point is, that this R^{-6} curve can be continued quite near the actual aurophilic bond distance.

Another textbook image of such interactions is that they are due to simultaneous dipole moments, excited in the two subsystems, A being excited to an excited state A′, and concomitantly B to B′, both excitations creating local dipole moments, which interact and cause the vdW attraction, see Fig. 4.

$$A \rightarrow A', B \rightarrow B'. \qquad (2)$$

This picture underlies the London derivation. When Runeberg, Schütz and Werner[381] analysed aurophilicity using local orbitals, this was, indeed, found to be the dominant term. In a similar calculation on solid AgCl and AuCl, this Au–Au contribution between two nearest neighbours was calculated to be 0.2 eV (19 kJ mol^{-1}) per pair, comparable with the molecular values. It should be added, that van der Waals forces in ionic crystals have been discussed since Mayer,[382] who considered silver and thallium halides. For summary, see refs. 383 and 384.

At this point we can quote the expression that "if it walks like a duck, swims like a duck and quacks like a duck, it is a duck".

Why is it so strong? Is the polarisability α particularly large for Au^+ or its compounds? No, it is only reasonably large, but comes from a compact volume, mainly corresponding to the $5d^{10}$ shell. It was instructive to compare aurophilicity with thallophilicity.[380] Tl(I) has a larger α than Au(I) but it also has a much larger size, due to the now occupied $6s^2$ shell on top of the $5d^{10}$ one. Therefore the interatomic repulsion stops the Tl(I)···Tl(I) interaction, on its lower-lying R^{-6} curve, before it becomes strong. Because Au(I) has a smaller size, it can dive to greater depths, before hitting the interatomic 'Pauli' repulsion, see Fig. 3.

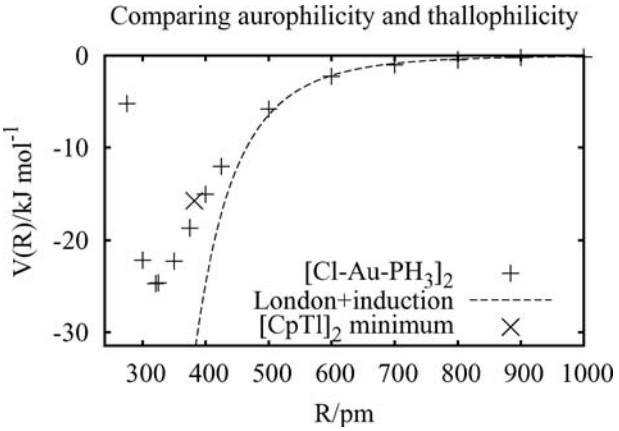

Fig. 3 The large-R agreement between the calculated points[379] for a perpendicular dimer [$(ClAuPH_3)_2$] and the R^{-6} long-distance limit, based on calculated monomer properties. The higher-lying minimum[380] for $[CpTl]_2$ is indicated by the cross.

Where does it stop? Is there a distance where aurophilicity disappears? This was discussed by Pyykkö in the reviews.[1,385] The interaction systematically weakens from as much as nearly 100 kJ mol^{-1} (per Au–Au pair!) around an R_{min} of 270 pm to about 10 kJ mol^{-1} around an R_{min} of 350 pm. It never vanishes. A curve relating V to R_{min} was presented.

The fine print. This simple picture must be completed by saying that the interacting molecules may have multipole moments and these are occasionally large. They can interact directly, or *via* an induction effect. This includes the net charges: If the interacting groups containing the two metals carry opposite net charges, the classical Coulomb attraction may be important. Note that in an ionic crystal or a liquid, it is the total Madelung potential of the system that counts.

In addition to the A → A′, B → B′ mechanism, in many metallophilic systems an A → A′, B → A′ mechanism[381] can cause up to half of the calculated attraction. This term corresponds to a virtual charge transfer, instead of the virtual double excitations (2) of the two systems.

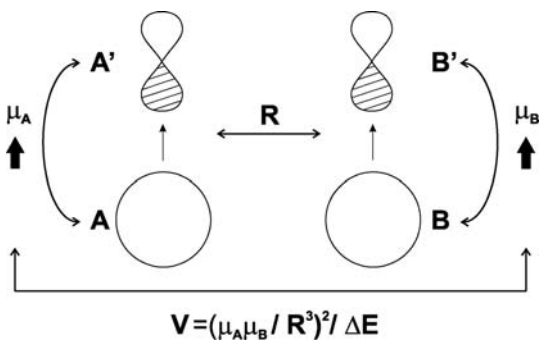

Fig. 4 How do van der Waals interactions arise? The wave function of subsystem A gets a small mixture of an excited state A′, and concomitantly the wave function of subsystem B a small mixture of its excited state B′. This creates the local dipole moments, μ_A and μ_B, respectively. In "second-order perturbation theory" one takes the square of the dipole–dipole energy, $\mu_A\mu_B R^{-3}$, divided by the energy of the excitations, ΔE. This results in the R^{-6} interaction law.

Technicalities. The virtual excitations mentioned require for their description 'correlated' quantum chemical methods going beyond a self-consistent field or Hartree–Fock (HF). In wave-function-based theories (WFT), there is a fairly clear hierarchy of methods, HF, MP2, (MP3), MP4, CCSD, CCSD(T),... where both cost and accuracy increase along the series. A large-basis CCSD(T) could be close to the truth. When it was said that aurophilicity is an 'electron correlation effect', it meant technically, that these theories should be used, and physically that the virtual electronic excitations (2) lie behind it. The qualitative fingerprint was that HF gave no attraction but MP2 did.[386]

When higher methods than MP2 were used,[387,388] it turned out that some trends changed sign. For instance the argentophilic attraction became comparable or stronger than the aurophilic one, while at MP2 level it was weaker. The direction of very large basis sets has just been studied, and only at the MP2 level.[65] The WFT theories of aurophilicity appear to rest on a sound foundation, but they have not yet converged.

Density functional theory (DFT) is an excellent tool for studying other forms of chemical bonding. It is, however, not applicable to the weaker interactions of the present type at the supramolecular level (A + B treated as one system). For instance the R^{-6} behaviour cannot be reproduced. Therefore all DFT studies of aurophilicity, even near the minimum, $V(R_{\min})$, should be regarded with suspicion. At best they mimic it *via* some unspecified mechanism.

Acknowledgements

The author belongs to the Finnish Centre of Excellence in Computational Molecular Science. The paper was partly written in May 2007 at Berlin in the laboratory of Helmut Schwarz during tenure of a Humboldt Research Prize. Ignazio Garzón, Eugene Kryachko, Catherine Louis, Helgard Raubenheimer and Michael Springborg made valuable remarks on the manuscript.

References

1 P. Pyykkö, *Angew. Chem., Int. Ed.*, 2004, **43**, 4412–4456.
2 P. Pyykkö, *Inorg. Chim. Acta*, 2005, **358**, 4113–4130.
3 P. Schwerdtfeger and M. Lein, in *Gold Chemistry. Current Trends and Future Directions*, ed. F. Mohr, Wiley, Weinheim, 2009.
4 J. M. L. Martin and A. Sundermann, *J. Chem. Phys.*, 2001, **114**, 3408–3420.
5 P. Pyykkö, N. Runeberg and F. Mendizabal, *Chem.–Eur. J.*, 1997, **3**, 1451–1457.
6 D. Schröder, H. Schwarz, J. Hrušák and P. Pyykkö, *Inorg. Chem.*, 1998, **37**, 624–632.
7 F. Weigend and R. Ahlrichs, *Phys. Chem. Chem. Phys.*, 2005, **7**, 3297–3305.
8 K. A. Peterson and C. Puzzarini, *Theor. Chem. Acc.*, 2005, **114**, 283–296.
9 D. Figgen, G. Rauhut, M. Dolg and H. Stoll, *Chem. Phys.*, 2005, **311**, 227–244.
10 S.-M. Hou, R. Li, Z.-K. Qian, J.-X. Zhang, Z.-Y. Shen, X.-Y. Zhao and Z.-Q. Xue, *J. Phys. Chem. A*, 2005, **109**, 8356–8360.
11 R. Rousseau, R. Mazzarello and S. Scandolo, *ChemPhysChem*, 2005, **6**, 1756–1760.
12 D. Naveh, L. Kronik, M. L. Tiago and J. R. Chelikowsky, *Phys. Rev. B*, 2007, **76**, 153407.
13 E. van Lenthe, J. G. Snijders and E. J. Baerends, *J. Chem. Phys.*, 1996, **105**, 6505–6516.
14 A. Hellweg, C. Hättig, S. Höfener and W. Klopper, *Theor. Chem. Acc.*, 2007, **117**, 587–597.
15 M. Pitoňák, P. Neogrády, V. Kellö and M. Urban, *Mol. Phys.*, 2006, **104**, 2277–2292.
16 P. Koskinen, H. Häkkinen, G. Seifert, S. Sanna, Th. Frauenheim and M. Moseler, *New J. Phys.*, 2006, **8**, 1–11.
17 J. Neugebauer and M. Reiher, *J. Comput. Chem.*, 2004, **25**, 587–597.
18 W. M. Itano, *Phys. Rev. A*, 2006, **73**, 022510.
19 Z.-J. Wu and Y. Kawazoe, *Chem. Phys. Lett.*, 2006, **423** 81–86.
20 L. Belpassi, F. Tarantelli, A. Sgamellotti and H. M. Quiney, *J. Phys. Chem. A*, 2006, **110**, 4543–4554.
21 V. Fivet, P. Quinet, É. Biémont and H. L. Xu, *J. Phys. B*, 2006, **39**, 3587–3598.
22 J.-L. Zeng, G. Zhao and J.-M. Yuan, *At. Data Nucl. Data Tables*, 2007, **93**, 183–354.
23 T. Pawluk, L. Xiao, J. Yukna and L.-C. Wang, *J. Chem. Theory Comput.*, 2007, **3**, 328–335.
24 L. Xiao, B. Tollberg, X.-K. Hu and L.-C. Wang, *J. Chem. Phys.*, 2006, **124**, 114309.
25 R. P. S. Fartaria, F. F. M. Freitas and F. M. S. Silva Fernandes, *Int. J. Quantum Chem.*, 2007, **107**, 2169–2177.
26 J. Kohanoff, A. Caro and M. W. Finnis, *ChemPhysChem*, 2005, **6**, 1848–1852.
27 A. Laguna and M. Laguna, *Coord. Chem. Rev.*, 1999, **193–195**, 837.
28 K. A. Barakat, T. R. Cundari, H. Rabaâ and M. A. Omary, *J. Phys. Chem. B*, 2006, **110**, 14645–14651.
29 N. C. Pyper and I. P. Grant, *Proc. R. Soc. London, Ser. A*, 1978, **360**, 525.
30 S. Riedel and M. Kaupp, *Inorg. Chem.*, 2006, **45**, 1228–1234.
31 A. A. Timakov, V. N. Prusakov and Y. V. Drobyshevskii, *Dokl. Akad. Nauk SSSR*, 1986, **291**, 125–128.
32 D. Himmel and S. Riedel, *Inorg. Chem.*, 2007, **46**, 5338–5342.
33 R. D. Hancock, L. J. Bartolotti and N. Kaltsoyannis, *Inorg. Chem.*, 2006, **45**, 10780–10785.
34 R. Cao, T. M. Anderson, P. M. B. Piccoli, A. J. Schultz, T. F. Koetzle, Yu. V. Geletii, E. Slonkina, B. Hedman, K. O. Hodgson, K. I. Hardcastle, X.-K. Fang, M. L. Kirk, S. Knottenbelt, P. Kögerler, D. G. Musaev, K. Morokuma, M. Takahashi and C. G. Hill, *J. Am. Chem. Soc.*, 2007, **129**, 11118–11133.
35 P. Pyykkö, S. Riedel and M. Patzschke, *Chem.–Eur. J.*, 2005, **11**, 3511–3520.
36 D. S. Laitar, P. Müller, T. G. Gray and J. P. Sadighi, *Organometallics*, 2005, **24**, 4503–4505.
37 P. Pyykkö and N. Runeberg, *Chem.–Asian J.*, 2006, **1** 623–628.
38 R. Tonner, F. Oxler, B. Neumüller, W. Petz and G. Frenking, *Angew. Chem., Int. Ed.*, 2006, **45**, 8038–8042.
39 R. Tonner, G. Heydenrych and G. Frenking, *Chem.–Asian J.*, 2007, **2**, 1555–1567.
40 H. Schmidbaur, *Angew. Chem., Int. Ed.*, 2007, **46** 2984–2985.
41 G. Frenking, B. Neumüller, W. Petz, R. Tonner and F. Öxler, *Angew. Chem., Int. Ed.*, 2007, **46**, 2986–2987.
42 F.-X. Li and P. B. Armentrout, *J. Chem. Phys.*, 2006, **125**, 133114.
43 R. Olson, S. Varganov, M. S. Gordon and H. Metiu, *Chem. Phys. Lett.*, 2005, **412**, 416–419.
44 D.-K. Lee, I. S. Lim, Y. S. Lee, D. Hagebaum-Reignier and G.-H. Jeung, *J. Chem. Phys.*, 2007, **126**, 244313.
45 H.-B. Yi, M. Diefenbach, Y. C. Choi, E. C. Lee, H. M. Lee, B. H. Hong and K. S. Kim, *Chem.–Eur. J.*, 2006, **12**, 4885–4892.
46 P. Pyykkö, *Mol. Phys.*, 1989, **67**, 871–878.
47 A. W. Ehlers, E. J. Baerends, F. M. Bickelhaupt and U. Radius, *Chem.–Eur. J.*, 1998, **4**, 210–221.
48 D. Yu. Zubarev, A. I. Boldyrev, J. Li, H.-J. Zhai and L.-S. Wang, *J. Phys. Chem. A*, 2007, **111**, 1648–1658.
49 J. Velasquez III, B. Njegic, M. S. Gordon and M. A. Duncan, *J. Phys. Chem. A*, 2008, **112**, 1907–1913.
50 J. U. Reveles, P. Calaminici, M. R. Beltrán, A. M. Köster and S. N. Khanna, *J. Am. Chem. Soc.*, 2007, **129**, 15565–15571.
51 G. Sini, O. Eisenstein and R. H. Crabtree, *Inorg. Chem.*, 2002, **41**, 602–604.

52 H. M. Lee, M. Diefenbach, S. B. Suh, P. Tarakeshwar and K. S. Kim, *J. Chem. Phys.*, 2005, **123**, 074328.
53 S. Afyon, P. Höhm, M. Armbrüster, A. Baranov, F. R. Wagner, M. Somer and R. Kniep, *Z. Anorg. Allg. Chem.*, 2006, **632**, 1671–1680.
54 S. Kokatam, K. Ray, J. Pap, E. Bill, W. E. Geiger, R. J. LeSuer, P. H. Rieger, T. Weyhermüller, F. Neese and K. Wieghardt, *Inorg. Chem.*, 2007, **46**, 1100–1111.
55 M. T. Räisänen, N. Runeberg, M. Klinga, M. Nieger, M. Bolte, P. Pyykkö, M. Leskelä and T. Repo, *Inorg. Chem.*, 2007, **46**, 9954–9960.
56 R. P. Krawczyk, A. Hammerl and P. Schwerdtfeger, *ChemPhysChem*, 2006, **7**, 2286–2289.
57 J. S. Golightly, L. Gao, A. W. Castleman, Jr, D. E. Bergeron, J. W. Hudgens, R. J. Magyar and C. A. Gonzalez, *J. Phys. Chem. C*, 2007, **111**, 14625–14627.
58 J. Granatier, M. Urban and A. J. Sadlej, *J. Phys. Chem. A*, 2007, **111**, 13238–13244.
59 A. Antušek, M. Urban and A. J. Sadlej, *J. Chem. Phys.*, 2003, **119**, 7247–7262.
60 H. Bilz, *Cryst. Lattice Defects Amorphous Mater.*, 1985, **12**, 31–40.
61 J. Muñiz and E. Sansores, *Mater. Avanzados*, 2007, **5**(9), 15–24.
62 H. de la Riva, A. Pintado-Alba, M. Nieuwenhuyzen, C. Hardacre and C. Lagunas, *Chem. Commun.*, 2005, 4970–4972.
63 K. M. Anderson, A. E. Goeta and J. W. Steed, *Inorg. Chem.*, 2007, **46**, 6444–6451.
64 O. Elbjeirami, S. Yockel, C. F. Campana, A. K. Wilson and M. A. Omary, *Organometallics*, 2007, **26**, 2550–2560.
65 P. Pyykkö and P. Zaleski-Ejgierd, *J. Chem. Phys.*, 2008, **128**, 124309.
66 J. Li and P. Pyykkö, *Inorg. Chem.*, 1993, **32**, 2630–2634.
67 H. Fang and S.-G. Wang, *J. Phys. Chem. A*, 2007, **111**, 1562–1566.
68 S. Riedel, P. Pyykkö, R. A. Mata and H.-J. Werner, *Chem. Phys. Lett.*, 2005, **405**, 148–152.
69 M. A. Carvajal, S. Alvarez and J. J. Novoa, *Theor. Chem. Acc.*, 2006, **116**, 472–479.
70 J. Li and P. Pyykkö, *Chem. Phys. Lett.*, 1992, **197**, 586–590.
71 M. Barysz and P. Pyykkö, *Chem. Phys. Lett.*, 2000, **325**, 225–231.
72 P. Pyykkö, W. Schneider, A. Bauer, A. Bayler and H. Schmidbaur, *Chem. Commun.*, 1997, 1111–1112.
73 L.-Y. Cao, M. C. Jennings and R. J. Puddephatt, *Inorg. Chem.*, 2007, **46**, 1361–1368.
74 E. J. Fernández, A. Laguna, J. M. López-de-Luzuriaga, M. Monge, M. E. Olmos and R. Q. Puelles, *J. Phys. Chem. B*, 2005, **109**, 20652–20656.
75 F. Mendizabal, D. Donoso, C. Olea-Azar and R. Mera, *THEOCHEM*, 2007, **803**, 39–44.
76 E. J. Fernández, A. Laguna, J. M. López-de-Luzuriaga, M. Monge, M. Nema, M. E. Olmos, J. Pérez and C. Silvestru, *Chem. Commun.*, 2007, 571–573.
77 E. J. Fernández, A. Laguna, J. M. López-de-Luzuriaga, M. Monge and F. Mendizabal, *THEOCHEM*, 2008, **851**, 121–126.
78 H. Nuss and M. Jansen, *Angew. Chem., Int. Ed.*, 2006, **45**, 4369–4371.
79 E. S. Kryachko and F. Remacle, *Chem. Phys. Lett.*, 2005, **404**, 142–149.
80 F. Remacle and E. S. Kryachko, *Nano Lett.*, 2005, **5**, 735–739.
81 E. S. Kryachko and F. Remacle, *J. Chem. Phys.*, 2007, **127**, 194305.
82 E. S. Kryachko and F. Remacle, *J. Phys. Chem. B*, 2005, **109**, 22746–22757.
83 E. S. Kryachko, A. Karpfen and F. Remacle, *J. Phys. Chem. A*, 2005, **109**, 7309–7318.
84 G. N. Khairallah, R. A. J. O'Hair and M. J. Bruce, *Dalton Trans.*, 2006, 3699–3707.
85 D. Yu. Zubarev, J. Li, L.-S. Wang and A. I. Boldyrev, *Inorg. Chem.*, 2006, **45**, 5269–5271.
86 B. Kiran, X. Li, H.-J. Zhai and L.-S. Wang, *J. Chem. Phys.*, 2006, **125**, 133204.
87 A. A. Mohamed, A. P. Mayer, H. E. Abdou, M. D. Irwin, L. M. Pérez and J. P. Fackler, Jr, *Inorg. Chem.*, 2007, **46**, 11165–11172.
88 M. S. Wickleder, *Z. Anorg. Allg. Chem.*, 2001, **627**, 2112–2114.
89 T. K. Ghanty, *J. Chem. Phys.*, 2005, **123**, 074323.
90 T. K. Ghanty, *J. Chem. Phys.*, 2006, **124**, 124304.
91 T. K. Ghanty, *J. Chem. Phys.*, 2005, **123**, 241101.
92 L. Belpassi, I. Infante, F. Tarantelli and L. Visscher, *J. Am. Chem. Soc.*, 2008, **130**, 1048–1060.
93 W. H. Breckenridge, V. L. Ayles and T. G. Wright, *J. Phys. Chem. A*, 2008, **112**, 4209–4214.
94 A. Yousef, S. Shrestha, L. A. Viehland, E. P. F. Lee, B. R. Gray, V. L. Ayles, T. G. Wright and W. H. Breckenridge, *J. Chem. Phys.*, 2007, **127**, 154309.
95 R. J. Plowright, V. L. Ayles, M. J. Watkins, A. M. Gardner, R. R. Wright, T. G. Wright and W. H. Breckenridge, *J. Chem. Phys.*, 2007, **127**, 204308.
96 M. O. Hakala and P. Pyykkö, *Chem. Commun.*, 2006, 2890–2892.
97 P. Pyykkö, M. O. Hakala and P. Zaleski-Ejgierd, *Phys. Chem. Chem. Phys.*, 2007, **9**, 3025–3030.
98 P. Zaleski-Ejgierd, M. Hakala and P. Pyykkö, *Phys. Rev. B*, 2007, **76**, 094104.
99 P. Pyykkö and P. Zaleski-Ejgierd, *Phys. Chem. Chem. Phys.*, 2008, **10**, 114–120.
100 L. E. Sansores, R. Salcedo, A. Martínez and N. Mireles, *THEOCHEM*, 2006, **763**, 7–11.
101 J. Repp, G. Meyer, S. Paavilainen, F. E. Olsson and M. Persson, *Science*, 2006, **312**, 1196–1199.
102 M. Sterrer, M. Yulikov, T. Risse, H.-J. Freund, J. Carrasco, F. Illas, C. Di Valentin, L. Giordano and G. Pacchioni, *Angew. Chem., Int. Ed.*, 2006, **45**, 2633–2635.
103 C. Puzzarini and K. A. Peterson, *Chem. Phys.*, 2005, **311**, 177–186.
104 L. Gagliardi and P. Pyykkö, *Angew. Chem., Int. Ed.*, 2004, **43**, 1573–1576.
105 M. Santos, J. Marçalo, A. Pires de Matos, J. K. Gibson and R. G. Haire, *Eur. J. Inorg. Chem.*, 2006, 3346–3349.
106 P. Hrobárik, M. Straka and P. Pyykkö, *Chem. Phys. Lett.*, 2006, **431**, 6–12.
107 S.-D. Li and C.-Q. Miao, *J. Phys. Chem. A*, 2005, **109** 7594–7597.
108 I. J. Blackmore, A. J. Bridgeman, N. Harris, M. A. Holdaway, J. F. Rooms, E. L. Thompson and N. A. Young, *Angew. Chem., Int. Ed.*, 2005, **44**, 6746–6750.
109 H. Grönbeck, M. Walter and H. Häkkinen, *J. Am. Chem. Soc.*, 2006, **128**, 10268–10275.
110 H.-J. Zhai, X. Li and L.-S. Wang, in *The Chemical Physics of Solid Surfaces*, Elsevier, Amsterdam, 2005, vol. 12, pp. 91–150.
111 I. L. Garzón, in *Dekker Encyclopedia of Nanoscience and Nanotechnology*, Marcel Dekker, New York, 2004, pp. 1287–1296.
112 Z.-F. Chen, S. Neukermans, X. Wang, E. Janssens, Z. Zhou, R. E. Silverans, R. B. King, P. von Ragué Schleyer and P. Lievens, *J. Am. Chem. Soc.*, 2006, **128**, 12829–12834.
113 P. Pyykkö and Y.-F. Zhao, *Chem. Phys. Lett.*, 1991, **177**, 103–106.
114 R. M. Olson and M. S. Gordon, *J. Chem. Phys.*, 2007, **126**, 214310.
115 Y.-K. Han, *J. Chem. Phys.*, 2006, **124**, 024316.
116 A. A. Rusakov, E. Rykova, G. E. Scuseria and A. Zaitsevskii, *J. Chem. Phys.*, 2007, **127**, 164322.
117 W. Fa, C.-F. Luo and J.-M. Dong, *Phys. Rev. B*, 2005, **72**, 205428.
118 M. P. Johansson, A. Lechtken, D. Schooss, M. M. Kappes and F. Furche, *Phys. Rev. A*, 2008, **77**, 053202.
119 S. Bulusu and X. C. Zeng, *J. Chem. Phys.*, 2006, **125**, 154303.
120 E. S. Kryachko and F. Remacle, *Int. J. Quantum Chem.*, 2007, **107**, 2922–2934.
121 K. J. Taylor, C. L. Pettiette-Hall, O. Chesnovsky and R. E. Smalley, *J. Chem. Phys.*, 1992, **96**, 3319–3329.
122 M. P. Johansson, D. Sundholm and J. Vaara, *Angew. Chem., Int. Ed.*, 2004, **43**, 2678–2681.
123 X. Gu, M. Ji, S. H. Wei and X. G. Gong, *Phys. Rev. B*, 2004, **70**, 205401.
124 M. J. Oila and A. M. P. Koskinen, *ARKIVOC*, 2006, **15** 76–83.
125 J.-L. Wang, J. Jellinek, J.-J. Zhao, Z.-F. Chen, R. B. King and P. von Ragué Schleyer, *J. Phys. Chem. A*, 2005, **109**, 9265–9269.
126 D.-X. Tian, J.-J. Zhao, B.-L. Wang and R. B. King, *J. Phys. Chem. A*, 2007, **111**, 411–414.
127 W. Fa and J.-M. Dong, *J. Chem. Phys.*, 2006, **124**, 114310.

128 S. Bulusu, X. Li, L.-S. Wang and X. C. Zeng, *Proc. Natl. Acad. Sci. U. S. A.*, 2006, **103**, 8326–8330.
129 P. Pyykkö, *J. Organomet. Chem.*, 2006, **691**, 4336–4340.
130 R. Ferrando, A. Fortunelli and G. Rossi, *Phys. Rev. B*, 2005, **72**, 085449.
131 E. M. Fernández, J. M. Soler and L. C. Balbás, *Phys. Rev. B*, 2006, **73**, 235433.
132 M. Walter, H. Häkkinen, J. Stanzel, M. Neeb and W. Eberhardt, *Phys. Rev. B*, 2007, **76**, 155422.
133 X.-P. Xing, B.-W. Yoon, U. Landman and J. H. Parks, *Phys. Rev. B*, 2006, **74**, 165423.
134 S. Bulusu, X. Li, L.-S. Wang and X. C. Zeng, *J. Phys. Chem. C*, 2007, **111**, 4190–4198.
135 B.-W. Yoon, P. Koskinen, B. Huber, O. Kostko, B. von Issendorf, H. Häkkinen, M. Moseler and U. Landman, *ChemPhysChem*, 2006, **8**, 157–161.
136 M. Ji, X. Gu, X.-G. Gong, J. Li and L.-S. Wang, *Angew. Chem., Int. Ed.*, 2005, **44**, 7119–7123.
137 A. Lechtken, D. Schooss, J. R. Stairs, M. N. Blom, F. Furche, N. Morgner, O. Kostko, B. von Issendorff and M. M. Kappes, *Angew. Chem., Int. Ed.*, 2007, **46**, 2944–2948.
138 P. Pyykkö, *Nat. Nanotechnol.*, 2007, **2**, 273–274.
139 K. Hansen, A. Herlert, L. Schweikhard and M. Vogel, *Phys. Rev. A*, 2006, **73**, 063202.
140 H. Häkkinen and M. Moseler, *Comput. Mater. Sci.*, 2006, **35**, 332–336.
141 A. J. Karttunen, M. Linnolahti, T. A. Pakkanen and P. Pyykkö, *Chem. Commun.*, 2008, 465–467.
142 G. Grochola, S. P. Russo and I. K. Snook, *J. Chem. Phys.*, 2007, **126**, 164707.
143 A. S. Barnard and L. A. Curtiss, *ChemPhysChem*, 2006, **7**, 1544–1553.
144 B. C. Curley, R. L. Johnston, N. P. Young, Z. Y. Li, M. Di Vece, R. E. Palmer and A. L. Bieloch, *J. Phys. Chem. C*, 2007, **111**, 17846–17851.
145 Y. Dong and M. Springborg, *J. Phys. Chem. C*, 2007, **111**, 12528–12535.
146 Y. Dong and M. Springborg, *Eur. Phys. J. D*, 2007, **43**, 15–18.
147 J. M. Soler, M. R. Beltrán, K. Michaelian, I. L. Garzón, P. Ordejón, D. Sánchez-Portal and E. Artacho, *Phys. Rev. B*, 2000, **61**, 5771–5780.
148 J. M. Soler, I. L. Garzón and J. D. Joannopoulos, *Solid State Commun.*, 2001, **117**, 621–625.
149 J.-L. Wang, M.-L. Yang, J. Jellinek and G.-H. Wang, *Phys. Rev. A*, 2006, **74**, 023202.
150 R. Popescu, E. Müller, M. Wanner, D. Gerthsen, M. Schowalter, A. Rosenauer, A. Böttcher, D. Löffler and P. Weis, *Phys. Rev. B*, 2007, **76**, 235411.
151 B. Soulé de Bas, M. J. Ford and M. B. Cortie, *J. Phys.: Condens. Matter*, 2006, **18**, 55–74.
152 P. Koskinen, H. Häkkinen, B. Huber, B. von Issendorff and M. Moseler, *Phys. Rev. Lett.*, 2007, **98**, 015701.
153 S. Krishnamurty, G. S. Shafai, D. G. Kanhere, B. Soulé de Bas and M. J. Ford, *J. Phys. Chem. A*, 2007, **111**, 10769–10775.
154 Y. H. Chui, I. K. Snook and S. P. Russo, *Phys. Rev. B*, 2007, **76**, 195427.
155 E. Mendez-Villuendas and R. K. Bowles, *Phys. Rev. Lett.*, 2007, **98**, 185503.
156 J. Stanzel, F. Burmeister, M. Neeb, W. Eberhardt, R. Mitrić, C. Bürgel and V. Bonačić-Koutecký, *J. Chem. Phys.*, 2007, **127**, 164312.
157 Z.-F. Chen and R. B. King, *Chem. Rev.*, 2005, **105**, 3613–3642.
158 Z.-F. Chen and R. B. King, *ChemTracts—Inorg. Chem.*, 2006, **19**, 45.
159 P. D. J. G. Calero, C. J. Ackerson, D. A. Bushneit and R. D. Kornberg, *Science*, 2007, **318**, 430–433.
160 R. L. Whetten and R. C. Price, *Science*, 2007, **318**, 407–408.
161 K. Spivey, J. I. Williams and L.-C. Wang, *Chem. Phys. Lett.*, 2006, **432**, 163–166.
162 J. Graciani, J. Oviedo and J. F. Sanz, *J. Phys. Chem. B*, 2006, **110**, 11600–11603.
163 Q. Sun, Q. Wang, P. Jena and Y. Kawazoe, *ACS Nano*, 2008, **2**, 341–347.
164 Y. Gao, S. Bulusu and X. C. Zeng, *J. Am. Chem. Soc.*, 2005, **127**, 15680–15681.
165 Y. Gao, S. Bulusu and X. C. Zeng, *ChemPhysChem*, 2006, **7**, 2275–2278.
166 L.-M. Wang, S. Bulusu, H.-J. Zhai, X.-C. Zeng and L.-S. Wang, *Angew. Chem., Int. Ed.*, 2007, **46**, 2915–2918.
167 M. Walter and H. Häkkinen, *Phys. Chem. Chem. Phys.*, 2006, **8**, 5407–5411.
168 L.-M. Wang, S. Bulusu, W. Huang, R. Pal, L.-S. Wang and X. C. Zheng, *J. Am. Chem. Soc.*, 2007, **129**, 15136–15137.
169 Q. Sun, Q. Wang, G. Chen and P. Jena, *J. Chem. Phys.*, 2007, **127**, 214706.
170 J.-L. Wang, J.-L. Bai, J. Jellinek and X. C. Zeng, *J. Am. Chem. Soc.*, 2007, **129**, 4110–4111.
171 X. Li, B. Kiran, L.-F. Cui and L.-S. Wang, *Phys. Rev. Lett.*, 2005, **95**, 253401.
172 R. Ferrando, A. Fortunelli and R. L. Johnston, *Phys. Chem. Chem. Phys.*, 2008, **10**, 640–649.
173 D. Cheng, S. Huang and W. Wang, *Eur. Phys. J. D*, 2006, **39**, 41–48.
174 F.-Y. Chen, B. C. Curley, G. Rossi and R. L. Johnston, *J. Phys. Chem. C*, 2007, **111**, 9157–9165.
175 D.-J. Cheng, S.-P. Huang and W.-C. Wang, *Phys. Rev. B*, 2006, **74**, 064117.
176 A. Spiekermann, S. D. Hoffmann, F. Kraus and T. F. Fässler, *Angew. Chem., Int. Ed.*, 2007, **46**, 1638–1640.
177 A. Kumar, P. C. Mishra and S. Suhai, *J. Phys. Chem. A*, 2006, **110**, 7719–7727.
178 R. J. C. Batista, M. S. C. Mazzoni, L. O. Ladeira and H. Chacham, *Phys. Rev. B*, 2005, **72**, 085447.
179 X.-L. Ding, J.-L. Yang, J. G. Hou and Q.-S. Zhu, *THEOCHEM*, 2005, **755**, 9–17.
180 H. Häkkinen, M. Walter and H. Grönbeck, *J. Phys. Chem. B*, 2006, **110**, 9927–9931.
181 P. Sevillano, O. Fuhr, M. Kattannek, P. Nava, O. Hampe, S. Lebedkin, R. Ahlrichs, D. Fenske and M. M. Kappes, *Angew. Chem., Int. Ed.*, 2006, **45**, 3702–3708.
182 I. L. Garzón, J. A. Reyes-Nava, J. I. Rodríguez-Hernández, I. Sigal, M. R. Beltrán and K. Michaelian, *Phys. Rev. B*, 2002, **66**, 073403.
183 F. R. Negreiros, E. A. Soares, V. E. de Carvalho and G. Bozzolo, *Phys. Rev. B*, 2007, **76**, 245432.
184 F. Naumkin, *Phys. Chem. Chem. Phys.*, 2006, **8**, 2539–2545.
185 X. López-Lozano, L. A. Pérez and I. L. Garzón, *Phys. Rev. Lett.*, 2006, **97**, 233401.
186 C. E. Román-Velázquez, C. Noguez and I. L. Garzón, *J. Phys. Chem. B*, 2007, **107**, 12035–12038.
187 G.-R. Zhou and Q.-M. Gao, *Solid State Commun.*, 2005, **136**, 32–35.
188 H. S. Park and J. A. Zimmerman, *Phys. Rev. B*, 2005, **72**, 054106.
189 J.-S. Lin, S.-P. Ju and W.-J. Lee, *Phys. Rev. B*, 2005, **72**, 085448.
190 H. S. Park, K. Gall and J. A. Zimmerman, *Phys. Rev. Lett.*, 2005, **95**, 255504.
191 P. Seal and S. Chakrabarti, *Chem. Phys.*, 2007, **335**, 201–204.
192 A. Ayuela, M. J. Puska, R. M. Nieminen and J. A. Alonso, *Phys. Rev. B*, 2005, **72**, 161403.
193 N. V. Skorodumova, S. I. Simak, A. E. Kochetov and B. Johansson, *Phys. Rev. B*, 2005, **72**, 193413.
194 I. K. Yanson, O. I. Shklyarevskii, Sz. Csonka, H. van Kempen, S. Speller, A. I. Yanson and J. M. van Ruitenbeek, *Phys. Rev. Lett.*, 2005, **95**, 256806.
195 A. Md. Asaduzzaman and M. Springborg, *Phys. Rev. B*, 2005, **72**, 165422.
196 F. D. Novaes, A. J. R. da Silva, E. Z. da Silva and A. Fazzio, *Phys. Rev. Lett.*, 2006, **96**, 016104.
197 F. D. Novaes, A. J. R. da Silva, A. Fazzio and E. Z. da Silva, *Appl. Phys. A*, 2005, **81**, 1551–1558.
198 E. Hobi, Jr, A. J. R. da Silva, F. D. Novaes, E. Z. da Silva and A. Fazzio, *Phys. Rev. Lett.*, 2005, **95**, 169601.
199 E. Anglada, J. A. Torres, F. Yndurain and J. M. Soler, *Phys. Rev. Lett.*, 2007, **98**, 096102.
200 A. I. Mares and J. M. van Ruitenbeek, *Phys. Rev. B*, 2005, **72**, 205402.
201 X.-P. Yang and J.-M. Dong, *Phys. Rev. B*, 2005, **71**, 233403.
202 R. T. Senger, S. Dag and S. Ciraci, *Turk. J. Phys.*, 2005, **29**, 269–276.
203 J. Zhou and J.-M. Dong, *Phys. Rev. B*, 2007, **75**, 155423.

204 F. Tielens and J. Andrés, *J. Phys. Chem. C*, 2007, **111**, 10342–10346.
205 G. Barcaro and A. Fortunelli, *J. Chem. Theory Comput.*, 2005, **1**, 972–985.
206 M. Walter, P. Frondelius, K. Honkala and H. Häkkinen, *Phys. Rev. Lett.*, 2007, **99**, 096102.
207 R. M. Ferullo, G. R. Garda, P. G. Belelli, M. M. Branda and N. J. Castellani, *THEOCHEM*, 2006, **769**, 217–223.
208 K. H. Lim, O. Zakharieva, A. M. Shor and N. Rösch, *Chem. Phys. Lett.*, 2007, **444**, 280–286.
209 L. M. Molina and J. A. Alonso, *J. Phys. Chem. C*, 2007, **111**, 6668–6677.
210 A. Locatelli, T. Pabisiak, A. Pavlovska, T. O. Mentes, L. Aballe, A. Klejna and E. Bauer, *J. Phys.: Condens. Matter*, 2007, **19**, 082202.
211 D. Pillay and G. S. Hwang, *THEOCHEM*, 2006, **771**, 129–133.
212 K. Okazaki, S. Ichikawa, Y. Maeda, M. Haruta and M. Kohyama, *Appl. Catal., A*, 2005, **291**, 45–54.
213 J. A. Rodriguez, F. Viñes, F. Illas, P. Liu, Y. Takahashi and K. Nakamura, *J. Chem. Phys.*, 2007, **127**, 211102.
214 R. Grau-Crespo, N. Cruz Hernandez, J. F. Sanz and N. H. de Leeuw, *J. Phys. Chem. C*, 2007, **111**, 10448–10454.
215 S. Chrétien and H. Metiu, *J. Chem. Phys.*, 2007, **127**, 084704.
216 S. Chrétien and H. Metiu, *J. Chem. Phys.*, 2008, **128**, 044714.
217 K. M. Neyman, C. Inntam, L. V. Moskaleva and N. Rösch, *Chem.–Eur. J.*, 2007, **13**, 277–286.
218 M. Walter and H. Häkkinen, *Phys. Rev. B*, 2005, **72**, 205440.
219 D. Ricci, A. Bongiorno, G. Pacchioni and U. Landman, *Phys. Rev. Lett.*, 2006, **97**, 036106.
220 U. Landman, B. Yoon, C. Zhang, U. Heiz and M. Arenz, *Top. Catal.*, 2007, **44**, 145–158.
221 P. Frondelius, H. Häkkinen and K. Honkala, *Phys. Rev. B*, 2007, **76**, 073406.
222 A. Del Vitto, G. Pacchioni, K. H. Lim, N. Rösch, J.-M. Antonietti, M. Michalski, U. Heiz and H. Jones, *J. Phys. Chem. B*, 2005, **109**, 19876–19884.
223 N. Cruz Hernández, J. Graciani, A. Márquez and J. Fdez Sanz, *Surf. Sci.*, 2005, **575**, 189–196.
224 J. Akola and H. Häkkinen, *Phys. Rev. B*, 2006, **74**, 165404.
225 J.-P. Jalkanen, M. Halonen, D. Fernández-Torre, K. Laasonen and L. Halonen, *J. Phys. Chem. A*, 2007, **111**, 12317–12326.
226 S. I. Bosko, L. V. Moskaleva, A. V. Matveev and N. Rösch, *J. Phys. Chem. A*, 2007, **111**, 6870–6880.
227 R. J. C. Batista, M. S. C. Mazzoni, I. L. Garzón, M. R. Beltrán and H. Chacham, *Phys. Rev. Lett.*, 2006, **96**, 116802.
228 K. Nobusada and T. Iwasa, *J. Phys. Chem. C*, 2007, **111**, 14279–14282.
229 A. M. Shikin, A. Varykhalov, G. V. Prudnikova, D. Usachov, V. K. Adamchuk, Y. Yamada, J. D. Riley and O. Rader, *Phys. Rev. Lett.*, 2008, **100**, 057601.
230 E. Cottancin, G. Celep, J. Lermé, M. Pellarin, J. R. Huntzinger, J. L. Vialle and M. Broyer, *Theor. Chem. Acc.*, 2006, **116**, 514–523.
231 F. Hao, C. L. Nehl, J. H. Hafner and P. Nordlander, *Nano Lett.*, 2007, **7**, 729–732.
232 S. Mazevet, J. Clérouin, V. Recoules, P. M. Anglade and G. Zerah, *Phys. Rev. Lett.*, 2005, **95**, 085002.
233 Y. Ping, D. Hanson, I. Koslow, T. Ogitsu, D. Prendergast, E. Schwegler, G. Collins and A. Ng, *Phys. Rev. Lett.*, 2006, **96**, 255003.
234 L. Dubrovinsky, N. Dubrovinskaia, W. A. Crichton, A. S. Mikhayluskin, S. I. Simak, I. A. Abrikosov, J. S. de Almeida, R. Ahuja, W. Luo and B. Johansson, *Phys. Rev. Lett.*, 2007, **98**, 045503.
235 W. Grochala, R. Hoffmann, J. Feng and N. W. Ashcroft, *Angew. Chem., Int. Ed.*, 2007, **46**, 3620–3642.
236 P. G. Etchegoin, E. C. Le Ru and M. Meyer, *J. Chem. Phys.*, 2006, **125**, 164705.
237 R. Yu and X. F. Zhang, *Phys. Rev. B*, 2005, **72**, 054103.
238 S. V. Barabash, V. Blum, S. Müller and A. Zunger, *Phys. Rev. B*, 2006, **74**, 035108.
239 M. H. F. Sluiter, C. Colinet and A. Pasturel, *Phys. Rev. B*, 2006, **73**, 174204.
240 S. Takeda, H. Fujii, Y. Kawakita, S. Tahara, S. Nakashima, S. Kohara and M. Itou, *J. Alloys Compd.*, 2008, **452**, 149–153.
241 Y. J. Feng, K. P. Bohnen and C. T. Chan, *Phys. Rev. B*, 2005, **72**, 125401.
242 V. M. Silkin, J. M. Pitarke, E. V. Chulkov and P. M. Echenique, *Phys. Rev. B*, 2005, **72**, 115435.
243 J. D. Walls and E. J. Heller, *Nano Lett.*, 2007, **7**, 3377–3382.
244 J.-W. Feng, W.-Q. Zhang and W. Jiang, *Phys. Rev. B*, 2005, **72**, 115423.
245 A. J. Karttunen and T. A. Pakkanen, *J. Phys. Chem. B*, 2006, **110**, 25926–25930.
246 G. Kyriakou, F. J. Williams, M. S. Tikhov, A. Wander and R. M. Lambert, *Phys. Rev. B*, 2005, **72**, 121408.
247 H. J. Gotsis, I. Rivalta, E. Sicilia and N. Russo, *Chem. Phys. Lett.*, 2007, **442**, 105–109.
248 P. Romaniello and P. L. de Boeij, *J. Chem. Phys.*, 2007, **127**, 174111.
249 E. J. Fernandez, A. Laguna and J. M. L. de Luzuriaga, *Dalton Trans.*, 2007, 1969–1981.
250 G. Hodes, *Adv. Mater.*, 2007, **19**, 639–655.
251 S. K. Ghosh and T. Pal, *Chem. Rev.*, 2007, **107**, 4797–4862.
252 C. M. Aikens and G. C. Schatz, *J. Phys. Chem. A*, 2006, **110**, 13317–13324.
253 S.-Q. Song, G.-F. Wang, A.-P. Ye and G. Jiang, *J. Phys. B*, 2007, **40**, 475–484.
254 J. Bieroń, C. Froese Fischer, P. Jönsson and P. Pyykkö, *J. Phys. B*, 2008, **41**, 115002.
255 M. Winkelmann, G. Fischer, B. Pilawa and M. S. S. Brooks, *Phys. Rev. B*, 2006, **73**, 165107.
256 H. Yakobi, E. Eliav and U. Kaldor, *J. Chem. Phys.*, 2007, **126**, 184305.
257 L. Belpassi, F. Tarantelli, A. Sgamellotti, H. M. Quiney, J. N. P. van Stralen and L. Visscher, *J. Chem. Phys.*, 2007, **126**, 064314.
258 C. Thierfelder, P. Schwerdtfeger and T. Saue, *Phys. Rev. A*, 2007, **76**, 034502.
259 J. David and A. Restrepo, *Phys. Rev. A*, 2007, **76**, 052511.
260 L. Fernández-Seivane and J. Ferrer, *Phys. Rev. Lett.*, 2007, **99**, 183401.
261 W.-D. Luo, S. J. Pennycook and S. T. Pantelides, *Nano Lett.*, 2007, **7**, 3134–3137.
262 P. Pyykkö and N. Runeberg, *Angew. Chem., Int. Ed.*, 2002, **41**, 2174–2176.
263 F. Michael, C. Gonzalez, V. Mujica, M. Marquez and M. Ratner, *Phys. Rev. B*, 2007, **76**, 224409.
264 R. P. S. Fartaria, F. F. M. Freitas and F. M. S. Silva Fernandes, *J. Electroanal. Chem.*, 2005, **574**, 321–331.
265 A. Grigoriev, N. V. Skorodumova, S. I. Simak, G. Wendin, B. Johansson and R. Ahuja, *Phys. Rev. Lett.*, 2006, **97**, 236807.
266 A. Fujii, M. Tsutsui, S. Kurokawa and A. Sakai, *Phys. Rev. B*, 2005, **72**, 045407.
267 M. Dreher, F. Pauly, J. Heurich, J. C. Cuevas, E. Scheer and P. Nielaba, *Phys. Rev. B*, 2005, **72**, 075435.
268 H. Basch and M. A. Ratner, *J. Chem. Phys.*, 2005, **123** 234704.
269 Z.-Y. Ning, J.-Z. Chen, S.-M. Hou, J.-X. Zhang, Z.-Y. Liang, J. Zhang and R.-S. Han, *Phys. Rev. B*, 2005, **72**, 155403.
270 G. C. Solomon, A. Gagliardi, A. Pecchia, T. Frauenheim, A. Di Carlo, J. R. Reimers and N. S. Hush, *J. Chem. Phys.*, 2006, **124**, 094704.
271 F. Remacle and R. D. Levine, *Faraday Discuss.*, 2005, **131**, 45–67.
272 J. K. Viljas, J. C. Cuevas, F. Pauly and M. Häfner, *Phys. Rev. B*, 2005, **72**, 245415.
273 X.-H. Zheng, X.-Q. Shi, Z.-X. Dai and Z. Zeng, *Phys. Rev. B*, 2006, **74**, 085418.
274 J. M. Seminario, A. G. Zacarias and J. M. Tour, *J. Am. Chem. Soc.*, 1999, **121**, 411–416.
275 S. Y. Quek, L. Venkataraman, H. J. Choi, S. G. Louie, M. S. Hybertsen and J. B. Neaton, *Nano Lett.*, 2007, **7**, 3477–3482.
276 L.-M. Yan and J. M. Seminario, *Int. J. Quantum Chem.*, 2007, **107**, 440–450.
277 N. Armstrong, R. C. Hoft, A. McDonagh, M. B. Cortie and M. J. Ford, *Nano Lett.*, 2007, **7**, 3018–3022.
278 J. Samela, J. Kotakoski, K. Nordlund and J. Keinonen, *Nucl. Instrum. Methods Phys. Res., Sect. B*, 2005, **239**, 331–346.
279 G. C. Bond, C. Louis and D. T. Thompson, *Catalysis by Gold*, Imperial College Press, London, 2006.
280 D. J. Gorin and F. D. Toste, *Nature*, 2007, **446**, 395–403.

281 A. S. K. Hashmi and G. J. Hutchings, *Angew. Chem., Int. Ed.*, 2006, **45**, 7896–7936.
282 A. S. K. Hashmi, F. Ata, J. W. Bats, M. C. Blanco, W. Frey, M. Hamzic, M. Rudolph, R. Salathé, S. Schäfer and M. Wölfle, *Gold Bull.*, 2007, **40**(1), 31–35.
283 A. S. K. Hashmi, *Chem. Rev.*, 2007, **107**, 3180–3211.
284 P. P. Edwards and J. M. Thomas, *Angew. Chem., Int. Ed.*, 2007, **46**, 5480–5486.
285 R. Burks, *Chem. Eng. News*, 2007, **85**(39), 87–91.
286 M. C. Kung, R. J. Davis and H. H. Kung, *J. Phys. Chem. C*, 2007, **111**, 11767–11775.
287 C. Louis, in *Nanoparticles and Catalysis*, ed. D. Astruc, Wiley-VCH, Weinheim, 2007, pp. 475–503.
288 T. Ishida and M. Haruta, *Angew. Chem., Int. Ed.*, 2007, **46**, 7154–7156.
289 C. W. Corti, R. J. Holliday and D. T. Thompson, *Top. Catal.*, 2007, **44**, 331–343.
290 D. T. Thompson, *NanoToday*, 2007, **2**(4), 40–43.
291 J. Roithová, J. Hrušák, D. Schröder and H. Schwarz, *Inorg. Chim. Acta*, 2005, **358**, 4287–4292.
292 A. Comas-Vives, C. González-Arellano, A. Corma, M. Iglesias, F. Sánchez and G. Ujaque, *J. Am. Chem. Soc.*, 2006, **128**, 4756–4765.
293 H. Rabaâ, B. Engels, T. Hupp and A. S. K. Hashmi, *Int. J. Quantum Chem.*, 2007, **107**, 359–365.
294 V. Bonačić-Koutecký and R. Mitrić, *Chem. Rev.*, 2005, **105**, 11–65.
295 D. Loffreda, *Surf. Sci.*, 2006, **600**, 2103–2112.
296 T.-F. Zhang, Z.-P. Liu, S. M. Driver, S. J. Pratt, S. J. Jenkins and D. A. King, *Phys. Rev. Lett.*, 2005, **95**, 266102.
297 M.-S. Chen and D. W. Goodman, *Acc. Chem. Res.*, 2006, **39**, 739–746.
298 M. Okumura, Y. Kitagawa, M. Haruta and K. Yamaguchi, *Appl. Catal., A*, 2005, **291**, 37–44.
299 L. Barrio, P. Liu, J. A. Rodríguez, J. M. Campos-Martín and J. L. G. Fierro, *J. Chem. Phys.*, 2006, **125**, 164715.
300 A. Corma, M. Boronat, S. González and F. Illas, *Chem. Commun.*, 2007, 3371–3373.
301 E. Bus, J. T. Miller and J. A. van Bokhoven, *J. Phys. Chem. B*, 2005, **109**, 14581–14587.
302 E. A. Ivanova Shor, V. A. Nasluzov, A. M. Shor, G. N. Vayssilov and N. Rösch, *J. Phys. Chem. C*, 2007, **111**, 12340–12351.
303 C. Sarpe-Tudoran, B. Fricke, J. Anton and V. Pers[h]ina, *J. Chem. Phys.*, 2007, **126**, 174702.
304 E. A. Rykova, A. Zaitsevskii, N. S. Mosyagin, T. A. Isaev and A. V. Titov, *J. Chem. Phys.*, 2006, **125**, 241102.
305 X.-L. Ding, Y.-Z. Li, J.-K. Yang, J. G. Hou and Q.-S. Zhu, *J. Chem. Phys.*, 2004, **120**, 9594–9600.
306 L. M. Molina and B. Hammer, *J. Chem. Phys.*, 2005, **123** 161104.
307 F. Tielens, J. Andrés, T.-D. Chau, T. Visart de Bocarmé, N. Kruse and P. Geerlings, *Chem. Phys. Lett.*, 2006, **421** 433–438.
308 M. L. Kimble, A. W. Castleman, Jr, C. Bürgel and V. Bonačić-Koutecký, *Int. J. Mass Spectrom.*, 2006, **254**, 163–167.
309 M. L. Kimble, A. W. Castleman, Jr, R. Mitrić, C. Bürgel and V. Bonačić-Koutecký, *J. Am. Chem. Soc.*, 2004, **126**, 2526–2535.
310 M. L. Kimble, N. A. Moore, G. E. Johnson and A. W. Castleman Jr., *J. Chem. Phys.*, 2006, **125**, 204311.
311 R. Mitrić, C. Bürgel and V. Bonačić-Koutecký, *Proc. Natl. Acad. Sci. U. S. A.*, 2007, **104**, 10314–10317.
312 L. Barrio, P. Liu, J. A. Rodríguez, J. M. Campos-Martín and J. L. G. Fierro, *J. Phys. Chem. C*, 2007, **111**, 19001–19008.
313 J. L. C. Fajín, M. N. D. S. Cordeiro and J. R. B. Gomes, *J. Phys. Chem. C*, 2007, **111**, 17311–17321.
314 M. Okumura, M. Haruta, Y. Kitagawa and K. Yamaguchi, *Gold Bull.*, 2007, **40**, 40–44.
315 D. C. Lim, I. Lopez-Salido, R. Dietsche, M. Bubek and Y. D. Kim, *Chem. Phys.*, 2006, **330**, 441–448.
316 H.-Q. Shi and C. Stampfl, *Phys. Rev. B*, 2007, **76**, 075327.
317 F. Tielens, J. Andrés, M. Van Brussel, C. Buess-Hermann and P. Geerlings, *J. Phys. Chem. B*, 2005, **109**, 7624–7630.
318 T. Visart de Bocarmé, T.-D. Chau, F. Tielens, J. Andrés, P. Gaspard, R. L. C. Wang, H. J. Kreuzer and N. Kruse, *J. Chem. Phys.*, 2006, **125**, 054703.
319 G. Teobaldi and F. Zerbetto, *J. Phys. Chem. C*, 2007, **111**, 13879–13885.
320 G. L. Beltramo, T. E. Shubina, S. J. Mitchell and M. T. M. Koper, *J. Electroanal. Chem.*, 2004, **563**, 111–120.
321 A. Fielicke, G. von Helden, G. Meijer, B. Simard and D. M. Rayner, *J. Phys. Chem. B*, 2005, **109**, 23935–23940.
322 N. S. Phala and E. van Steen, *Gold Bull.*, 2007, **40** 150–153.
323 K. P. McKenna and A. L. Shluger, *J. Phys. Chem. C*, 2007, **111**, 18848–18852.
324 L. Giordano, J. Carrasco, C. Di Valentin and G. Pacchioni, *J. Chem. Phys.*, 2006, **124**, 174709.
325 L. Giordano and G. Pacchioni, *Phys. Chem. Chem. Phys.*, 2006, **8**, 3335–3341.
326 E. M. Fernández and L. C. Balbás, *J. Phys. Chem. B*, 2006, **110**, 10449–10454.
327 A. M. Joshi, M. H. Tucker, W. N. Delgass and K. T. Thomson, *J. Chem. Phys.*, 2006, **125**, 194707.
328 L.-C. Wang, *Chem. Phys. Lett.*, 2007, **443**, 304–308.
329 C.-R. Song, Q.-F. Ge and L.-C. Wang, *J. Phys. Chem. B*, 2005, **109**, 22341–22350.
330 L. Piccolo, D. Loffreda, F. J. Cadete Santos Aires, C. Deranlot, Y. Jugnet, P. Sautet and J. C. Bertolini, *Surf. Sci.*, 2004, **566–568**, 995–1000.
331 D. Loffreda and P. Sautet, *J. Phys. Chem. B*, 2005, **109**, 9596–9603.
332 D. Loffreda, L. Piccolo and P. Sautet, *Phys. Rev. B*, 2005, **71**, 113414.
333 F. Tielens, L. Gracia, V. Polo and J. Andrés, *J. Phys. Chem. A*, 2007, **111**, 13255–13263.
334 A. Prestianni, A. Martorana, F. Labat, I. Ciofini and C. Adamo, *J. Phys. Chem. B*, 2006, **110**, 12240–12248.
335 A. Fielicke, G. von Helden, G. Meijer, B. Simard and D. M. Rayner, *Phys. Chem. Chem. Phys.*, 2005, **7**, 3906–3909.
336 U. Ekström, H. Ottosson and P. Norman, *J. Phys. Chem. C*, 2007, **111**, 13846–13850.
337 C. Vericat, M. E. Vela and R. C. Salvarezza, *Phys. Chem. Chem. Phys.*, 2005, **7**, 3258–3268.
338 C. Vericat, M. E. Vela, G. A. Benitez, J. A. Martin Gago, X. Torrelles and R. C. Salvarezza, *J. Phys.: Condens. Matter*, 2006, **18**, R867–R900.
339 N. Gonzalez-Lakunza, N. Lorente and A. Arnau, *J. Phys. Chem. C*, 2007, **111**, 12383–12390.
340 P. Maksymovych, D. C. Sorescu and J. T. Yates, Jr, *Phys. Rev. Lett.*, 2006, **97**, 146103.
341 R. Mazzarello, A. Cossaro, A. Verdini, R. Rousseau, L. Casalis, M. F. Danisman, L. Floreano, S. Scandolo, A. Morgante and G. Scoles, *Phys. Rev. Lett.*, 2007, **98**, 016102.
342 M. Yu, N. Bovet, C. J. Satterley, S. Bengió, K. R. J. Lovelock, P. K. Milligan, R. G. Jones, D. P. Woodruff and V. Dhanak, *Phys. Rev. Lett.*, 2006, **97**, 166102.
343 F. P. Cometto, P. Paredes-Oliveira, V. A. Macagno and E. M. Patrito, *J. Phys. Chem. B*, 2005, **109**, 21737–21748.
344 Y.-S. Leng, P. S. Krstić, J. C. Wells, P. T. Cummings and D. J. Dean, *J. Chem. Phys.*, 2005, **122**, 244721.
345 V. Perebeinos and M. Newton, *Chem. Phys.*, 2005, **319**, 159–166.
346 G. Heimel, L. Romaner, J.-L. Brédas and E. Zojer, *Phys. Rev. Lett.*, 2006, **96**, 196806.
347 T. Doneux, F. Tielens, P. Geerlings and Cl. Buess-Herman, *J. Phys. Chem. A*, 2006, **110**, 11346–11352.
348 T. Iwasa and K. Nobusada, *Chem. Phys. Lett.*, 2007, **441**, 268–272.
349 T. Iwasa and K. Nobusada, *J. Phys. Chem. C*, 2007, **111** 45–49.
350 S. Y. Quek, M. M. Biener, J. Biener, Bhattacharjee, C. M. Friend, U. V. Waghmare and E. Kaxiras, *J. Chem. Phys.*, 2007, **127**, 104704.
351 R. S. Neves, A. J. Motheo, R. P. S. Fartaria and F. M. S. Silva Fernandes, *J. Electroanal. Chem.*, 2007, **609**, 140–146.
352 R. S. Neves, A. J. Motheo, R. P. S. Fartaria and F. M. S. Silva Fernandes, *J. Electroanal. Chem.*, 2007, **612**, 179–185.
353 W.-K. Chen, S.-H. Liu, M.-J. Cao, Q.-G. Yan and C.-H. Lu, *THEOCHEM*, 2006, **770**, 87–91.
354 R. S. Neves, A. J. Motheo, F. M. S. Silva Fernandes and R. P. S. Fartaria, *J. Braz. Chem. Soc.*, 2004, **15**, 224–231.

355 A. M. McDonagh, H. M. Zareie, M. J. Ford, C. S. Barton, M. Ginic-Markovic and J. G. Matisons, *J. Am. Chem. Soc.*, 2007, **129**, 3533–3538.
356 W.-K. Chen, M.-J. Cao, S.-H. Liu, C.-H. Lu, Y. Xu and J.-Q. Li, *Chem. Phys. Lett.*, 2006, **417**, 414–418.
357 A. Bilić, J. R. Reimers, N. S. Hush, R. C. Hoft and M. J. Ford, *J. Chem. Theory Comput.*, 2006, **2**, 1093–1105.
358 K. Leung, S. B. Rempe, P. A. Schultz, E. M. Sproviero, V. S. Batista, M. E. Chandross and C. J. Medforth, *J. Am. Chem. Soc.*, 2006, **128**, 3659–3668.
359 K.-H. Lee, J.-J. Yu and Y. Morikawa, *Phys. Rev. B*, 2007, **75**, 045402.
360 G. Schull and R. Berndt, *Phys. Rev. Lett.*, 2007, **99**, 226105.
361 J. A. Rodriguez, M. Pérez, J. Evans, G. Liu and J. Hrbek, *J. Chem. Phys.*, 2005, **122**, 241101.
362 M. Arenz, U. Landman and U. Heiz, *ChemPhysChem*, 2006, **7**, 1871–1879.
363 A. Bongiorno and U. Landman, *Phys. Rev. Lett.*, 2005, **95**, 106102.
364 L. M. Molina and B. Hammer, *Appl. Catal., A*, 2005, **291**, 21–31.
365 Z.-P. Liu, *Phys. Rev. B*, 2006, **73**, 233410.
366 N. Cruz Hernández, J. Fdez. Sanz and J. A. Rodriguez, *J. Am. Chem. Soc.*, 2006, **126**, 15600–15601.
367 I. N. Remediakis, N. Lopez and J. K. Nørskov, *Appl. Catal., A*, 2005, **291**, 13–20.
368 A. Shiga and M. Haruta, *Appl. Catal., A*, 2005, **291**, 6–12.
369 C. Zhang, B.-W. Yoon and U. Landman, *J. Am. Chem. Soc.*, 2007, **129**, 2228–2229.
370 O. Guliamov, A. I. Frenkel, L. D. Menard, R. G. Nuzzo and L. Kronik, *J. Am. Chem. Soc.*, 2007, **129**, 10978–10979.
371 L. M. Liu, B. McAllister, H. Q. Ye and P. Hu, *J. Am. Chem. Soc.*, 2006, **128**, 4017–4022.
372 H. Kobayashi and Y. Shimodaira, *THEOCHEM*, 2006, **762**, 57–67.
373 F. Wang, D.-J. Zhang, H. Sun and Y. Ding, *J. Phys. Chem. C*, 2007, **111**, 11590–11597.
374 N. Marion, P. Carlqvist, R. Gealageas, P. de Frémont, F. Maseras and S. P. Nolan, *Chem.–Eur. J.*, 2007, **13** 6437–6451.
375 T. V. W. Janssens, B. S. Clausen, B. Hvolbæk, H. Falsig, C. H. Christensen, T. Bligaard and J. K. Nørskov, *Top. Catal.*, 2007, **44**, 15–26.
376 J. A. Rodriguez, S. Ma, P. Liu, J. Hrbek, J. Evans and M. Pérez, *Science*, 2007, **318**, 1757–1760.
377 J. G. Wang and B. Hammer, *Phys. Rev. Lett.*, 2006, **97** 136107.
378 J.-Y. Raty, F. Gygi and G. Galli, *Phys. Rev. Lett.*, 2005, **95**, 096103.
379 P. Pyykkö and F. Mendizabal, *Chem.–Eur. J.*, 1997, **3**, 1458–1465.
380 P. Pyykkö, M. Straka and T. Tamm, *Phys. Chem. Chem. Phys.*, 1999, **1**, 3441–3444.
381 N. Runeberg, M. Schütz and H.-J. Werner, *J. Chem. Phys.*, 1999, **110**, 7210–7215.
382 J. E. Mayer, *J. Chem. Phys.*, 1933, **1**, 327–334.
383 M. Dolg, in *Encyclopedia of Computational Chemistry*, Wiley, Chichester, New York, 1998, vol. 2, pp. 1478–1486.
384 M. Bucher, *Phys. Rev. B*, 1984, **30**, 947–956.
385 P. Pyykkö, *Chem. Rev.*, 1997, **97**, 597–636.
386 P. Pyykkö and Y.-F. Zhao, *Angew. Chem.*, 1991, **103**, 622–623.
387 L. Magnko, M. Schweizer, G. Rauhut, M. Schütz, H. Stoll and H.-J. Werner, *Phys. Chem. Chem. Phys.*, 2002, **4**, 1006–1013.
388 E. O'Grady and N. Kaltsoyannis, *J. Chem. Soc., Dalton Trans.*, 2002, 1233–1239.
389 N. Cruz Hernández and J. Fdez. Sanz, *J. Chem. Phys.*, 2005, **123**, 244706.
390 P. Schaposchnikow, R. Pool and T. J. H. Vlugt, *Comput. Phys. Commun.*, 2007, **177**, 154–157.
391 E. Eliav, U. Kaldor and Y. Ishikawa, *Phys. Rev. A*, 1994, **49**, 1724–1729.
392 V. A. Dzuba, V. V. Flambaum and C. Harabati, *Phys. Rev. A*, 2000, **62**, 042504.
393 T. M. Miller, in *CRC Handbook of Chemistry and Physics*, ed. D. R. Lide, CRC, Boca Raton, FL, 2002, ch. 10, vol. 83, pp. 147–162.
394 K. A. Barakat, T. R. Cundari and M. A. Omary, *J. Am. Chem. Soc.*, 2003, **125**, 14228–14229.
395 V. R. Bojan, E. J. Fernández, A. Laguna, J. M. López-de-Luzuriaga, M. Monge, M. E. Olmos and C. Silvestru, *J. Am. Chem. Soc.*, 2005, **127**, 11564–11565.
396 Z.-X. Cao and Q.-E. Zhang, *J. Comput. Chem.*, 2005, **26**, 1214–1221.
397 E. J. Fernández, A. Laguna and J. M. López-de-Luzuriaga, *Coord. Chem. Rev.*, 2005, **249**, 1423–1433.
398 Y.-R. Guo, Q.-J. Pan, G.-Z. Fang and Z.-M. Liu, *Chem. Phys. Lett.*, 2005, **413**, 59–64.
399 K. K. Saha and A. Mookerjee, *J. Phys.: Condens. Matter*, 2005, **17**, 4559–4566.
400 P. Sinha, A. K. Wilson and M. A. Omary, *J. Am. Chem. Soc.*, 2005, **127**, 12488–12489.
401 M. Bardají, M. J. Calhorda, P. J. Costa, P. G. Jones, A. Laguna, M. Reyes Pérez and M. D. Villacampa, *Inorg. Chem.*, 2006, **45**, 1059–1068.
402 E. J. Fernández, A. Laguna, J. M. López-de-Luzuriaga, M. Monge, M. Montiel, M. E. Olmos and M. Rodríguez-Castillo, *Organometallics*, 2006, **25**, 3639–3646.
403 Y. Liao, G.-C. Yang, J.-K. Feng, L.-L. Shi, S.-Y. Yang, L. Yang and A.-M. Ren, *J. Phys. Chem. A*, 2006, **110** 13036–13044.
404 F. Mendizabal, C. Olea-Azar and R. Briones, *THEOCHEM*, 2006, **764**, 187–194.
405 Q.-J. Pan, H.-G. Fu, H.-T. Yu and H.-X. Zhang, *Chem. Phys. Lett.*, 2006, **426**, 257–262.
406 M.-X. Zhang, C.-Y. Mang and K.-C. Wu, *THEOCHEM*, 2006, **759**, 35–39.
407 R. K. Arvapally, P. Sinha, S. R. Hettiarachchi, N. L. Coker, C. E. Bedel, H. H. Patterson, R. C. Elder, A. K. Wilson and M. A. Omary, *J. Phys. Chem. C*, 2007, **111**, 10689–10699.
408 E. J. Fernández, A. Laguna, J. M. López-de-Luzuriaga, M. Monge, M. Montiel and M. E. Olmos, *Inorg. Chem.*, 2007, **46**, 2953–2955.
409 E. J. Fernández, P. G. Jones, A. Laguna, J. M. López-de-Luzuriaga, M. Monge, M. E. Olmos and R. C. Puelles, *Organometallics*, 2007, **26**, 5931–5939.
410 M.-Z. Liu, P. Guyot-Sionnest, T.-W. Lee and S. K. Gray, *Phys. Rev. B*, 2007, **76**, 235428.
411 F. Mendizabal, B. Aguilera and C. Olea-Azar, *Chem. Phys. Lett.*, 2007, **447**, 345–351.
412 J. Muñiz, L. E. Sansores, A. Martínez and R. Salcedo, *THEOCHEM*, 2007, **820**, 141–147.
413 A. Perrier, F. Maurel and J. Aubard, *J. Phys. Chem. A*, 2007, **111**, 9688–9698.
414 M. Stener, A. Nardelli, R. De Francesco and G. Fronzoni, *J. Phys. Chem. C*, 2007, **111**, 11862–11871.
415 K. M.-C. Wong, L.-L. Hung, W. H. Lam, N.-Y. Zhu and V. W.-W. Yam, *J. Am. Chem. Soc.*, 2007, **129**, 4350–4365.
416 Y.-L. Zhu, S.-Y. Zhou, Y.-H. Kan, L.-K. Yan and Z.-M. Su, *J. Chem. Phys.*, 2007, **126**, 245106.
417 Q.-J. Pan, X. Zhou, H.-X. Zhang and H.-G. Fu, *Chem. Phys. Lett.*, 2008, **453**, 7–12.
418 L.-F. Cui, Y.-C. Lin, D. Sundholm and L.-S. Wang, *J. Phys. Chem. A*, 2007, **111**, 7555–7561.
419 J. Gao, W.-L. Zou, W.-J. Liu, Y.-L. Xiao, D.-L. Peng, B. Song and C.-B. Liu, *J. Chem. Phys.*, 2005, **123**, 054102.
420 J. M. H. Lo and M. Klobukowski, *Theor. Chem. Acc.*, 2007, **118**, 607–622.
421 E. Tellgren, J. Henriksson and P. Norman, *J. Chem. Phys.*, 2007, **126**, 064313.
422 W. Q. Tian, M.-F. Ge, F.-L. Gu, T. Yamada and Y. Aoki, *J. Phys. Chem. A*, 2006, **110**, 6285–6293.
423 O. Kullie, H. Zhang, J. Kolb and D. Kolb, *J. Chem. Phys.*, 2006, **125**, 244303.
424 Z. J. Wu and Z. M. Su, *J. Chem. Phys.*, 2006, **124**, 184306.
425 V. Pershina, J. Anton and B. Fricke, *J. Chem. Phys.*, 2007, **127**, 134310.
426 L. O'Brien, A. E. Oberlink and B. O. Roos, *J. Phys. Chem. A*, 2006, **110**, 11954–11957.
427 Z. J. Wu, *J. Phys. Chem. A*, 2005, **109**, 5951–5955.
428 C. Inntam, L. V. Moskaleva, I. V. Yudanov, K. M. Neyman and N. Rösch, *Chem. Phys. Lett.*, 2006, **417**, 515–520.

429 M. Samah, M. Bouguerra, L. Guerbous and M. Berd, *Phys. Scr.*, 2007, **75**, 411–413.
430 C. Majumder and S. K. Kulshreshta, *Phys. Rev. B*, 2006, **73**, 155427.
431 P. K. Jain, *Struct. Chem.*, 2005, **16**, 421–426.
432 R. C. Longo and L. J. Gallego, *Phys. Rev. B*, 2006, **74** 193409.
433 X.-B. Li, H.-Y. Wang, X.-D. Yang, Z.-H. Zhu and Y.-J. Tang, *J. Chem. Phys.*, 2007, **126**, 084505.
434 Y. Dai, D. Dai, B. Huang and C. Yan, *Eur. Phys. J. D*, 2005, **34**, 105–107.
435 W. Fa, J. Zhou, C.-F. Luo and J.-M. Dong, *Phys. Rev. B*, 2006, **73**, 085405.
436 A. F. Jalbout, F. F. Contreras-Torres, L. A. Pérez and I. L. Garzón, *J. Phys. Chem. A*, 2008, **112**, 353–357.
437 I. L. Garzón, K. Michaelian, M. R. Beltrán, A. Posada-Amarillas, P. Ordejón, E. Artacho, D. Sánchez-Portal and J. M. Soler, *Eur. Phys. J. D*, 1999, **9**, 211–215.
438 V. G. Grigoryan, D. Alamanova and M. Springborg, *Eur. Phys. J. D*, 2005, **34**, 187–190.
439 O. Olvera-Neria, A. Cruz, H. Luna-García, A. Anguiano-García, E. Poulain and S. Castillo, *J. Chem. Phys.*, 2005, **123**, 164302.
440 L.-F. Cui, X. Huang, L.-M. Wang, J. Li and L.-S. Wang, *Angew. Chem., Int. Ed.*, 2007, **46**, 742–745.
441 C.-Y. Mang, C.-P. Liu, J. Zhou, Z.-G. Li and K.-C. Wu, *Chem. Phys. Lett.*, 2007, **438**, 20–25.
442 J.-J. Guo, J.-X. Yang and D. Die, *THEOCHEM*, 2006, **764**, 117–121.
443 Q. Ge, C. Song and L. Wang, *Comput. Mater. Sci.*, 2006, **35**, 247–253.
444 A. Spiekermann, S. D. Hoffmann, T. F. Fässler, I. Krossing and U. Preiss, *Angew. Chem., Int. Ed.*, 2007, **46**, 5310–5313.
445 F.-L. Liu, Y.-F. Zhao, X.-Y. Li and F.-Y. Hao, *THEOCHEM*, 2007, **809**, 189–194.
446 C. A. Tsipis, I. G. Depastas and C. E. Kefalidis, *J. Comput. Chem.*, 2007, **28**, 1893–1908.
447 Y.-C. Lin, D. Sundholm, J. Jusélius, L.-F. Cui, X. Li, H.-J. Zhai and L.-S. Wang, *J. Phys. Chem. A*, 2006, **110**, 4244–4250.
448 J. L. Rao, G. K. Chaitanya, S. Basavaraja, K. Bhanuprakash and A. Venkataramana, *THEOCHEM*, 2007, **803**, 89–93.
449 S. F. Li, X.-L. Xue, Y. Jia, G.-F. Zhao, N.-F. Zhang and X. G. Gong, *Phys. Rev. B*, 2006, **73**, 165401.
450 H.-J. Zhai, L.-S. Wang, D. Yu. Zubarev and A. I. Boldyrev, *J. Phys. Chem. A*, 2006, **110**, 1689–1693.
451 K. Michaelian and I. L. Garzón, *Eur. Phys. J. D*, 2005, **34**, 183–186.
452 M.-X. Chen, X. H. Yan and S. H. Wei, *J. Phys. Chem. A*, 2007, **111**, 8659–8662.
453 G. F. Zhao and Z. Zeng, *J. Chem. Phys.*, 2006, **125**, 014303.
454 G.-F. Zhao, J.-M. Sun and Z. Zheng, *Chem. Phys.*, 2007, **342**, 267–274.
455 H.-Y. Wang, X.-B. Li, Y.-J. Tang, R. B. King and H. F. Schaefer III, *Chin. Phys.*, 2007, **16**, 1660–1664.
456 H. Woldeghebriel and A. Kshirsagar, *J. Chem. Phys.*, 2007, **127**, 224708.
457 W. Q. Tian, M.-F. Ge, F.-L. Gu and Y. Aoki, *J. Phys. Chem. A*, 2005, **109**, 9860–9866.
458 M. Neumaier, F. Weigend, O. Hampe and M. M. Kappes, *J. Chem. Phys.*, 2006, **125**, 104308.
459 C. Corminboeuf, *Chem. Phys. Lett.*, 2006, **418**, 437–441.
460 C. Corminboeuf, C. S. Wannere, D. Roy, R. B. King and P. v. R. Schleyer, *Inorg. Chem.*, 2006, **45**, 214–219.
461 E. M. Fernández, L. C. Balbás, L. A. Peréz, K. Michaelian and I. L. Garzón, *Int. J. Mod. Phys. B*, 2005, **19**, 2339–2344.
462 P. J. Hsu and S. K. Lai, *J. Chem. Phys.*, 2006, **124**, 044711.
463 B. C. Curley, G. Rossi, R. Ferrando and R. L. Johnston, *Eur. Phys. J. D*, 2007, **43**, 53–56.
464 M. Zhang and R. Fournier, *THEOCHEM*, 2006, **762**, 49–56.
465 S.-T. Sun, X.-P. Xing, H.-T. Liu and Z.-C. Tang, *J. Phys. Chem. A*, 2005, **109**, 11742–11751.
466 A. C. Tsipis and C. A. Tsipis, *J. Am. Chem. Soc.*, 2005, **127**, 10623–10638.
467 A. H. Pakiari and Z. Jamshidi, *J. Phys. Chem. A*, 2007, **111**, 4391–4396.
468 O. Schuster, U. Monkowius, H. Schmidbaur, R. S. Ray, S. Krüger and N. Rösch, *Organometallics*, 2006, **25**, 1004–1011.
469 D.-Y. Wu, B. Ren and Z.-Q. Tian, *ChemPhysChem*, 2006, **7**, 619–628.
470 G. P. Li and I. P. Hamilton, *Chem. Phys. Lett.*, 2006, **420**, 474–479.
471 H. W. Ghebriel and A. Kshirsagar, *J. Chem. Phys.*, 2007, **126**, 244705.
472 C. Majumder, A. K. Kandalam and P. Jena, *Phys. Rev. B*, 2006, **74**, 205437.
473 H.-J. Zhai, B. Kiran, B. Dai, J. Li and L.-S. Wang, *J. Am. Chem. Soc.*, 2005, **127**, 12098–12106.
474 G. S. Shafai, S. Shetty, S. Krishnamurthy, V. Shah and D. G. Kanhere, *J. Chem. Phys.*, 2007, **126**, 014704.
475 C.-F. Luo, W. Fa and J.-M. Dong, *J. Chem. Phys.*, 2006, **125**, 084707.
476 Y. Wang and X. G. Gong, *J. Chem. Phys.*, 2006, **125**, 124703.
477 G.-C. Yang, L. Fang, K. Tan, S.-Q. Shi, Z.-M. Su and R.-S. Wang, *Organometallics*, 2007, **26**, 2082–2087.
478 S. Chrétien and H. Metiu, *J. Chem. Phys.*, 2007, **126**, 104701.
479 Y. Okamoto, *Chem. Phys. Lett.*, 2006, **420**, 382–386.
480 C. Gourlaouen, J.-P. Piquemal, T. Saue and O. Parisel, *J. Comput. Chem.*, 2006, **27**, 142–156.
481 J. M. Standard, B. W. Gregory and B. K. Clark, *THEOCHEM*, 2007, **803**, 103–113.
482 S. Mishra, V. Vallet and W. Domcke, *ChemPhysChem*, 2006, **7**, 723–727.
483 S. Mishra, *J. Phys. Chem. A*, 2007, **111**, 9164–9168.
484 X.-F. Wang and L. Andrews, *Chem. Commun.*, 2005, 4001–4003.
485 X.-F. Wang and L. Andrews, *Inorg. Chem.*, 2005, **44**, 9076–9083.
486 Q. Xu and L. Jing, *J. Phys. Chem. A*, 2006, **110**, 2655–2662.
487 Q.-M. Surong, Y.-F. Zhao, X.-G. Jing, F.-L. Liu, X.-Y. Li and W.-H. Su, *Aust. J. Chem.*, 2005, **58**, 792–798.
488 H. V. R. Dias, M. Fianchini, T. R. Cundari and C. F. Campana, *Angew. Chem., Int. Ed.*, 2008, **47**, 556–559.
489 K. Koyasu, M. Niemietz, M. Götz and G. Ganteför, *Chem. Phys. Lett.*, 2007, **450**, 96–100.
490 Q.-M. Su Rong, Y.-F. Zhao, X.-G. Jing, X.-Y. Li and W.-H. Su, *THEOCHEM*, 2005, **717**, 91–97.
491 A. J. Esswein, J. L. Dempsey and D. G. Nocera, *Inorg. Chem.*, 2007, **46**, 2362–2364.
492 S. M. Mendoza, C. M. Whelan, J.-P. Jalkanen, F. Zerbello, F. G. Gatti, E. R. Kay, D. A. Leigh, M. Lubomska and P. Rudolf, *J. Chem. Phys.*, 2005, **123**, 244708.
493 M. Y. Wang, X. J. Liu, J. Meng and Z. J. Wu, *THEOCHEM*, 2007, **804**, 47–55.
494 H. G. Raubenheimer, M. W. Esterhuysen, G. Frenking, A. Y. Timoshkin, C. Esterhuysen and U. E. I. Horvath, *Dalton Trans.*, 2006, 4580–4589.
495 A. M. Joshi, W. N. Delgass and K. T. Thomson, *J. Phys. Chem. C*, 2007, **111**, 7841–7844.
496 R. Wesendrup, T. Hunt and P. Schwerdtfeger, *J. Chem. Phys.*, 2000, **112**, 9356–9362.
497 F. Furche, R. Ahlrichs, P. Weis, C. Jacob, S. Gilb, T. Bierweiler and M. M. Kappes, *J. Chem. Phys.*, 2002, **117**, 6982–6990.
498 R. Guo, K. Balasubramanian, X.-F. Wang and L. Andrews, *J. Chem. Phys.*, 2002, **117**, 1614–1620.
499 S. Gilb, P. Weis, F. Furche, R. Ahlrichs and M. M. Kappes, *J. Chem. Phys.*, 2003, **116**, 4094–4101.
500 H. Häkkinen, B. Yoon, U. Landman, X. Li, H.-J. Zhai and L.-S. Wang, *J. Phys. Chem. A*, 2003, **107**, 6168–6175.
501 H. Häkkinen and U. Landman, *Phys. Rev. B*, 2000, **62**, R2287–R2290.
502 L. Xiao and L.-C. Wang, *Chem. Phys. Lett.*, 2004, **392**, 452–455.
503 F. Remacle and E. S. Kryachko, *J. Chem. Phys.*, 2005, **122**, 044304.
504 A. V. Walker, *J. Chem. Phys.*, 2005, **122**, 094310.
505 J. Li, X. Li, H.-J. Zhai and L.-S. Wang, *Science*, 2003, **299**, 864–867.
506 X. Gu, S. Bulusu, X. Li, X. C. Zeng, J. Li, X. G. Gong and L.-S. Wang, *J. Phys. Chem. C*, 2007, **111**, 8228–8232.
507 I. L. Garzón and A. Posada-Amarillas, *Phys. Rev. B*, 1996, **54**, 11796–11802.
508 L. Miao and J. M. Seminario, *J. Chem. Phys.*, 2007, **126** 184706.

509 J.-G. Wang and A. Selloni, *J. Phys. Chem. A*, 2007, **111**, 12381–12385.
510 Y. Wang, N. S. Hush and J. R. Reimers, *J. Am. Chem. Soc*., 2007, **129**, 14532–14533.
511 A. Filippetti and V. Fiorentini, *Phys. Rev. B*, 2005, **72**, 135128.
512 L.-S. Hsu, Y.-K. Wang, Y.-L. Tai and J.-F. Lee, *Phys. Rev. B*, 2005, **72**, 115115.
513 B. Li and J. D. Corbett, *Inorg. Chem*., 2005, **44**, 6515–6517.
514 H. Reichert, A. Schöps, I. B. Ramsteiner, V. N. Bugaev, O. Shchyglo, A. Udyansky, H. Dosch, M. Asta, R. Drautz and V. Honkimäki, *Phys. Rev. Lett*., 2005, **95**, 235703.
515 C.-J. Zhang and A. Alavi, *J. Am. Chem. Soc*., 2005, **127**, 9808–9817.
516 J. Gegner, T. C. Koethe, H. Wu, Z. Hu, H. Hartmann, T. Lorenz, T. Fickensher, R. Pöttgen and L. H. Tjeng, *Phys. Rev. B*, 2006, **74**, 073102.
517 S. Lange, F. M. Schappacher, D. Johrendt, T. Nilges, R.-D. Hoffmann and R. Pöttgen, *Z. Anorg. Allg. Chem*., 2006, **632**, 1432–1436.
518 M. A. McGuire, T. K. Reynolds and F. J. DiSalvo, *J. Alloys Compd*., 2006, **425**, 81–87.
519 T. Miyazaki and H. Kino, *Phys. Rev. B*, 2006, **73**, 035107.
520 P. D. Semalty, *J. Alloys Compd*., 2006, **419**, 1–6.
521 G. Ugur and F. Soyalp, *J. Phys.: Condens. Matter*, 2006, **18**, 6777–6784.
522 J.-C. Dai and J. D. Corbett, *Inorg. Chem*., 2007, **46** 4592–4598.
523 A. Dal Corso, *Phys. Rev. B*, 2007, **76**, 054308.
524 M. Hodak, S.-C. Wang, W.-C. Lu and J. Bernholc, *Phys. Rev. B*, 2007, **76**, 085108.
525 S.-H. Lee and G. S. Hwang, *J. Chem. Phys*., 2007, **127**, 224710.
526 Q.-S. Lin and J. D. Corbett, *Inorg. Chem*., 2007, **46**, 8722–8727.
527 X.-L. Song, J.-M. Zhang and K.-W. Xu, *J. Alloys Compd*., 2007, **436**, 23–29.
528 H.-Q. Shi, R. Asahi and C. Stampfl, *Phys. Rev. B*, 2007, **75**, 205125.
529 D. Kurzydłowski and W. Grochala, *Chem. Commun*., 2008, 1073–1075.